

DTIC FILE COPY

1

AD-A202 598



EFFECTS OF DIFFERENT FABRICATION  
TECHNIQUES ON THE  
YTTRIUM-BARIUM-COPPER OXIDE  
HIGH TEMPERATURE SUPERCONDUCTOR

THESIS

Paul A. Rhea  
First Lieutenant, USAF

DTIC  
ELECTE  
JAN 18 1989  
S  
&  
D

DISTRIBUTION STATEMENT A

Approved for public release  
Distribution Unlimited

DEPARTMENT OF THE AIR FORCE  
AIR UNIVERSITY  
**AIR FORCE INSTITUTE OF TECHNOLOGY**

Wright-Patterson Air Force Base, Ohio

80 1 17 097

AFIT/GE/ENG/88D-42

1

DTIC  
ELECTE  
JAN 18 1989  
S D<sup>3</sup> D

EFFECTS OF DIFFERENT FABRICATION  
TECHNIQUES ON THE  
YTTRIUM-BARIUM-COPPER OXIDE  
HIGH TEMPERATURE SUPERCONDUCTOR

THESIS

Paul A. Rhea  
First Lieutenant, USAF

AFIT/GE/ENG/88D-42

Approved for public release; distribution unlimited

AFIT/GE/ENG/88D-42

EFFECTS OF DIFFERENT FABRICATION TECHNIQUES ON THE YTTRIUM-  
BARIUM-COPPER OXIDE HIGH TEMPERATURE SUPERCONDUCTOR

THESIS

Presented to the Faculty of the School of Engineering  
of the Air Force Institute of Technology

Air University

In Partial Fulfillment of the  
Requirements for the Degree of  
Master of Science in Electrical Engineering



Paul A. Rhea  
First Lieutenant, USAF

December 1988

|               |                                     |
|---------------|-------------------------------------|
| Accession For |                                     |
| NTIS GRA&I    | <input checked="" type="checkbox"/> |
| DTIC TAB      | <input type="checkbox"/>            |
| Unannounced   | <input type="checkbox"/>            |
| Justification |                                     |
| By            |                                     |
| Date          |                                     |
| Approved      |                                     |
| Dist          |                                     |
| A-1           |                                     |

Approved for public release; distribution unlimited

### Acknowledgements

I am greatly indebted to many people who helped me complete the experimentation and writing of this thesis. First, my appreciation to the Physics Department, Air Force Institute of Technology, for giving me the opportunity to carry out this project. I wish to thank Dr. Y. K. Yeo, my thesis advisor, for his guidance and direction. A special thanks to the Materials Laboratory for sponsoring this effort and providing the necessary equipment and materials. I am also thankful to Dr. P. Hemenger, of the Materials Laboratory, for his assistance from the start of this endeavor and, especially, for his valuable advice in writing this thesis. I thank Ron Kerans, Materials Laboratory, for his assistance in designing this project. I would also like to thank Tim Peterson for his patient instructing. I thank Mark Battison for sharing his knowledge of materials fabrication and for taking the x-ray diffraction measurements for this project. I thank Iman Maartense for taking magnetic susceptibility measurements and spending hours helping me interpret them. Finally, I would like to thank my wife, Shirlene, whose unwaivering support gave me the inspiration to complete this project.

## Table of Contents

|   | Page |
|---|------|
| Acknowledgements . . . . .                                  | ii   |
| List of Figures . . . . .                                   | vi   |
| List of Tables . . . . .                                    | xii  |
| Abstract . . . . .  | xiii |
| I. Background . . . . .                                     | 1    |
| Importance of Superconductivity . . . . .                   | 1    |
| Overview . . . . .  | 3    |
| Statement of Problem . . . . .                              | 4    |
| Scope . . . . .   | 5    |
| Assumptions . . . . .                                       | 6    |
| Purpose of the Study . . . . .                              | 7    |
| Approach/Methodology . . . . .                              | 7    |
| Materials and Equipment . . . . .                           | 8    |
| Conclusions . . . . .                                       | 10   |
| Subsequent Chapters . . . . .                               | 10   |
| II. Summary of Current Knowledge . . . . .                  | 11   |
| Early High Temperature Superconductors . . . . .            | 11   |
| Problems with High Temperature<br>Superconductors . . . . . | 12   |
| Critical Current Density . . . . .                          | 12   |
| Brittle Materials . . . . .                                 | 13   |
| Instability . . . . .                                       | 14   |
| Recent High Temperature Superconductors . . . . .           | 14   |
| Theory . . . . .  | 16   |
| Conclusions . . . . .                                       | 18   |

|  | Page |
|--|------|
| III. Experimental Procedure . . . . .                                  | 19   |
| Sample Preparation . . . . .   | 19   |
| Structural Measurements . . . . .                                      | 20   |
| Density Measurements . . . . .   | 20   |
| X-ray Diffraction Measurements . . . . .                               | 22   |
| Electrical and Magnetic Measurements . . . . .                         | 22   |
| Magnetic Susceptibility Measurements . . . . .                         | 22   |
| Resistivity Measurements . . . . .                                     | 23   |
| Cutting Samples . . . . .  | 24   |
| Contacts . . . . .   | 24   |
| Electrical Connections . . . . .                                       | 25   |
| Cooling the Sample . . . . .   | 25   |
| Critical Current Density Measurements . . . . .                        | 27   |
| IV. Results and Analysis . . . . .                                     | 29   |
| Introduction . . . . .   | 29   |
| Results . . . . .  | 29   |
| Sample Preparation . . . . .   | 29   |
| Density Measurements . . . . .   | 30   |
| X-ray Diffraction Measurements . . . . .                               | 31   |
| Magnetic Susceptibility Measurements . . . . .                         | 32   |
| Resistivity Measurements . . . . .                                     | 59   |
| Critical Current Density Measurements . . . . .                        | 64   |
| Analysis . . . . .   | 71   |
| Conclusions . . . . .  | 76   |
| V. Conclusions and Recommendations . . . . .                           | 77   |
| Introduction . . . . .   | 77   |
| Conclusions . . . . .  | 78   |
| Recommendations . . . . .  | 84   |
| Appendix A: Calculations of Amounts of Starting<br>Materials . . . . . | 86   |

|  | Page |
|--|------|
| Appendix B: Density Measurements . . . . . | 89   |
| Bibliography . . . . .                     | 92   |
| Vita . . . . .                             | 94   |

## List of Figures

| Figure  | Page |
|---|------|
| 1. Historical Improvement in the Superconducting Critical Temperature . . . . .                                     | 4    |
| 2. Samples Prepared . . . . .   | 9    |
| 3. Density Measurement Equipment . . . . .  | 21   |
| 4. Magnetic Susceptibility Equipment . . . . .  | 23   |
| 5. Ideal Dimensions of Sample . . . . .   | 24   |
| 6. Sample with Contacts . . . . .   | 25   |
| 7. Electrical Connections to Sample . . . . .   | 26   |
| 8. Dewar Used to Make Resistivity Measurements . . .  | 27   |
| 9. Density Measurements . . . . .   | 31   |
| 10. X-ray Diffraction Pattern for Barium Carbonate Derived Sample, Sintered at 850 °C, Annealed in Oxygen . . . . . | 33   |
| 11. X-ray Diffraction Pattern for Barium Carbonate Derived Sample, Sintered at 850 °C, Not Annealed                 | 34   |
| 12. X-ray Diffraction Pattern for Barium Carbonate Derived Sample, Sintered at 950 °C, Annealed in Oxygen . . . . . | 35   |
| 13. X-ray Diffraction Pattern for Barium Carbonate Derived Sample, Sintered at 950 °C, Not Annealed                 | 36   |
| 14. X-ray Diffraction Pattern for Barium Carbonate Derived Sample, Sintered at 900 °C, Annealed in Oxygen . . . . . | 37   |



| Figure |  | Page |
|--------|--|------|
| 15.    | X-ray Diffraction Pattern for Barium Carbonate<br>Derived Sample, Sintered at 900 °C, Not Annealed   | 38   |
| 16.    | X-ray Diffraction Pattern for Barium Peroxide<br>Derived Sample, Sintered at 850 °C, Annealed in<br>Oxygen . . . . .                           | 39   |
| 17.    | X-ray Diffraction Pattern for Barium Peroxide<br>Derived Sample, Sintered at 850 °C, Not Annealed  | 40   |
| 18.    | X-ray Diffraction Pattern for Barium Peroxide<br>Derived Sample, Sintered at 900 °C, Annealed in<br>Oxygen . . . . .                           | 41   |
| 19.    | X-ray Diffraction Pattern for Barium Peroxide<br>Derived Sample, Sintered at 900 °C, Not Annealed  | 42   |
| 20.    | X-ray Diffraction Pattern for Barium Peroxide<br>Derived Sample, Sintered at 950 °C, Annealed in<br>Oxygen . . . . .                           | 43   |
| 21.    | X-ray Diffraction Pattern for Barium Peroxide<br>Derived Sample, Sintered at 950 °C, Not Annealed  | 44   |
| 22.    | Magnetic Susceptibility versus Temperature for<br>the Barium Peroxide Derived Sample, Sintered<br>at 850 °C, Annealed in Oxygen . . . . .      | 45   |
| 23.    | Magnetic Susceptibility versus Temperature for<br>the Barium Peroxide Derived Sample, Sintered<br>at 850 °C, Not Annealed . . . . .            | 45   |
| 24.    | Magnetic Susceptibility Loss versus Temperature<br>for the Barium Peroxide Derived Sample, Sintered<br>at 850 °C, Annealed in Oxygen . . . . . | 47   |
| 25.    | Magnetic Susceptibility Loss versus Temperature<br>for the Barium Peroxide Derived Sample, Sintered<br>at 850 °C, Not Annealed . . . . .       | 47   |

| Figure  | Page |
|---|------|
| 26. Magnetic Susceptibility versus Temperature for the Barium Carbonate Derived Sample, Sintered at 850 °C, Annealed in Oxygen . . . . .      | 48   |
| 27. Magnetic Susceptibility versus Temperature for the Barium Carbonate Derived Sample, Sintered at 850 °C, Not Annealed . . . . .            | 48   |
| 28. Magnetic Susceptibility Loss versus Temperature for the Barium Carbonate Derived Sample, Sintered at 850 °C, Annealed in Oxygen . . . . . | 49   |
| 29. Magnetic Susceptibility Loss versus Temperature for the Barium Carbonate Derived Sample, Sintered at 850 °C, Not Annealed . . . . .       | 49   |
| 30. Magnetic Susceptibility versus Temperature for the Barium Carbonate Derived Sample, Sintered at 950 °C, Not Annealed . . . . .            | 50   |
| 31. Magnetic Susceptibility Loss versus Temperature for the Barium Carbonate Derived Sample, Sintered at 950 °C, Not Annealed . . . . .       | 50   |
| 32. Magnetic Susceptibility versus Temperature for the Barium Carbonate Derived Sample, Sintered at 950 °C, Annealed in Oxygen . . . . .      | 52   |
| 33. Magnetic Susceptibility Loss versus Temperature for the Barium Carbonate Derived Sample, Sintered at 950 °C, Annealed in Oxygen . . . . . | 52   |
| 34. Magnetic Susceptibility versus Temperature for the Barium Peroxide Derived Sample, Sintered at 900 °C, Not Annealed . . . . .             | 53   |
| 35. Magnetic Susceptibility versus Temperature for the Barium Peroxide Derived Sample, Sintered at 900 °C, Annealed in Oxygen . . . . .       | 53   |

| Figure  | Page |
|---|------|
| 36. Magnetic Susceptibility Loss versus Temperature for the Barium Peroxide Derived Sample, Sintered at 900 °C, Not Annealed . . . . .        | 54   |
| 37. Magnetic Susceptibility Loss versus Temperature for the Barium Peroxide Derived Sample, Sintered at 900 °C, Annealed in Oxygen . . . . .  | 54   |
| 38. Magnetic Susceptibility versus Temperature for the Barium Peroxide Derived Sample, Sintered at 950 °C, Annealed in Oxygen . . . . .       | 55   |
| 39. Magnetic Susceptibility versus Temperature for the Barium Peroxide Derived Sample, Sintered at 950 °C, Not Annealed . . . . .             | 55   |
| 40. Magnetic Susceptibility Loss versus Temperature for the Barium Peroxide Derived Sample, Sintered at 950 °C, Annealed in Oxygen . . . . .  | 56   |
| 41. Magnetic Susceptibility Loss versus Temperature for the Barium Peroxide Derived Sample, Sintered at 950 °C, Not Annealed . . . . .        | 56   |
| 42. Magnetic Susceptibility versus Temperature for the Barium Carbonate Derived Sample, Sintered at 900 °C, Annealed in Oxygen . . . . .      | 57   |
| 43. Magnetic Susceptibility versus Temperature for the Barium Carbonate Derived Sample, Sintered at 900 °C, Not Annealed . . . . .            | 57   |
| 44. Magnetic Susceptibility Loss versus Temperature for the Barium Carbonate Derived Sample, Sintered at 900 °C, Annealed in Oxygen . . . . . | 58   |
| 45. Magnetic Susceptibility Loss versus Temperature for the Barium Carbonate Derived Sample, Sintered at 900 °C, Not Annealed . . . . .       | 58   |

| Figure   | Page |
|--|------|
| 46. Resistivity versus Temperature for the Barium Peroxide Sample, Sintered at 850 °C, Annealed in Oxygen . . . . .  | 60   |
| 47. Resistivity versus Temperature for the Barium Peroxide Sample, Sintered at 850 °C, Not Annealed                  | 61   |
| 48. Resistivity versus Temperature for the Barium Peroxide Sample, Sintered at 900 °C, Annealed in Oxygen . . . . .  | 62   |
| 49. Resistivity versus Temperature for the Barium Peroxide Sample, Sintered at 900 °C, Not Annealed                  | 63   |
| 50. Resistivity versus Temperature for the Barium Peroxide Sample, Sintered at 950 °C, Annealed in Oxygen . . . . .  | 65   |
| 51. Resistivity versus Temperature for the Barium Peroxide Sample, Sintered at 950 °C, Not Annealed                  | 66   |
| 52. Resistivity versus Temperature for the Barium Carbonate Sample, Sintered at 900 °C, Annealed in Oxygen . . . . . | 67   |
| 53. Resistivity versus Temperature for the Barium Carbonate Sample, Sintered at 900 °C, Not Annealed . . . . .       | 68   |
| 54. Resistivity versus Temperature for the Barium Carbonate Sample, Sintered at 950 °C, Annealed in Oxygen . . . . . | 69   |
| 55. Resistivity versus Temperature for the Barium Carbonate Sample, Sintered at 950 °C, Not Annealed . . . . .       | 70   |
| 56. Critical Current Density versus Temperature for All Samples Measured . . . . .                                   | 72   |

| Figure |  | Page |
|--------|--|------|
| 57.    | Resistivity versus Temperature for All Oxygen<br>Annealed, Barium Peroxide Derived Samples . . . . | 80   |
| 58.    | Resistivity versus Temperature for All Unannealed<br>Barium Peroxide Derived Samples . . . . .     | 81   |
| 59.    | Resistivity versus Temperature for All Oxygen<br>Annealed, Barium Carbonate Derived Samples . . .  | 82   |
| 60.    | Resistivity versus Temperature for All Unannealed<br>Barium Carbonate Derived Samples . . . . .    | 83   |

## List of Tables

| Figure  | Page |
|---|------|
| 1. Density Measurements for Samples Annealed in<br>Oxygen . . . . . | 90   |
| 2. Density Measurements for Samples Not Annealed . .                | 91   |

Abstract

This study examines how several different parameters were changed in the yttrium-barium-copper oxide superconductor when the fabrication techniques were altered by using different barium precursors, including barium peroxide and barium carbonate; sintering at different temperatures, including 850, 900, 950 °C; and annealing in an above ambient oxygen environment. Twelve different pellets were fabricated, and measurements were taken on them which included density, x-ray diffraction, critical temperature, critical current density, and magnetic susceptibility. The results showed that the barium peroxide derived samples had higher densities, better critical current densities, and lower resistivities in the normal state. The samples sintered at 900 °C for both barium precursors, had higher critical temperatures, higher critical current densities, sharper transitions from the normal to the superconducting state, and lower resistivities in the normal state. The samples which were annealed in an oxygen environment varied little from those samples measured as-sintered.

# EFFECTS OF DIFFERENT FABRICATION TECHNIQUES ON THE YTTRIUM-BARIUM-COPPER OXIDE HIGH TEMPERATURE SUPERCONDUCTOR

## I. Background

### Importance of Superconductivity

High temperature superconductivity is a phenomenon which could revolutionize our society in much the same way as the transistor has since it was developed in the 1950's. As an example, in the area of generation and transmission of electrical power, superconductors could produce enormous energy savings. As much as 20 per cent of the energy sent through transmission lines is lost in heat due to resistance in the lines (5:65). If these lines were replaced with superconductive lines, transmission losses would be greatly reduced. This would mean that less electricity would have to be generated and fewer power plants would have to be built, producing enormous savings for the power companies. In addition, it would take fewer superconductive lines to carry the same amount of electricity as is currently being transmitted, and, since it could be transmitted further, power plants could be built in remote areas (6:30).



Generators produced with superconductive materials could double output (5:69). Transformers could be made smaller and more efficient: able to convert more power since there would be no heat produced in the coils. With the introduction of superconductivity, large underground rings of superconducting cable could store vast amounts of electricity for use during the peak hours (5:70). A superconducting magnetic energy storage (SMES) unit with a capacity of 20 megawatt hours is being built as a demonstration and will be available for the Strategic Defense Initiative (SDI) pulsed power weapon tests (7:5).

An area of great promise for superconductors in the short term appears to be in the field of microelectronics (6:30). Eliminating the generation of heat in computer circuits will significantly reduce the size constraints being encountered today (5:65). Superconductivity could bring about smaller, faster computers with increased memory. One way speed could be increased is in high-speed interconnects on and between computer chips. Another way to increase speed could be through the use of Josephson junctions, which are superconductive devices which switch like transistors but have no gain (13:1189). They perform as fast switches at speeds of less than 10 picoseconds and with less than a microwatt of power dissipated (6:30). Since switching speed is currently a limiting factor in computer speed, Josephson junctions could greatly increase the speed of computers.

Josephson junctions, kept at liquid helium temperatures, are already being used in many applications (5:69).

The present high temperature superconductors, however, are limited in many ways. For these materials the critical current density,  $J_C$  (A/cm<sup>2</sup>), which is defined as the amount of current density necessary to drive the material from the superconductive state to the normal state at a fixed temperature, is much less than that of earlier superconductors and is much less than that needed for most applications. These materials are ceramics so they are brittle and easily broken. Finally, for these materials the critical temperature,  $T_C$  (K), which is defined as the temperature at which the resistivity of a material drops to zero as it is cooled, is still too low for many applications.

### Overview

The objective of most of the research in the field of superconductivity has been to find materials which maintain their superconductivity at higher temperatures. One of the most significant advances in  $T_C$  was the discovery of a lanthanum-barium-copper oxide, with a  $T_C$  of 35 K (9:1134), which was followed by a similar compound in which the lanthanum was replaced by yttrium, with a  $T_C$  of 98 K (5:68). The highest known  $T_C$  prior to these discoveries, as shown in Figure 1, was that of Nb<sub>3</sub>Ge at 23 K (9:1134). These new compounds are not fully understood, and theorists are still

puzzled as to what mechanism is responsible for the superconductivity in these materials. They do not behave in a manner consistent with current theories. More information must be obtained if researchers are to fully understand these materials so their properties can be exploited.

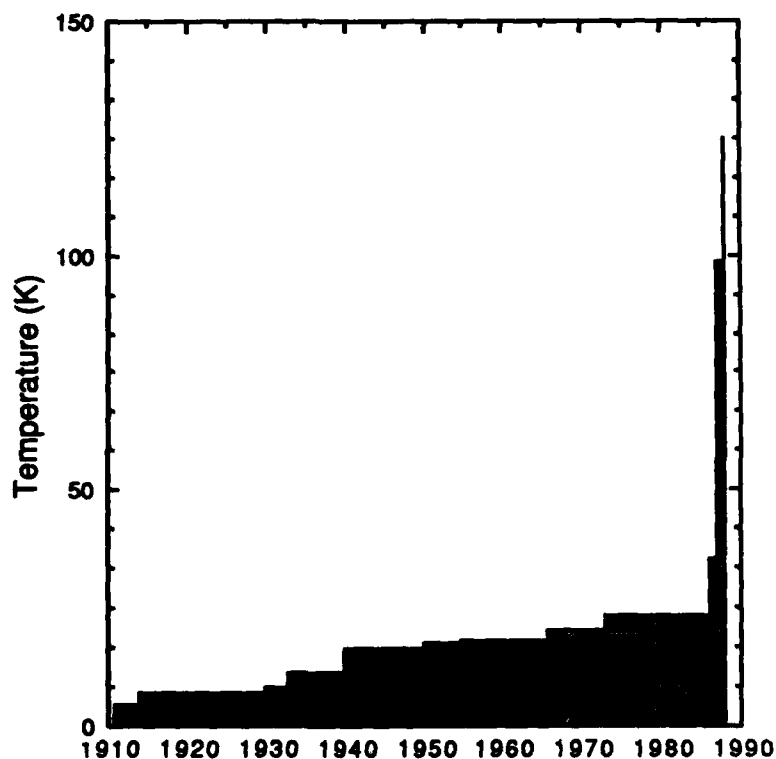


Figure 1. Historical Improvement in the Superconducting Critical Temperature (Values from 9:1134, 4:22, and 16:1243)

#### Statement of Problem

This research will examine two yttrium-barium-copper oxide compounds to determine how selected parameters change

when different barium precursors are used and when different fabrication techniques are used.

#### Scope

This research will be limited to examining with structural, electrical, and magnetic measurements, two yttrium-barium-copper oxide compounds to determine how selected parameters change when different barium precursors are used and when different fabrication techniques are used. The two barium precursors under investigation are barium carbonate and barium peroxide. The experimental design includes barium carbonate as a precursor since it is a commonly used starting material for the compound sought (13:1). The choice of barium peroxide was not as obvious. The possible barium precursors were barium peroxide, barium carbonate, barium oxide, barium acetate, barium hydroxide, and barium fluoride. Barium oxide was not selected because it is not stable in air. Barium acetate was not used because it would require liquid mixing, which would make for poorer comparisons. Barium hydroxide melts at much lower temperatures than barium carbonate so these two precursors could not be used in identical fabrication techniques. Barium fluoride was not selected because it only reacts at temperatures much higher than those at which barium carbonate reacts. Barium peroxide was selected because it is more

stable than the other choices and it can be processed in the same manner as barium carbonate.

The different fabrication techniques to be considered include sintering samples at three different temperatures and annealing half of the samples in oxygen.

The parameters to be examined are density, x-ray diffraction, critical temperature, critical current density, and magnetic susceptibility.

#### Assumptions

As the material is cooled below the critical temperature so that the resistivity drops to zero, it is assumed that the resistivity will remain at zero through any further cooling. Any effects which might cause the non-zero resistance to return once the superconductive state is reached, other than the current density or the magnetic field present, such as the Kondo effect (2:15), are not under investigation. This assumption indicates that measurements taken well below the critical temperature are not necessary.

Secondly, hysteretic effects will not be considered while taking resistivity versus temperature measurements; thus, these measurements will begin at a temperature below the material's  $T_c$  and proceed as the samples are heated up to room temperature. Since all of the samples are measured in the same manner, hysteretic effects do not impair a comparison of the data taken from different samples.

### Purpose of the Study

This research will show how the various precursors and fabrication techniques employed affect the properties of the finished material. The objective is to gain a better understanding of how purer, more homogeneous superconductors may be fabricated so that new materials with better properties will be developed.

### Approach/Methodology

The approach used is to substitute barium peroxide for barium carbonate in the fabrication of the yttrium-barium-copper oxide superconductor and do a systematic study of the resulting materials. In addition to varying the barium precursor, the sintering temperatures were varied, using 850, 900, or 950 °C. Finally, half of the pellets were annealed in an oxygen environment as shown in Figure 2.

Structural differences in the final materials were evaluated by density measurements and x-ray diffraction patterns.

Electrical and magnetic properties were evaluated by magnetic susceptibility measurements, resistivity versus temperature measurements, and critical current density measurements. If the magnetic susceptibility measurements indicated that a pellet was not superconducting at even very low temperatures, no electrical measurements were made.

This approach to the problem yields 12 sets of two identical samples fabricated from different barium precursors, different sintering temperatures, and different annealing procedures as shown in Figure 2. Using different barium precursors shows how the parameters under investigation are affected by changes in the barium precursor. Using different processing techniques shows how sintering at different temperatures and annealing in oxygen will affect the parameters under investigation.

#### Materials and Equipment

The materials needed for this study were provided by the Air Force Wright Aeronautical Laboratory's Materials Lab. The materials used were yttrium oxide, copper oxide, barium carbonate, barium peroxide, oxygen, ethyl alcohol, silver paint, liquid nitrogen, liquid helium, pure indium solder, gold wire, epoxy with acetate, and Epomet molding compound.

The equipment needed for this study were provided by the Materials Lab. The equipment needed was a balance, beakers, spatula, ball milling equipment, oven for calcinations, thermocouple, Doric meter, crucible, plastic beaker, tongs, mortar and pestle, dry box, cold press and half inch dies, petree dish, oven for sintering, crucible boats, oven rod, 100 ml beaker, platform to elevate ethyl alcohol above balance dish, wire to suspend sample in ethyl alcohol, tweezers, hacksaw, ruler, sandpaper, microscope slides, x-ray

diffractometer, mounting press, AC magnetometer, DC current source, DC field coil, sensor coils, glass dewar, thermocouple, variable temperature dewar, ammeter, and nanovoltmeter.













|                  |                    | Sintering Temperature   |  |   |
|------------------|--------------------|---|--|---|
|                  |                    | 850   | 900  | 950   |
| Barium Carbonate | Annealed in Oxygen |    |    |    |
|                  | Not Annealed       |    |    |    |
| Barium Peroxide  | Annealed in Oxygen |  |  |  |
|                  | Not Annealed       |  |  |  |

Figure 2. Samples Prepared



## Conclusions

The objective of most of the research in the field of superconductivity has been to find materials which maintain their superconductivity at higher temperatures and carry larger currents. The most significant recent advance in critical temperature was the discovery of a lanthanum-barium-copper oxide, which was followed by a similar compound in which lanthanum was replaced by yttrium. The mechanisms responsible for the superconductivity in these materials are still not understood. The purpose of this research is to produce purer, more homogeneous samples and to add information to the existing knowledge of the subject with the hope that a better understanding of the phenomenon of high temperature superconductivity may be achieved. This will be accomplished by varying the starting materials and the fabrication techniques and seeing how specific parameters are affected.

## Subsequent Chapters

Chapter II will include a review of current literature dealing with high temperature superconductivity. Chapter III will detail the methodology used in the exercise. Chapter IV will analyze the results achieved. Finally, Chapter V will draw conclusions based on the analysis of the results and give recommendations for further study in this field.

## II. Summary of Current Knowledge

### Early High Temperature Superconductors

In 1983 Karl Alex Müller and Johannes Georg Bednorz of IBM began to consider ceramics in their search for higher critical temperatures. In December of 1985 they discovered a compound of barium, lanthanum, copper, and oxygen that displayed superconductive properties at 35 K (Figure 1). This was considered a phenomenal breakthrough in a field which had been stagnant for many years (5:66). Shortly after this discovery, researchers at Bell Labs reached a critical temperature,  $T_C$ , of 38 K (5:67).

Paul C. W. Chu of the University of Houston found that under pressures 10,000 to 12,000 times atmospheric pressure the compound discovered at IBM had a  $T_C$  of 52 K. Chu replaced the barium in the IBM compound with strontium, which is chemically similar but has a smaller atomic structure. This new compound exhibited a  $T_C$  of 54 K. He then tried replacing the barium with calcium, which has an even smaller atomic structure, but the attempt was unsuccessful. After this attempt, Maw-Kuen Wu, the head of the unit of Chu's team located at the University of Alabama, replaced the lanthanum in the compound with yttrium. The result was a  $T_C$  of 93 K. In February of 1987, Chu and Wu repeated the process together, in order to verify the results. They found the  $T_C$  to be 98 K (5:68).

### Problems with High Temperature Superconductors

Though the compound Chu discovered greatly increased the temperature at which a superconductor may operate, it has some problems associated with it. First, the materials can not carry a large enough current for most practical applications. Second, the materials being ceramics are brittle so it is difficult to produce them in useful geometries, and once the materials are produced they can easily be broken. Finally, the materials' properties are not stable enough for most practical uses, because the material degrades in the atmosphere.

Critical Current Density. The yttrium-barium-copper-oxygen compounds made to date do not carry as high a current density as the low temperature superconductors (5:70). The superconductive current is thought to be interrupted at the grain boundaries of the polycrystalline material, but at low current densities a proximity effect allows current to flow through these boundaries with no voltage drop.

To improve the current carrying capacity of these materials, it is necessary to reduce their polycrystalline nature or to control the grain boundaries. A major improvement was achieved by an IBM team with a process that involves using electron beams to evaporate material from yttrium, barium, and copper targets in a vacuum system with low oxygen pressure. The metal atoms in the vapor and oxygen

atoms deposit on a heated substrate, such as strontium titanate. The films deposited have small grains and no superconductivity; however, heating them to 900-1000 °C in oxygen causes the grains to grow significantly, up to 1 cm in diameter, changes the oxidation state of the copper, and the films become superconducting with a  $T_c$  of about 90 K. This process increases the current carrying capacity into the range needed for interconnects in microelectronics applications, which is typically on the order of  $10^5$  A/cm<sup>2</sup> (13:1189).

Brittle Materials. A second problem with the yttrium-barium-copper-oxygen compounds is that they have the brittleness typical of ceramics so they can not be easily formed into useful shapes. For example, they break easily if one attempts to bend the material into the shape of a coil (5:70).

Present methods for making ceramic superconductors include reacting the starting materials to form the proper compound, grinding it into a powder, and sintering the powder to form a comparatively homogeneous solid. The very low ductility may be partially compensated for by sintering the material after it has been shaped appropriately. An alternative to this method is to melt the metallic elements, yttrium, barium, and copper, which then solidifies into a ternary metal alloy. The alloy can then be formed into the desired shape and heated in an oxygen atmosphere, where it is

converted into the oxide superconductor (14:1526).

Researchers at Argonne National Laboratory have succeeded in drawing wires made from these superconductive materials.

Also, researchers at Bell Labs have formed these materials into thin flexible films (6:30).

Instability. Another problem with the yttrium-barium-copper oxide is that it is prone to breaking down when exposed to moisture and carbon dioxide. Some researchers linked this problem with impurities in the sample and reported that the stability problem diminished as purer samples were developed (12:27). Other researchers placed the blame on the barium in the compound. They sought a replacement for barium which was not prone to reacting with moisture and carbon dioxide, such as calcium and strontium (10:2).

#### Recent High Temperature Superconductors

A new record high  $T_C$  of 105 K was reported in January of 1988. The compound discovered by a group led by Hiroshi Maeda of Japan's National Research Institute for Metals was composed of bismuth, calcium, strontium, copper, and oxygen (4:22).

In addition to the increased  $T_C$ , the bismuth-containing compound had several advantages over the yttrium-containing compound. The bismuth-containing compound is much more stable and more flexible than its predecessor. It does not

have to be processed at as high a temperature, and it does not require a final annealing step in order to add oxygen. However, workers have not succeeded in making materials composed of only the high  $T_C$  phase. There has not yet been a report indicating whether or not the critical current density of this material exceeds that of the yttrium-containing compound (12:27).

On the same day the bismuth-containing compound was announced, Allen Hermann and Zhengzhi Sheng of the University of Arkansas announced a thallium-barium-copper oxide with a  $T_C$  of 81 K. Later, they found that by adding calcium to the compound, they developed a new material with a  $T_C$  of 106 K. On March 3, 1988, researchers at the IBM Almaden Research Center reported the discovery of a compound containing these same elements which had a  $T_C$  of 125 K. This is by far the highest temperature at which superconductivity has been reported to date (16:1243).

The thallium-containing compound is considered in the same class as the bismuth-containing compound. Indeed, it shares many of the same advantages over the yttrium-containing compound. Since it does not contain a rare-earth element, it should also be considerably cheaper to produce than the yttrium-containing compound (16:1243).

The most significant contribution of these latest discoveries might be the insight they give as to how high

temperature superconductors work, and they may provide clues as to how higher  $T_C$ 's may be reached (11:146).

### Theory

The discoveries of the thallium- and bismuth-containing compounds may have led to a clarification of what is responsible for the superconductivity in the high temperature superconductors. Researchers have reported a correlation between the number of copper-oxide layers in the structure and the  $T_C$  of the material. For the thallium-containing compound, if the material is prepared such that it has one copper-oxide layer, the  $T_C$  is 80 K. Two copper-oxide layers yield a  $T_C$  of 110 K. Finally, three copper-oxide layers yield a  $T_C$  of 125 K. Similar results have been reported for the bismuth-containing compound (11:146).

Based on these observations some researchers believe that the supercurrents propagate in the copper-oxide planes rather than primarily in the copper-oxide chains as originally proposed for the yttrium-containing compound. The bismuth- and thallium-containing compounds contain copper-oxide planes rather than chains (11:146).

The conventional theory concerning superconductivity, known as the BCS theory, is generally perceived as having limited applicability to the high temperature superconductors; therefore, most researchers believe the theory needs modifications (15:280). The central feature of

the BCS theory is the pairing of electrons. Researchers report that several experiments have shown that electron pairing occurs in the high temperature superconductors (15:281).

Also central to the BCS theory is the mechanism that causes pairing, namely that electron pairs are bound together by electron-phonon interactions. Though this means of pairing may play a part in the high temperature superconductors, it is generally believed that electron-phonon interactions are not the only and probably not the dominant mechanism. One mechanism proposed is that if the normal harmonic vibrations in the lattice do not cause sufficient attraction between the electrons in each pair, then strong anharmonic vibrations can cause electrons to interact with greater attraction. A second mechanism involves electric charge fluctuations which should give rise to a net attractive force if the fluctuations can be exchanged between electrons. Another mechanism involves spin-mediated and magnetic interactions. The spins of electrons can experience spin fluctuations, which can result in energy being given to or taken from electrons. Through these fluctuations an attractive force may result and cause pairing between electrons (15:281).



## Conclusions

The field of high temperature superconductivity is rapidly changing. Researchers are finding materials which maintain their superconductivity at ever higher temperatures. The major advances include lanthanum-barium-copper oxide, yttrium-barium-copper oxide, bismuth-strontium-calcium-copper oxide, and thallium-calcium-barium-copper oxide. These discoveries have led to a better understanding of how these high temperature superconductors work. Future discoveries will surely further clarify the mechanism for superconductivity in these materials.

### III. Experimental Procedure

#### Sample Preparation

The first step was to mix the appropriate amounts of the starting materials into two 200 gram batches. One of these two batches used barium carbonate as the barium precursor and the other used barium peroxide. The first mixture was composed of 30.20 grams of yttrium oxide, 64.00 grams of copper oxide, and 105.8 grams of barium carbonate. The second mixture was composed of 32.80 grams of yttrium oxide, 69.20 grams of copper oxide, and 98.20 grams of barium peroxide. Appendix A shows the calculations performed to arrive at these amounts.

The two batches were each separately ball milled and then successively calcined for 16 hours at each of four temperatures. The mixtures were hand ground after each calcination. These repeated calcinations were performed to insure that all of the starting materials were fully reacted. The temperatures used for calcination were 850, 900, 925, and 950 °C. After the fourth calcination, the barium carbonate based compound was unevenly colored, so the two batches were calcined again at 950 °C, with their positions switched in the furnace to compensate for any temperature variation within the furnace.

After a final hand grinding, 12 one-half inch diameter pellets were cold pressed from each mixture at a pressure of

52,000 lb/in<sup>2</sup>. The resulting as-pressed pellets were approximately one-quarter inch thick, varying from 0.20 to 0.32 inches. There was a total of 24 pellets.

These 24 samples were separated into 3 groups of eight samples each, four from each compound, which were sintered in air for 16 hours at one of the following temperatures: 850, 900, or 950 °C.

Each group of eight samples was then separated into two sets of four samples each with two from each mixture, and one set was then annealed in an above ambient oxygen environment at 450 °C for 16 hours.

The result was 12 sets of two samples each with variations in starting materials and processing as shown in Figure 2.

### Structural Measurements

Structural measurements included density and x-ray diffraction. Density measurements were taken on all 24 pellets. For the remaining measurements, one pellet was selected from each set of two identical pellets. Thus, x-ray diffraction patterns were taken on 12 samples.

Density Measurements. The density of each pellet was determined by using Archimedes principle. Each pellet was weighed dry and then submerged in ethyl alcohol and weighed again. The final measurement was the weight of the wire itself hanging in the ethyl alcohol. Appendix B shows the

measurements taken for each sample. The equipment was set up as shown in Figure 3. The formula used to determine density,  $\rho_s$ , was

$$\rho_s = \frac{w_d d}{w_d - (w_s - w_w)} \quad (1)$$

where

$w_d$  = weight of sample dry (g)

$w_s$  = weight of sample plus weight of wire both suspended in ethyl alcohol (g)

$w_w$  = weight of wire suspended in ethyl alcohol (g)

$\rho_s$  = density of sample ( $\text{g}/\text{cm}^3$ )

$d$  = specific gravity of ethyl alcohol ( $0.7893 \text{ g}/\text{cm}^3$ ).

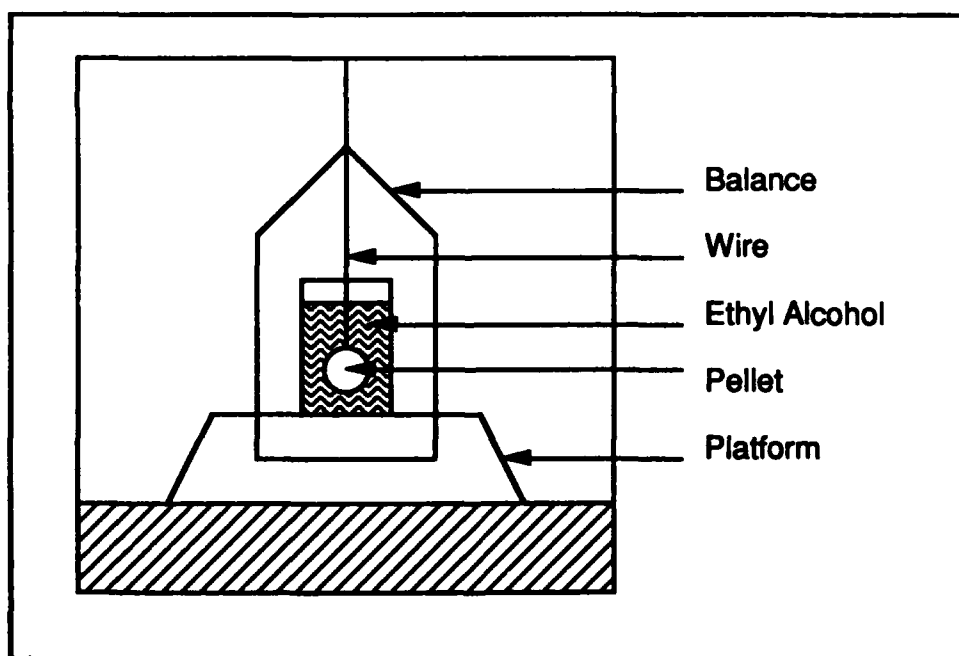


Figure 3. Density Measurement Equipment

( X-ray Diffraction Measurements. Portions of each pellet were crushed using a mortar and pestle. The resulting powder was then placed on a glass slide and mixed with an adherent to form a thin layer which was then allowed to dry. An x-ray diffractometer was then used to determine the crystal structures of the compounds present in each sample.

Electrical and Magnetic Measurements

Electrical and magnetic measurements were taken on each pellet, which included magnetic susceptibility, resistivity versus temperature, and critical current density. If the magnetic susceptibility measurement indicated that the pellet was not superconducting at even very low temperatures, no electrical measurements were made.

Magnetic Susceptibility Measurements. To measure magnetic susceptibility, samples must be cut approximately 2 X 2 X 7 mm, then mounted in a dewar as shown in Figure 4. The dewar allows the sample to be cooled down to liquid helium temperatures. Data is taken as the temperature increases at a rate of 1 or 2 K/min. The AC sensing field is near 4 kHz with the amplitude variable from 0.01 to 4.0 Oe. A DC magnetic field can also be applied to the samples to evaluate their DC as well as their AC magnetic response; however, the field generated by the DC coils for the samples measured in this experiment is kept at zero. As the sample is warmed, the real and imaginary parts of the susceptibility

are measured as the AC field is stepped over several values. The temperature is measured after each AC field scan (8:2).

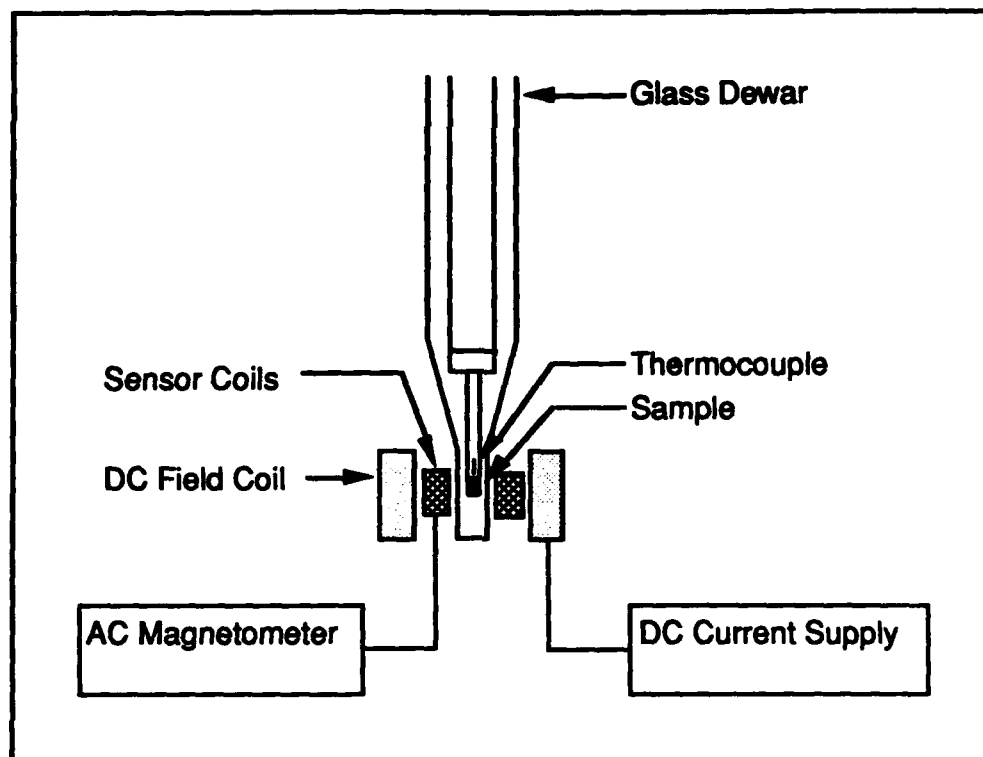


Figure 4. Magnetic Susceptibility Equipment

Resistivity Measurements. To measure resistivity at temperatures other than the boiling point of liquid nitrogen (77 K), it was necessary to cut each pellet into a sample of appropriate size for mounting into a variable temperature dewar, and contacts for four point measurements had to be applied. Next, the samples had to be mounted onto the sample holder and electrical connections made. Finally, the sample holder had to be placed into a liquid helium variable

temperature dewar which can cool the sample and control its temperature.

Cutting Samples. Samples were cut out of each pellet for resistivity measurements using a hacksaw. Emery paper was used to smooth the edges and square them. The ideal sample dimensions are shown in Figure 5.

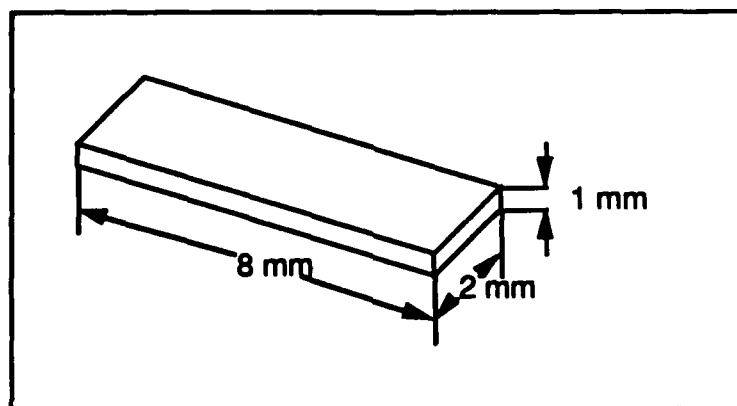


Figure 5. Ideal Dimensions of Sample

Contacts. Silver paint was spread in four strips across each sample as shown in Figure 6. The samples were then placed in an oven at 350 °C for two hours to allow the silver to diffuse into the material forming a low resistance contact and to remove the organic binder in the paint. Another layer of silver paint was then added to assure better adherence of the indium solder. The cross-sectional area of each sample was measured, along with the distance between the centers of the two voltage contacts.

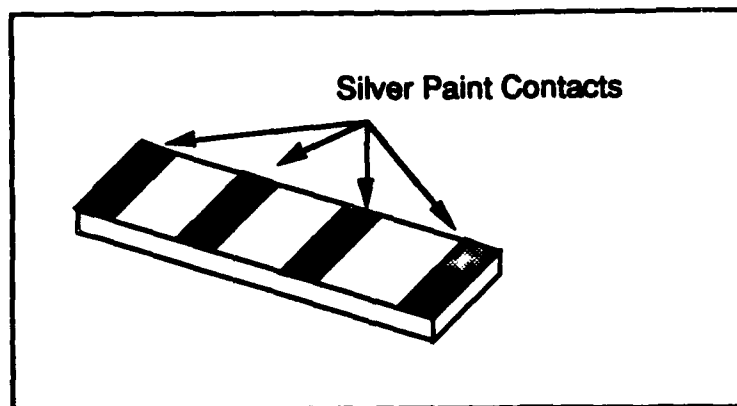


Figure 6. Sample with Contacts

Electrical Connections. Three mil (0.003 inch in diameter) gold wires were attached to each contact by indium solder. The sample was mounted on a beryllium oxide pad which gives electrical isolation but good thermal contact to the copper block assembly containing heaters and thermometers used to measure and control the temperature of the sample. The contacts on the ends of the sample were connected through an ammeter to a current source, while the contacts in the center were connected to a voltmeter, as shown in Figure 7.

Cooling the Sample. The sample was lowered into a dewar used to cool it below liquid nitrogen temperatures (Figure 8). A constant current was passed through the sample so that the voltage drop across the sample was approximately 0.5 to 1.0 mV. The sample was then cooled until no voltage was observed across the voltage contacts. The sample was then heated slowly with measurements being taken at several temperatures. The measurements taken included temperature,



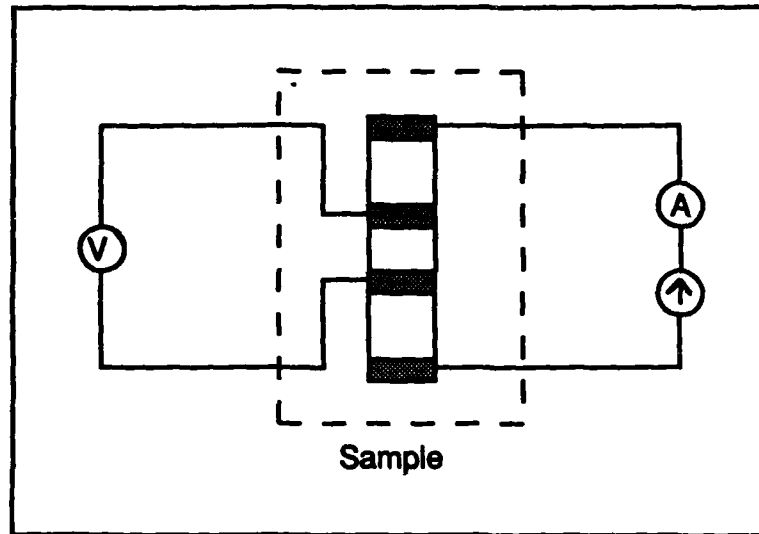


Figure 7. Electrical Connections to Sample

current, and voltage. The resistance between the voltage contacts could then be calculated using Ohm's Law:

$$R = \frac{V}{I} \quad (2)$$

where

$R$  = resistance between voltage contacts ( $\Omega$ )

$I$  = current flowing through sample (A)

$V$  = voltage across the voltage contacts (V)

The resistivity could then be calculated by the formula

$$\rho = \frac{AR}{l} \quad (3)$$

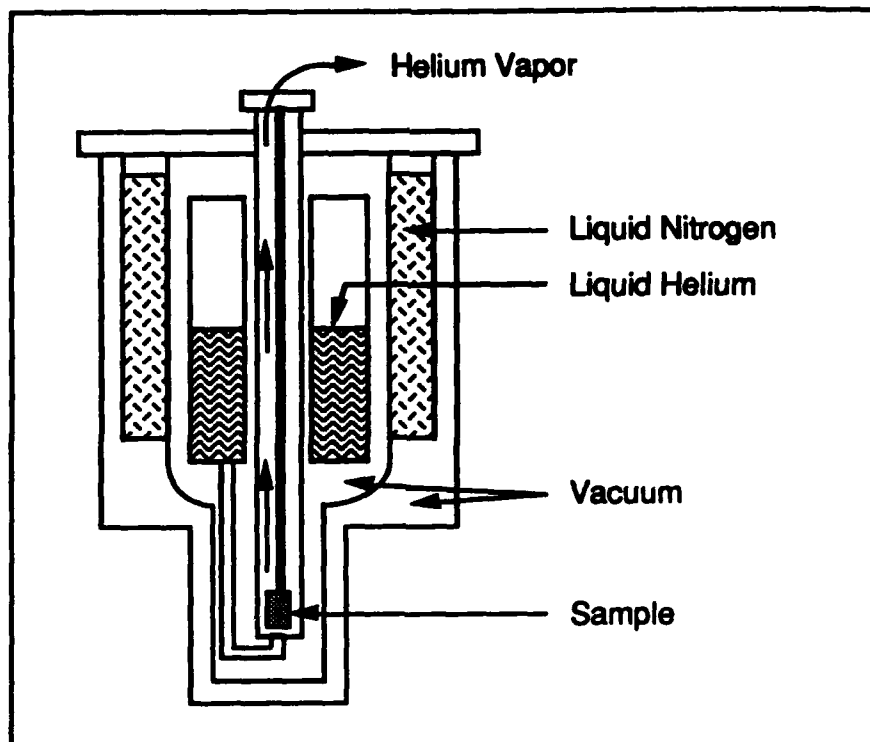


Figure 8. Dewar Used to Make Resistivity Measurements

where

$\rho$  = resistivity ( $\Omega\text{-cm}$ )

$A$  = cross-sectional area of the sample ( $\text{cm}^2$ )

$l$  = distance between the centers of the voltage contacts  
(cm)

$R$  = resistance between voltage contacts ( $\Omega$ )

Critical Current Density Measurements. The samples to be used for critical current density measurements were prepared in a similar manner as those used in the resistivity measurements. However, an attempt was made to reduce the cross-sectional area of the samples so that less current would be needed to reach the critical current density. The

sample was cooled until the maximum current available did not drive it out of the superconductive state. In order to avoid contact heating due to  $I^2R$  losses, the maximum current was limited to 280 mA. Also, the samples were not cooled below 25 K.

The temperature was then raised until the sample went into the normal state, where the temperature was fixed. The current was lowered until no voltage was observed across the sample. The current was recorded. The temperature was then raised to a higher value, and measurements were taken again. This process was repeated until the amount of current was too small to be measured.

#### IV. Results and Analysis

##### Introduction

The results of this research include observations made during sample preparation, the results of the structural measurements, and the data obtained from electrical and magnetic measurements. The analysis of these results will include an examination of the data as well as a look at how the results from the electrical measurements correlate with the results of the structural and magnetic measurements.

##### Results

Sample Preparation. During the repeated calcinations and hand-grindings, observations were made which could be useful in understanding the materials and reaching conclusions.

First, of the two batches mixed and calcined, the batch derived from barium carbonate was much harder to grind than the batch derived from the barium peroxide. Second, the barium carbonate derived batch was also a much less homogeneous mixture and specks of barium carbonate were noticed throughout the sample preparation process, which made it more difficult to ensure that all of the barium carbonate had reacted. Third, the barium peroxide derived batch was much more homogeneous in nature, containing no visible evidence of unreacted starting materials during any part of

( the sample preparation process. Fourth, the barium carbonate derived pellets sintered at 950 °C melted during the sintering process.

Finally, the pellets sintered at 850 °C were cooled at an average rate of 2.39 °C/min until they reached 360 °C after which they were removed from the furnace. The pellets sintered at 900 °C were cooled at an average rate of 2.62 °C/min until they reached 480 °C. The pellets sintered at 950 °C were cooled at an average rate of 2.49 °C/min until they reached 415 °C. The pellets which were annealed in an above ambient oxygen environment at 450 °C, cooled in the above ambient oxygen environment at an average rate of 2.50 °C/min until they reached 22 °C.

After the sintering and annealing processes were completed, it was noted that the furnace used was approximately 20 °C hotter than the temperature at which it was set due to a thermocouple offset error.

Density Measurements. The results of the density measurements show that the pellets derived from barium peroxide were consistently more dense than those derived from barium carbonate (Figure 9). Annealing the pellets in an above ambient oxygen environment had a small effect upon the density of the samples. Of the pellets derived from barium peroxide, those which were sintered at 850 °C were the most dense. The density then dropped as the sintering temperature increased as shown in Figure 9. Of the pellets derived from

barium carbonate, those which were sintered at 900 °C were the most dense. The density then dropped as the sintering temperature either increased or decreased as shown in Figure 9.

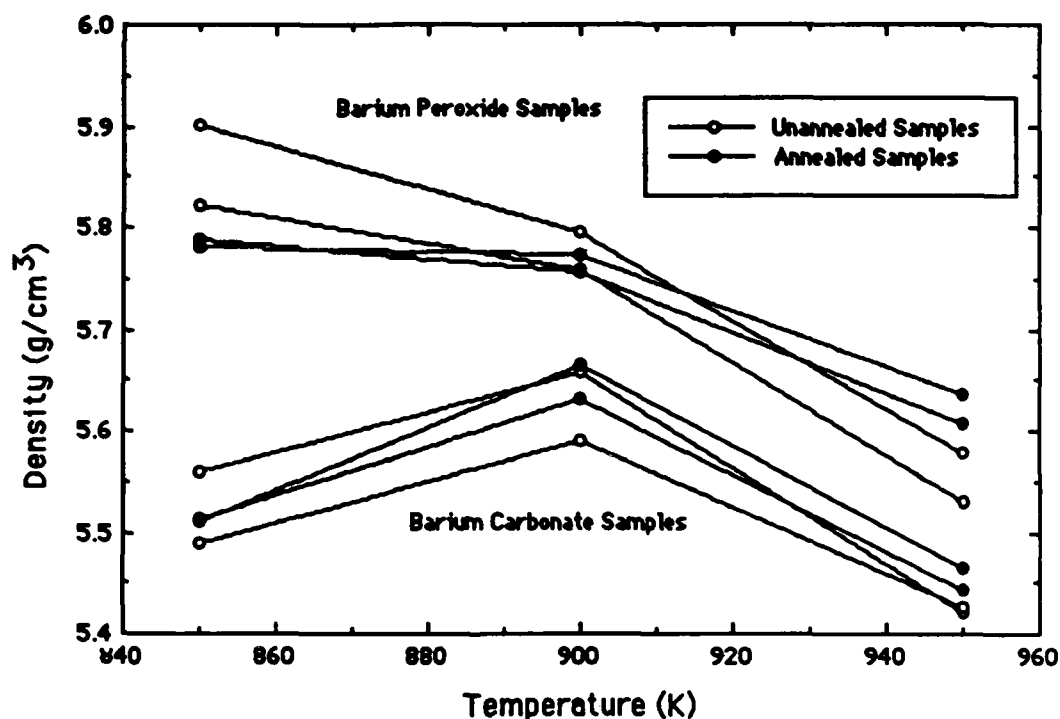


Figure 9. Density Measurements

X-ray Diffraction Measurements. The x-ray diffraction measurements showed little structural difference between the oxygen annealed samples and the unannealed samples.

The most significant observation made based on the x-ray diffraction data is that for the samples derived from barium carbonate, the samples sintered at 850 °C and 950 °C show

( relatively large peaks at a 2 theta of about  $24^\circ$  which corresponds to the maximum peak of the barium carbonate x-ray diffraction pattern as shown in Figures 10-13. Thus it is evident that these samples contain a considerable amount of unreacted barium carbonate. In the barium carbonate derived samples which were sintered at  $900^\circ\text{C}$ , this peak is nonexistent as shown in Figures 14 and 15.

Also, for the barium peroxide derived samples the x-ray diffraction patterns show little difference between the samples sintered at different temperatures as shown in Figures 16-21. These samples do not show the peak at a 2 theta of about  $24^\circ$ . The middle figures in Figures 10-21 show the x-ray diffraction of a typical yttrium-barium-copper oxide sample (17:571).

Magnetic Susceptibility Measurements. Generally, the magnetic susceptibility data shows a sudden occurrence of magnetic susceptibility at about 88 K, indicating that at least part of the bulk superconductor has gone superconducting. In some cases, the individual regions of superconductivity are surrounded by non-superconductive phases which do not allow them to link up until a much colder temperature is reached.

( For the samples derived from barium peroxide which were sintered at  $850^\circ\text{C}$ , the magnetic susceptibility curves show a sudden occurrence of magnetic susceptibility at about 88 K (Figures 22 and 23). At that point, all of the AC field

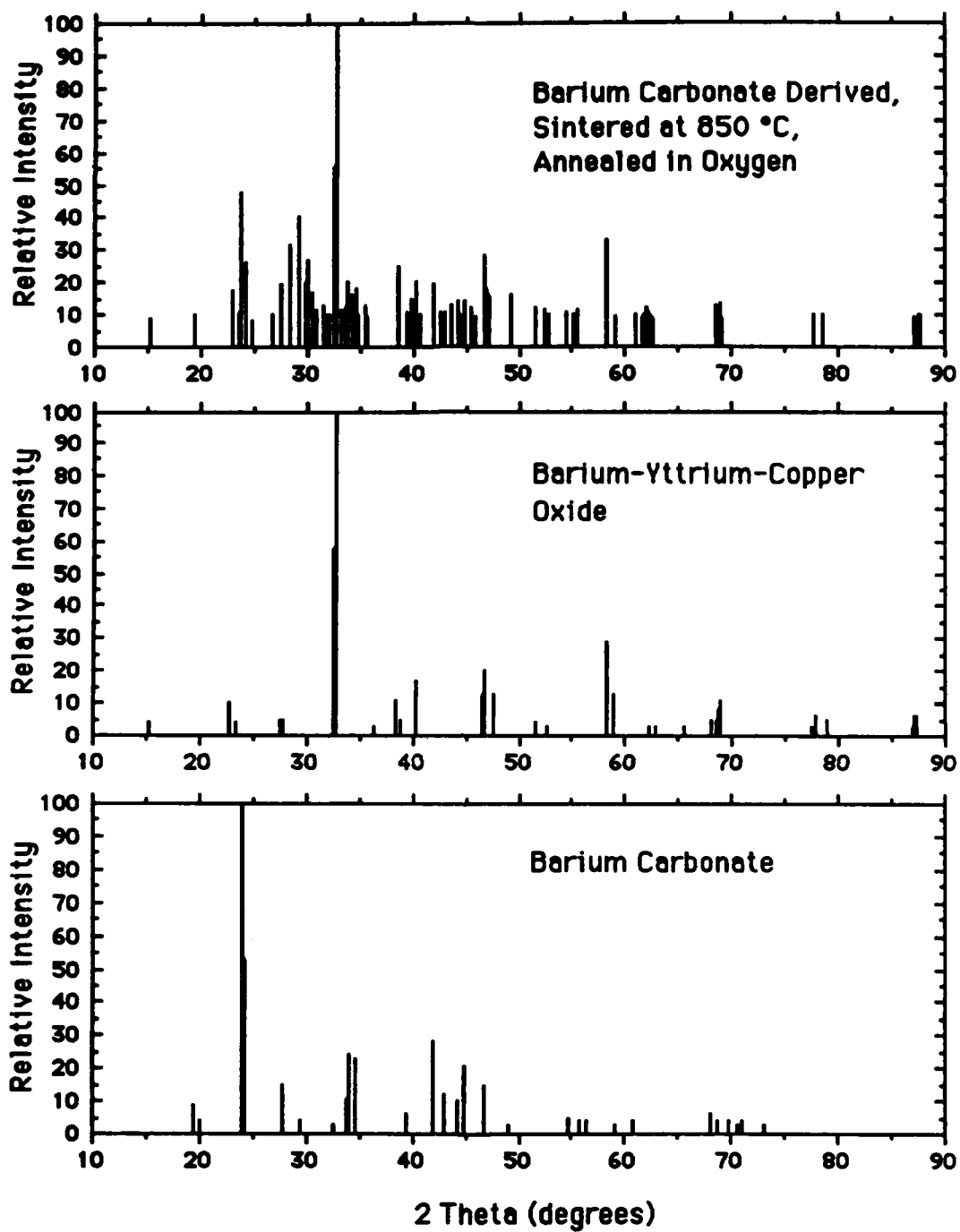


Figure 10. X-ray Diffraction Pattern for Barium Carbonate Derived Sample, Sintered at 850 °C, Annealed in Oxygen



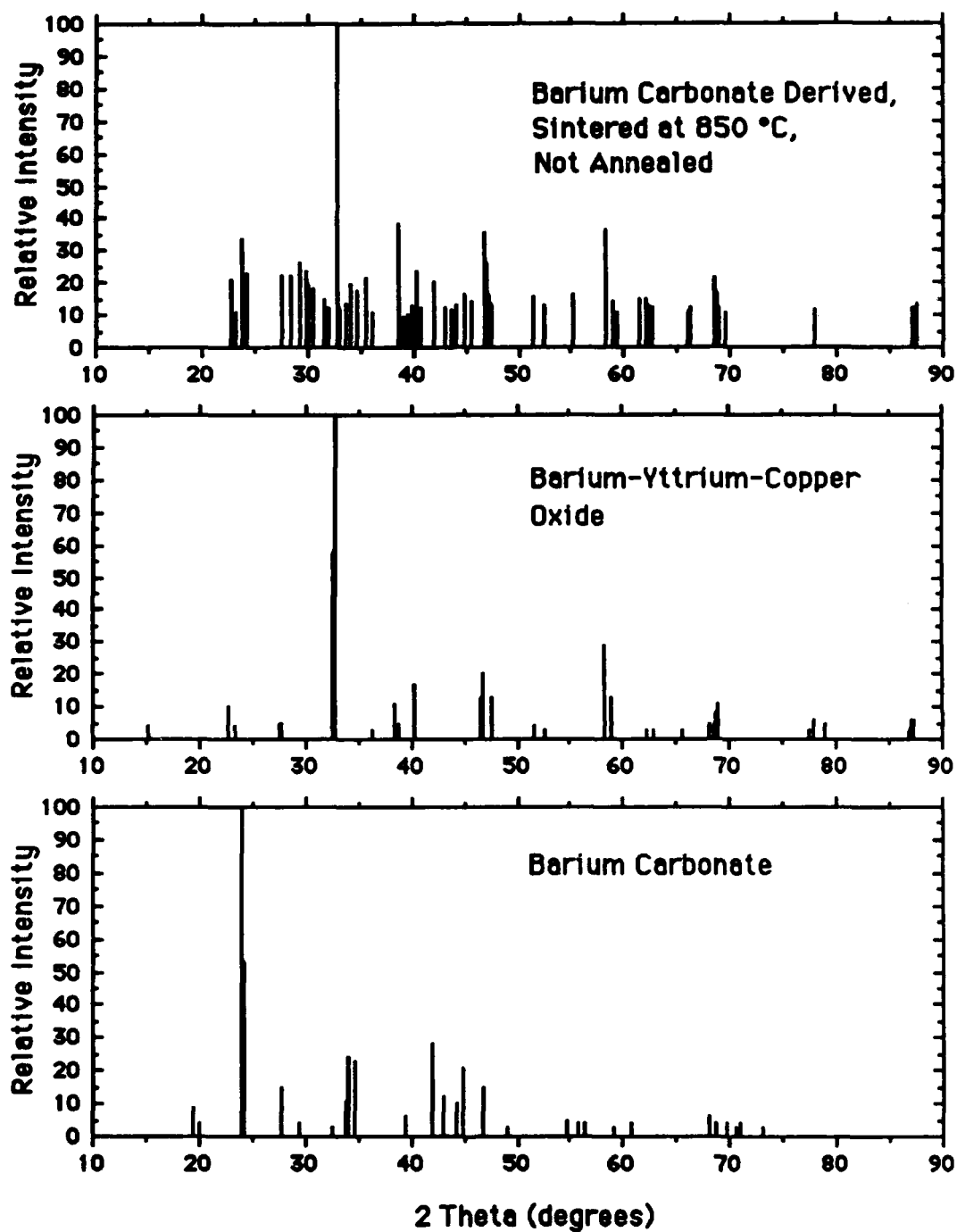


Figure 11. X-ray Diffraction Pattern for Barium Carbonate Derived Sample, Sintered at 850 °C, Not Annealed

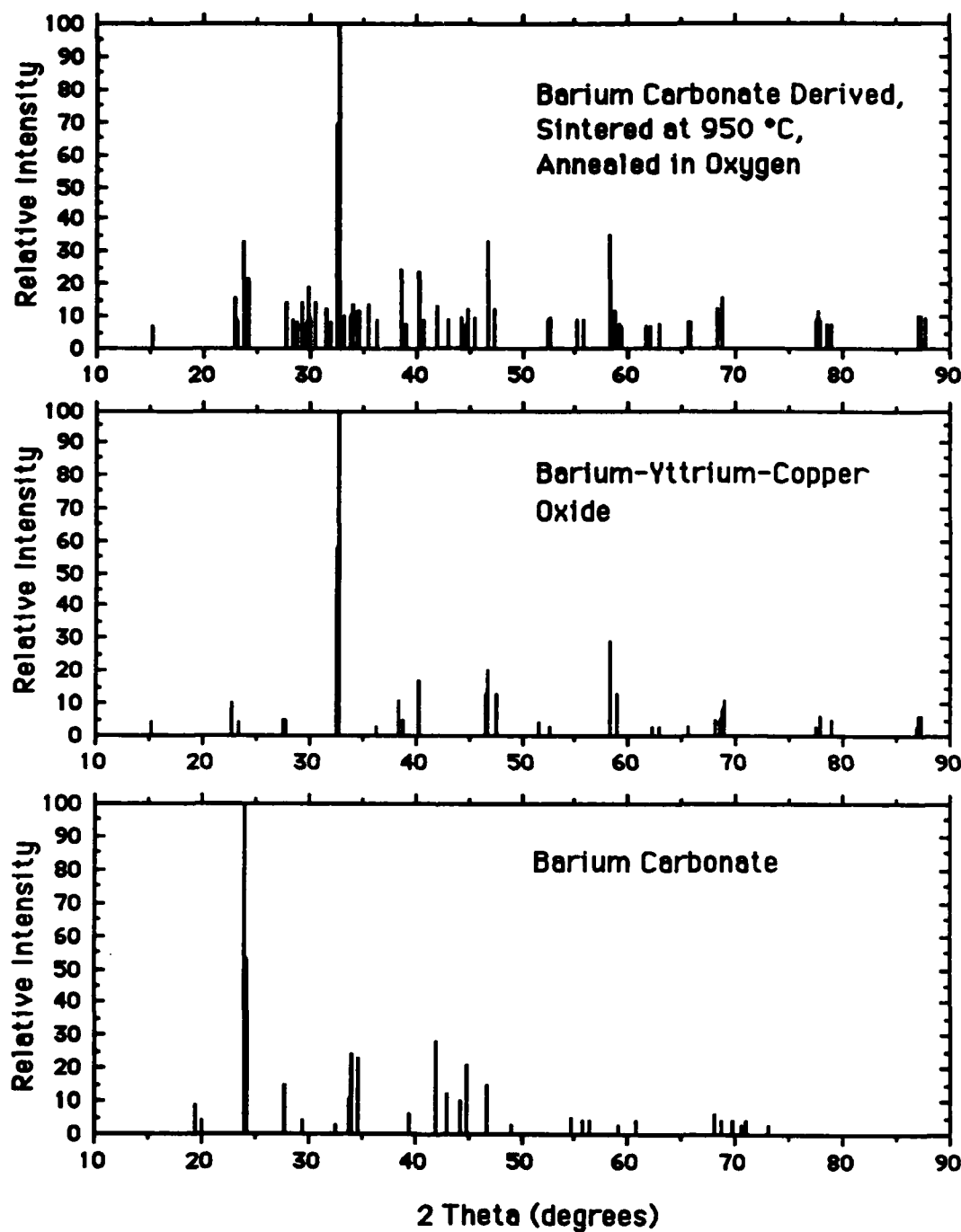


Figure 12. X-ray Diffraction Pattern for Barium Carbonate Derived Sample, Sintered at 950 °C, Annealed in Oxygen

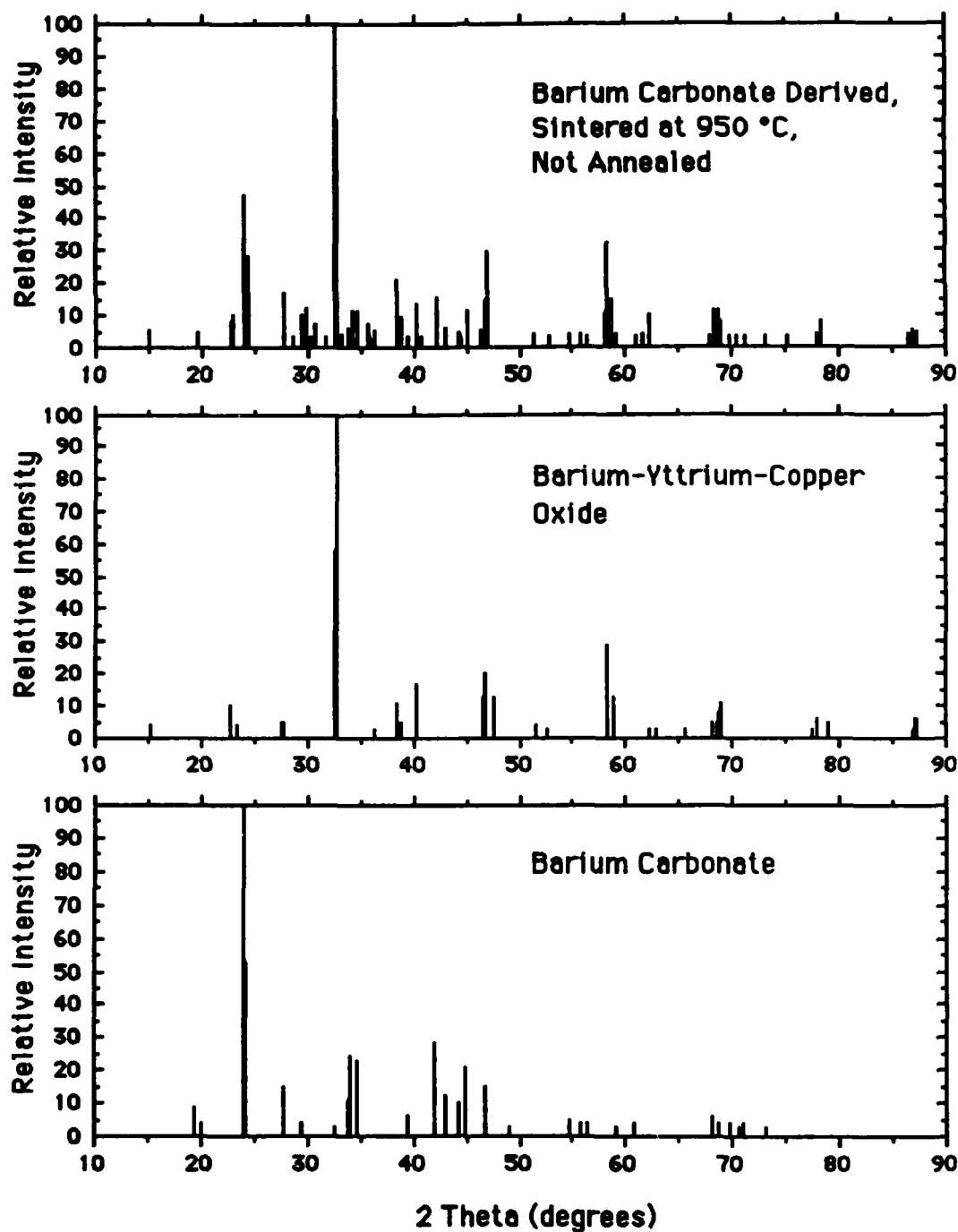


Figure 13. X-ray Diffraction Pattern for Barium Carbonate Derived Sample, Sintered at 950 °C, Not Annealed

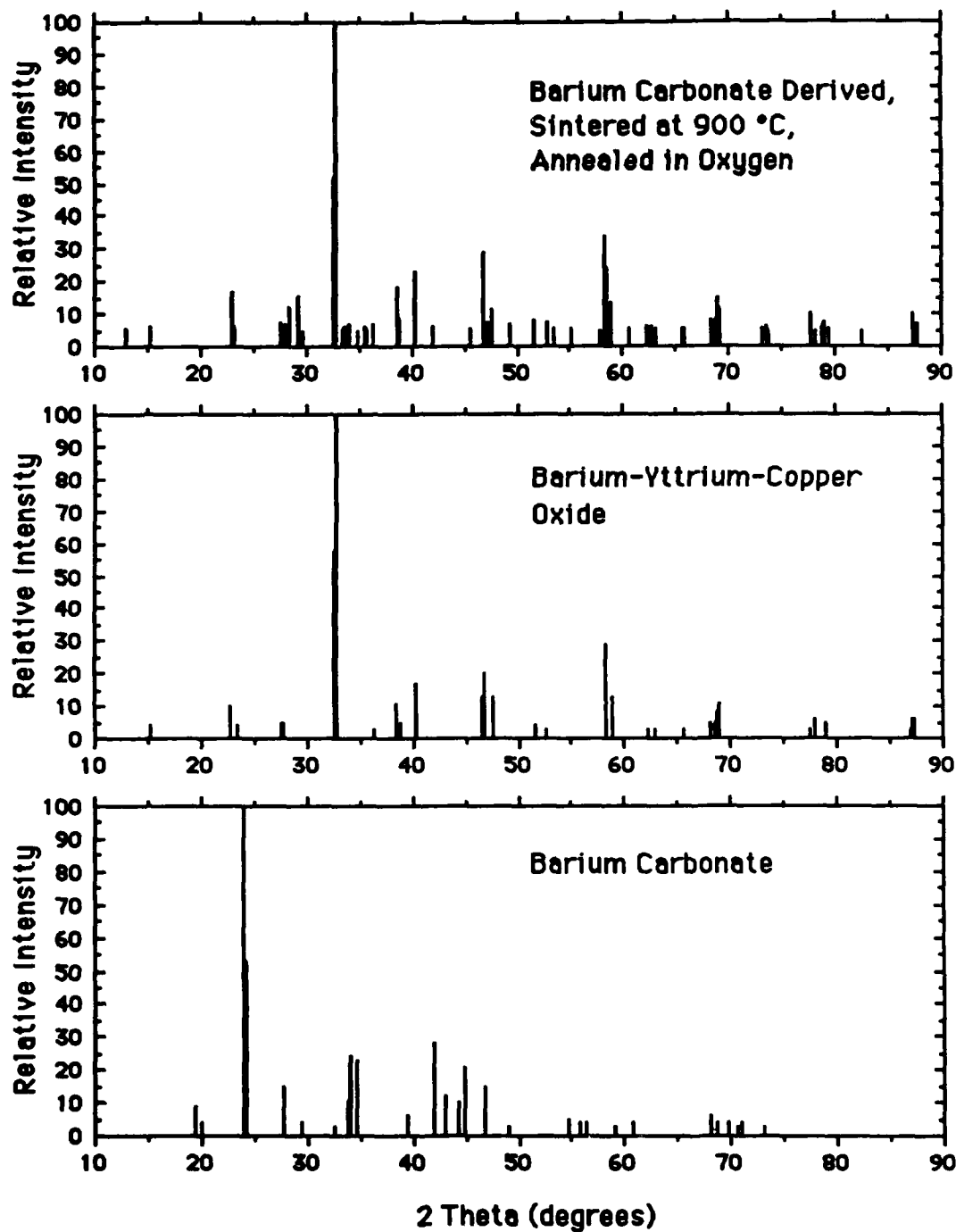


Figure 14. X-ray Diffraction Pattern for Barium Carbonate Derived Sample, Sintered at 900 °C, Annealed in Oxygen

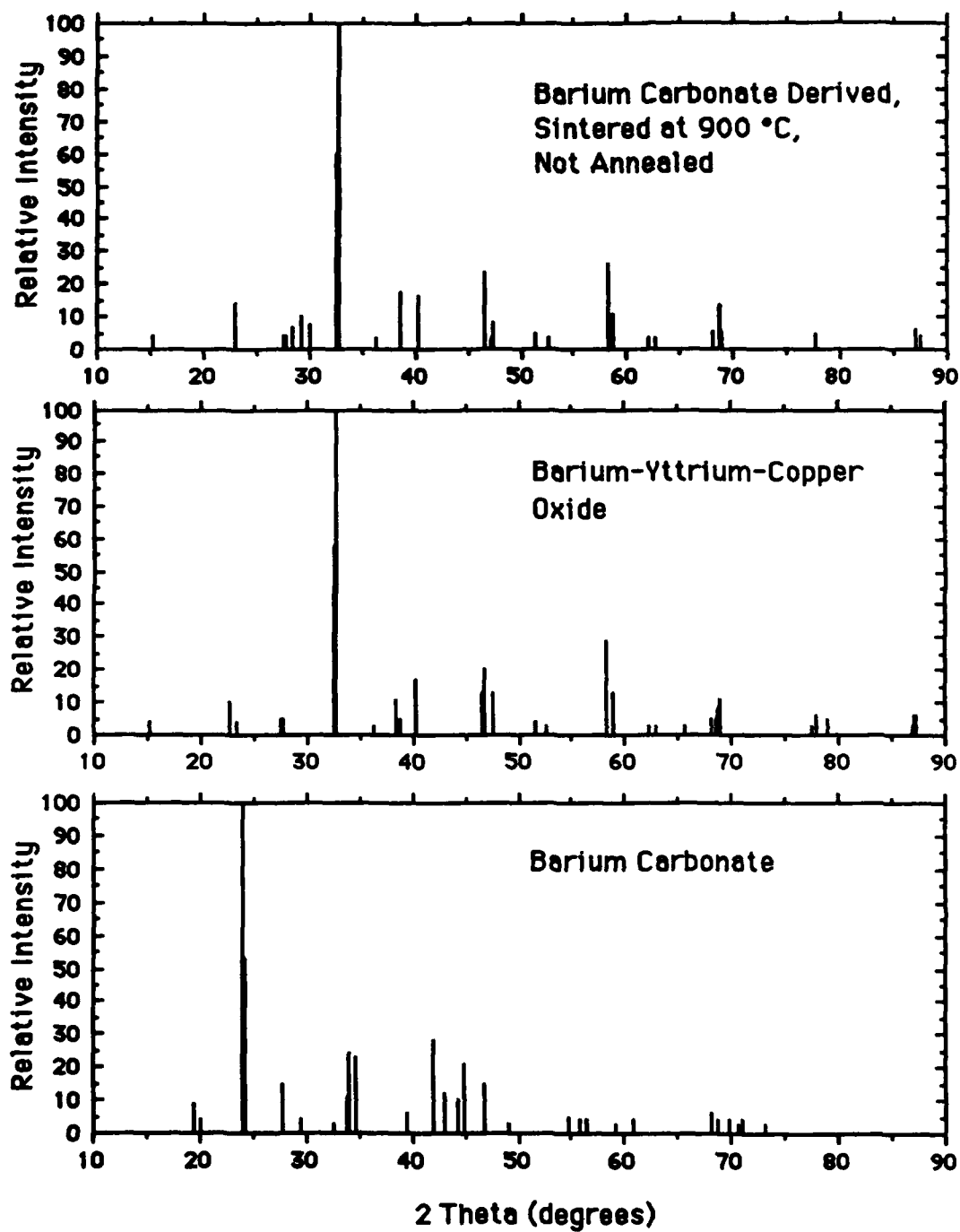


Figure 15. X-ray Diffraction Pattern for Barium Carbonate Derived Sample, Sintered at 900 °C, Not Annealed

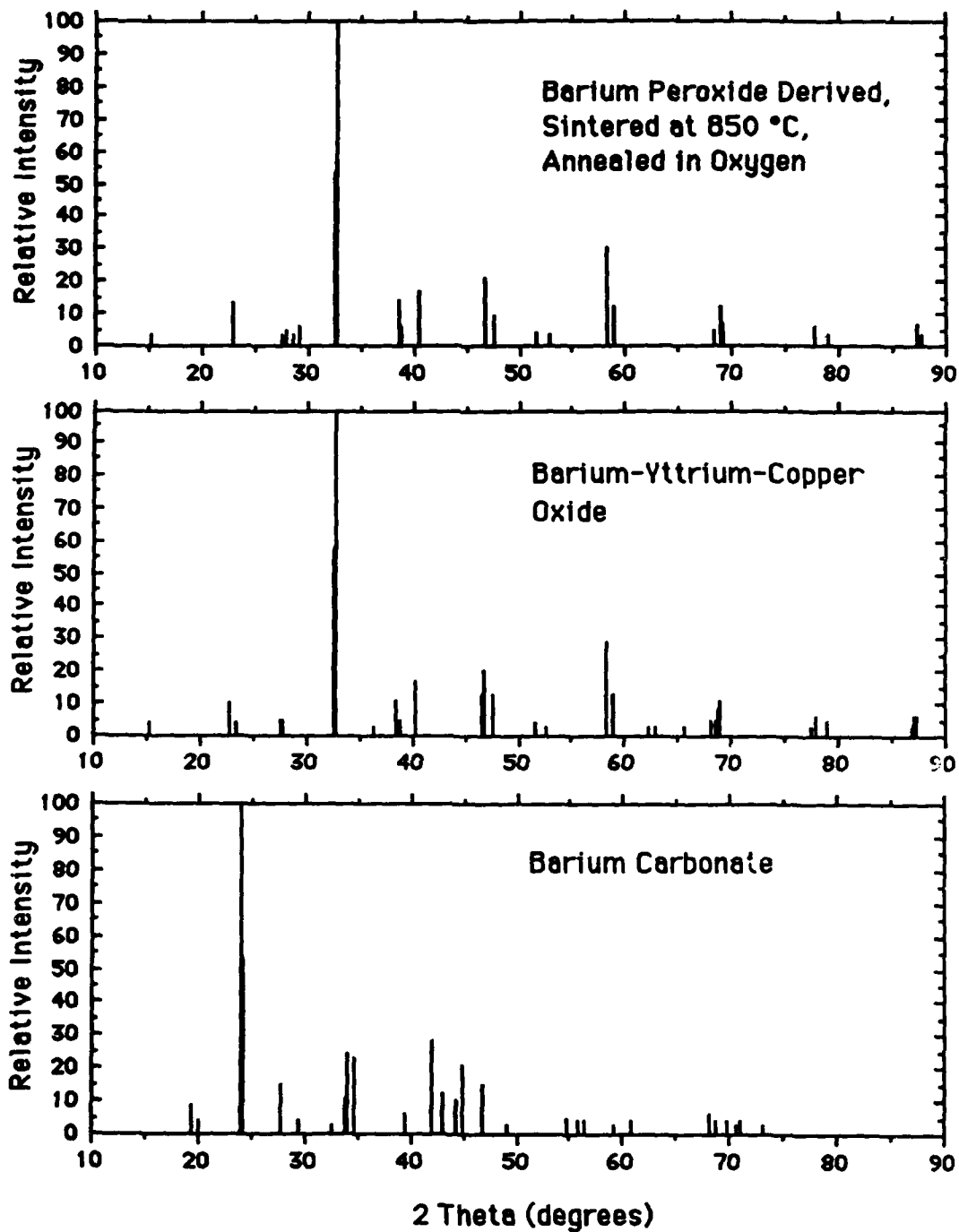


Figure 16. X-ray Diffraction Pattern for Barium Peroxide Derived Sample, Sintered at 850 °C, Annealed in Oxygen

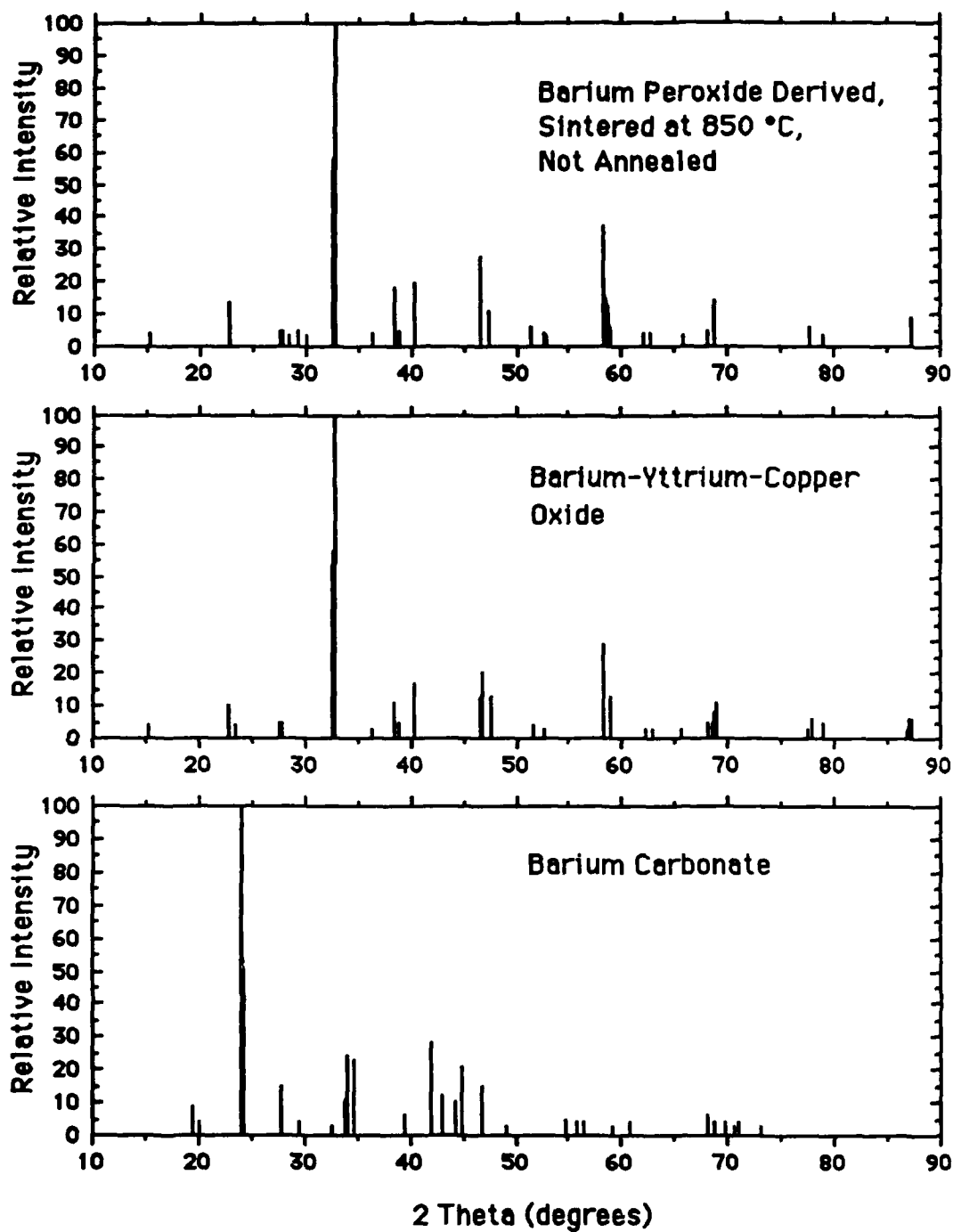


Figure 17. X-ray Diffraction Pattern for Barium Peroxide Derived Sample, Sintered at 850 °C, Not Annealed

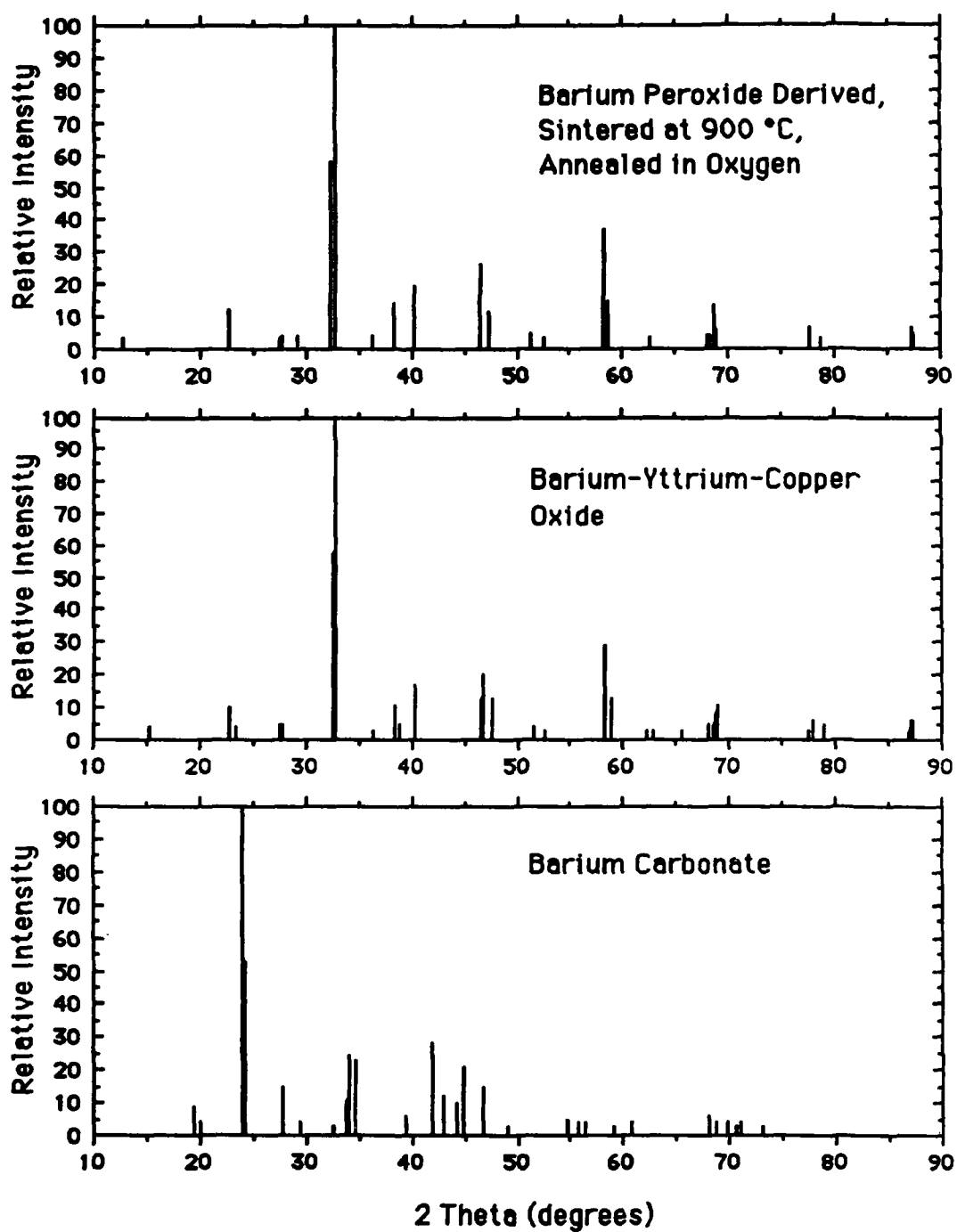


Figure 18. X-ray Diffraction Pattern for Barium Peroxide Derived Sample, Sintered at 900 °C, Annealed in Oxygen



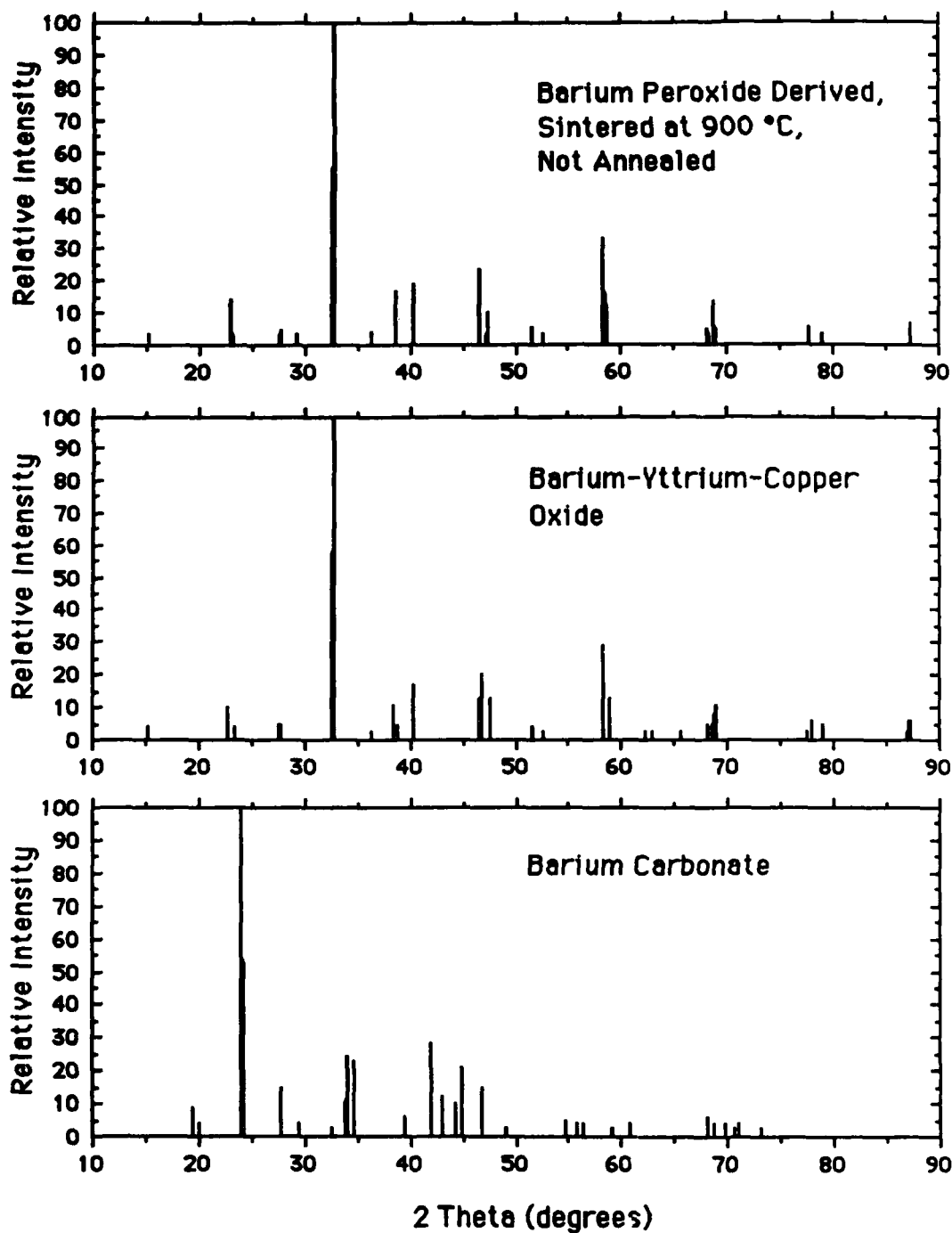


Figure 19. X-ray Diffraction Pattern for Barium Peroxide Derived Sample, Sintered at 900 °C, Not Annealed

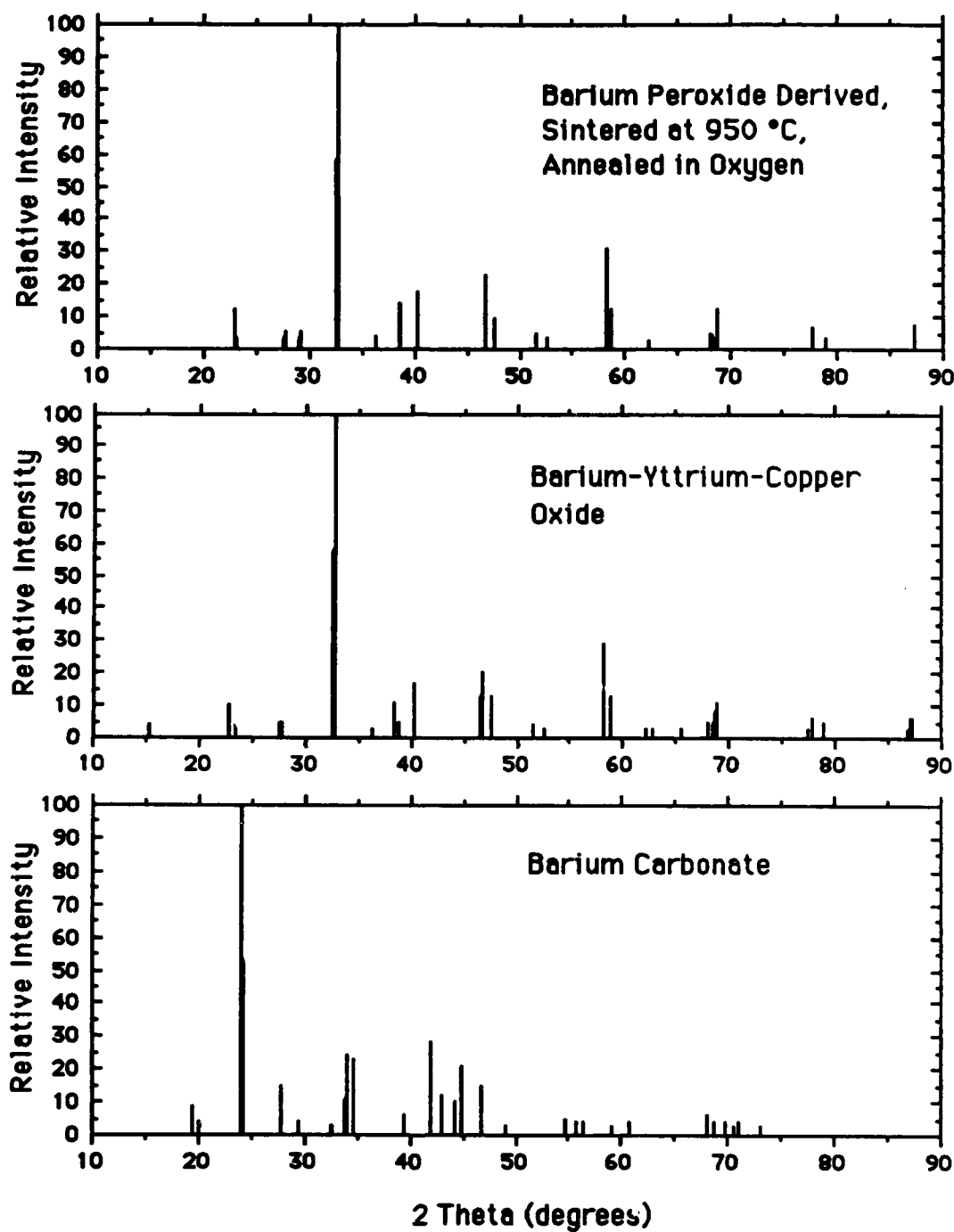


Figure 20. X-ray Diffraction Pattern for Barium Peroxide Derived Sample, Sintered at 950 °C, Annealed in Oxygen

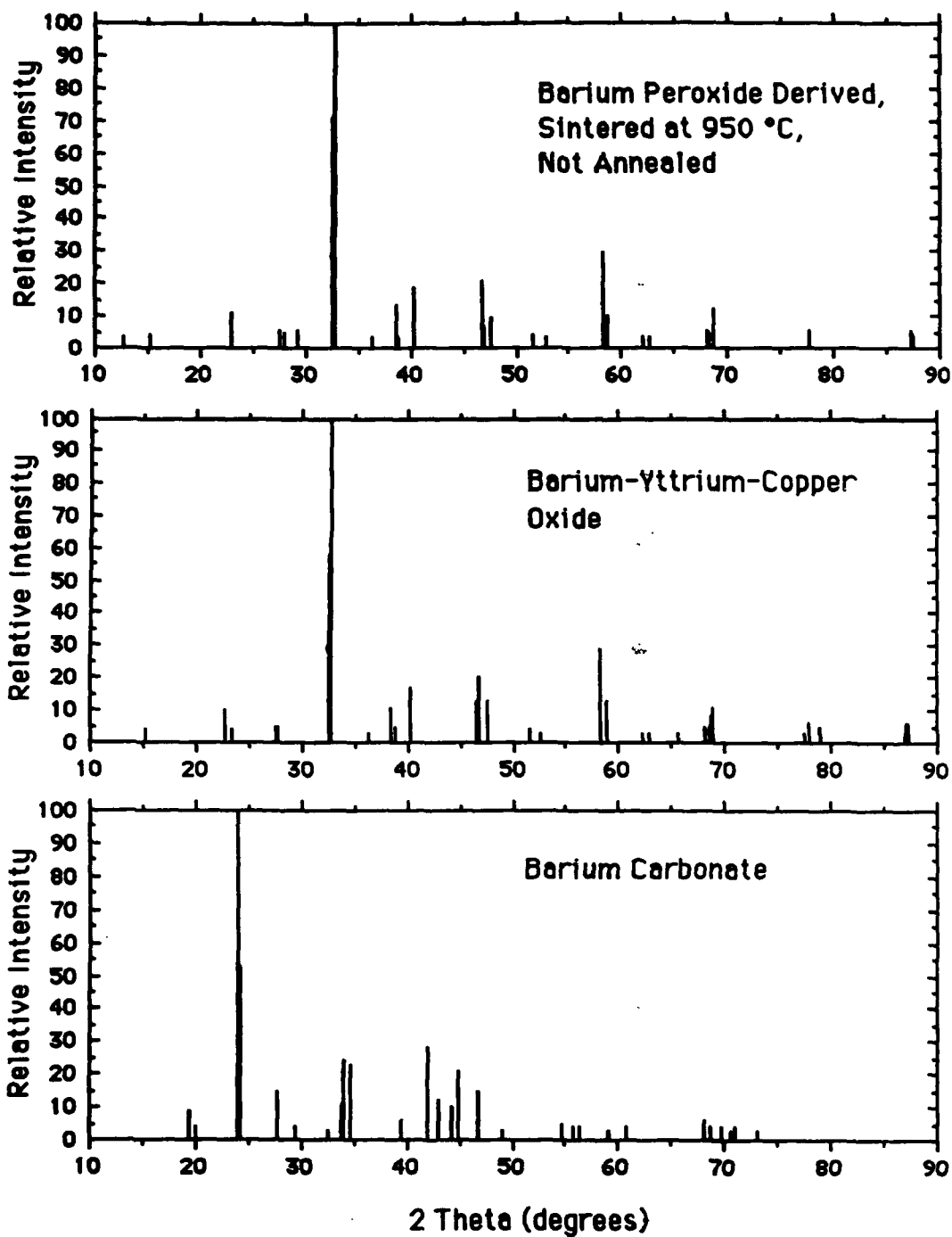


Figure 21. X-ray Diffraction Pattern for Barium Peroxide Derived Sample, Sintered at 950 °C, Not Annealed

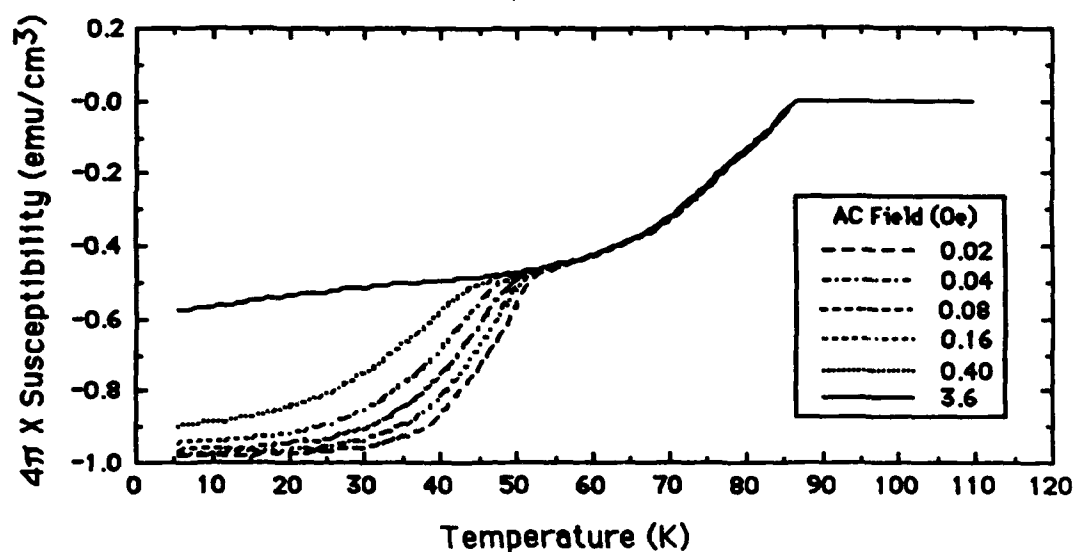


Figure 22. Magnetic Susceptibility versus Temperature for the Barium Peroxide Derived Sample, Sintered at 850 °C, Annealed in Oxygen

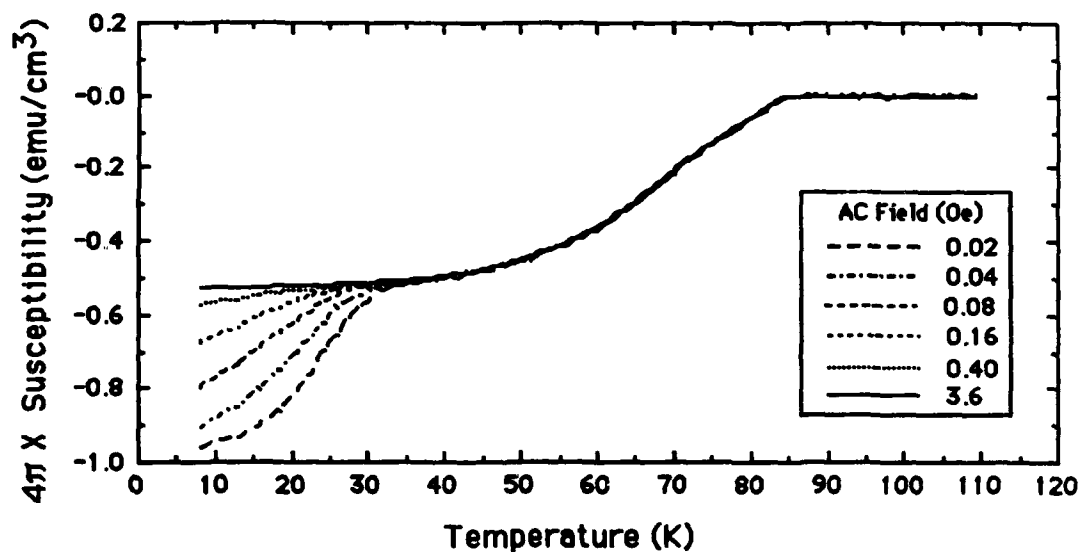


Figure 23. Magnetic Susceptibility versus Temperature for the Barium Peroxide Derived Sample, Sintered at 850 °C, Not Annealed

curves drop at the same rate until the temperature reaches about 55 K for the sample annealed in oxygen and about 35 K for the sample not annealed. At this point the AC field curve corresponding to the strongest field (3.6 Oe), follows the same path, while the AC field curve corresponding to the weakest field (0.02 Oe) drops suddenly. This is the point for this sample where the AC field curves begin splitting up. This point corresponds to the first occurrence of loss shown on the loss curves (Figures 24 and 25).

For the samples derived from barium carbonate which were sintered at 850 °C, the magnetic susceptibility curves show that the susceptibility never came close to  $-1/4\pi$  (emu/cm<sup>3</sup>) (Figures 26 and 27). The loss curves for these samples show no indication of a peak, which would indicate that the superconductive grains have not linked up (Figures 28 and 29). Thus, the samples did not reach bulk superconductivity, and no electrical measurements were made on these samples. Similarly, the sample derived from barium carbonate which was sintered at 950 °C and not annealed in oxygen did not reach  $-1/4\pi$  (emu/cm<sup>3</sup>) and thus did not show bulk superconductivity (Figure 30). The loss curves for this sample also showed no peaks (Figure 31).

The remaining samples had very similar curves. For these samples the magnetic susceptibility curves show a

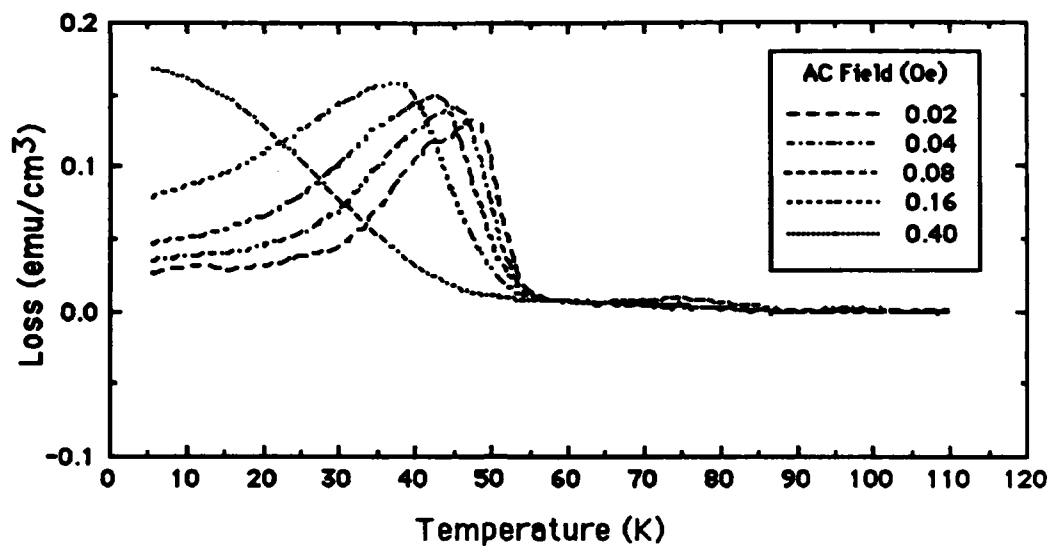


Figure 24. Magnetic Susceptibility Loss versus Temperature for the Barium Peroxide Derived Sample, Sintered at 850 °C, Annealed in Oxygen

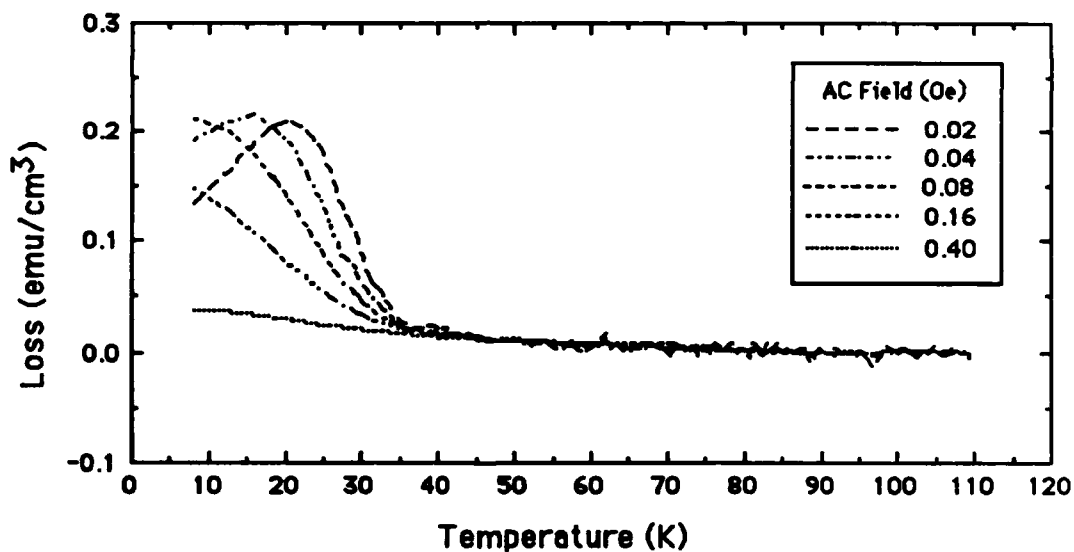


Figure 25. Magnetic Susceptibility Loss versus Temperature for the Barium Peroxide Derived Sample, Sintered at 850 °C, Not Annealed

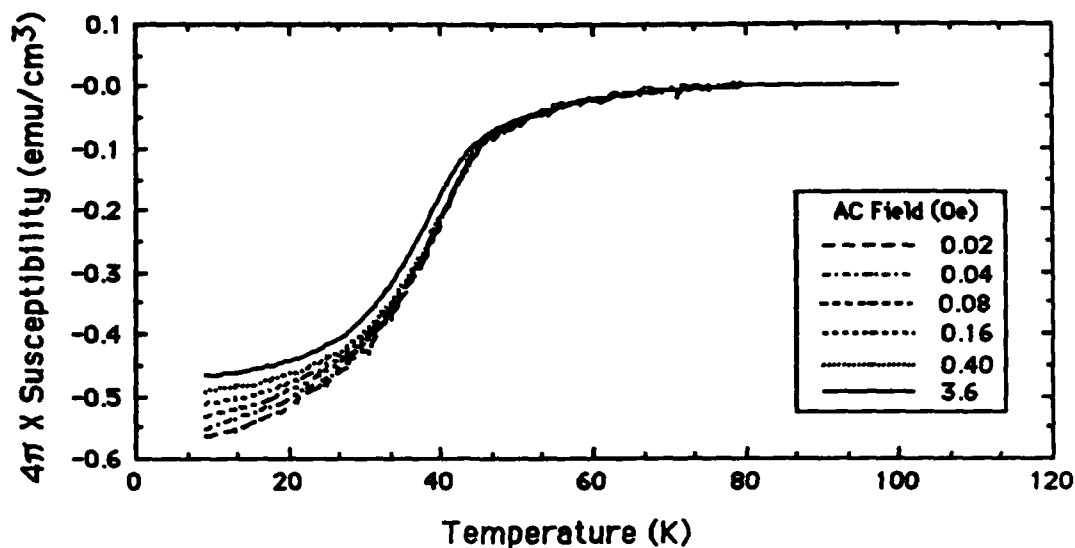


Figure 26. Magnetic Susceptibility versus Temperature for the Barium Carbonate Derived Sample, Sintered at 850 °C, Annealed in Oxygen

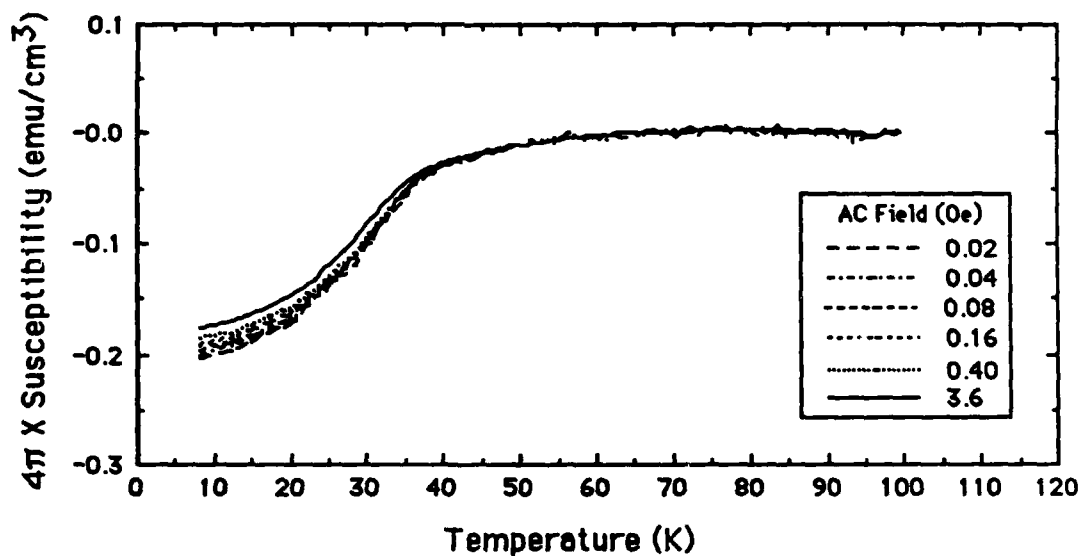


Figure 27. Magnetic Susceptibility versus Temperature for the Barium Carbonate Derived Sample, Sintered at 850 °C, Not Annealed

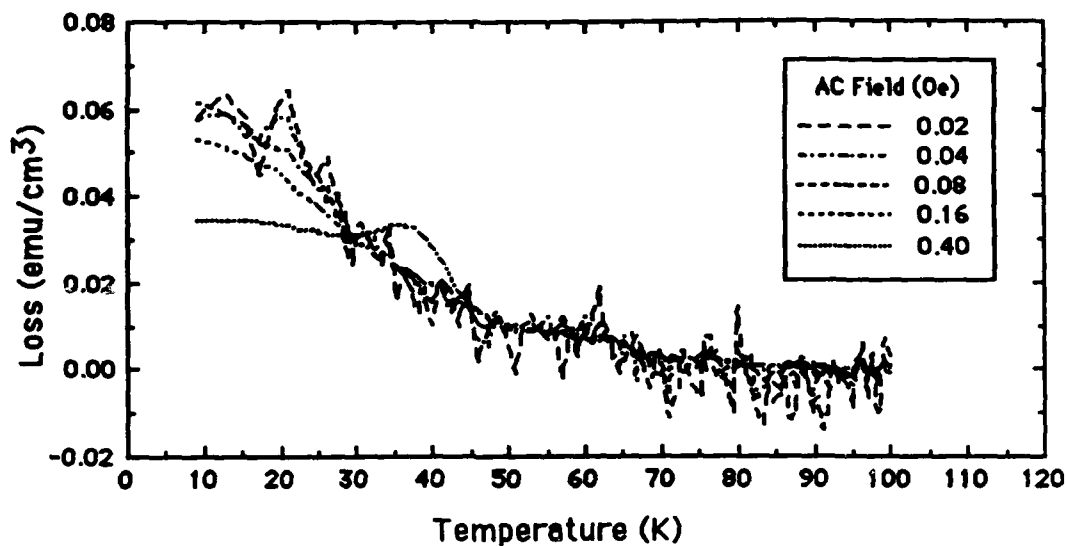


Figure 28. Magnetic Susceptibility Loss versus Temperature for the Barium Carbonate Derived Sample, Sintered at 850 °C, Annealed in Oxygen

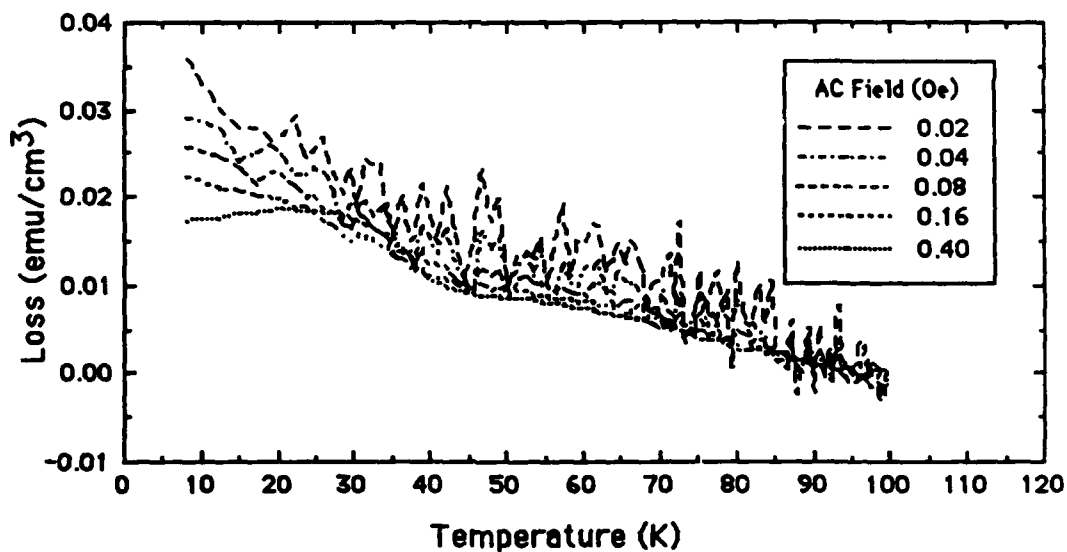


Figure 29. Magnetic Susceptibility Loss versus Temperature for the Barium Carbonate Derived Sample, Sintered at 850 °C, Not Annealed



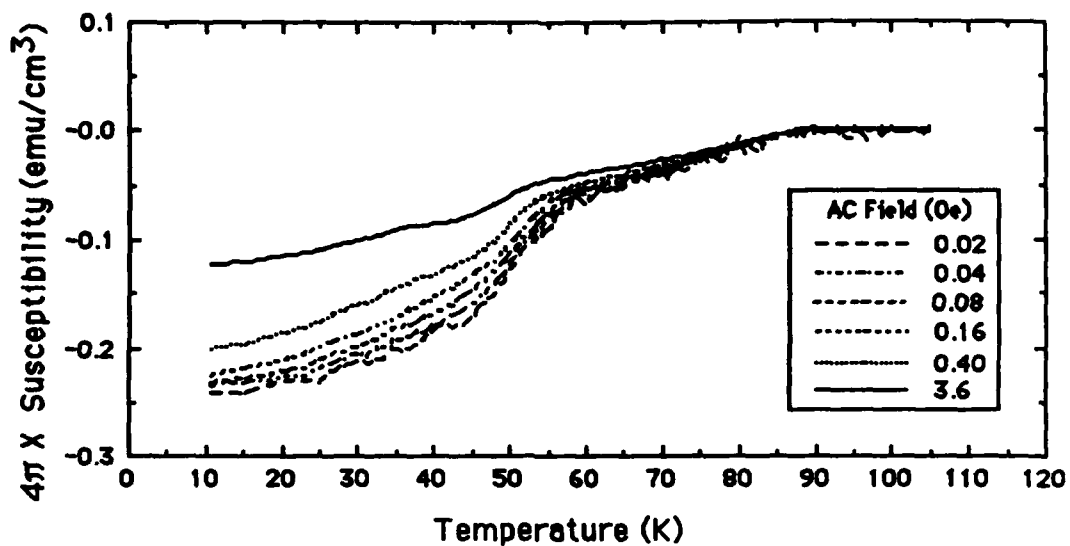


Figure 30. Magnetic Susceptibility versus Temperature for the Barium Carbonate Derived Sample, Sintered at 950 °C, Not Annealed

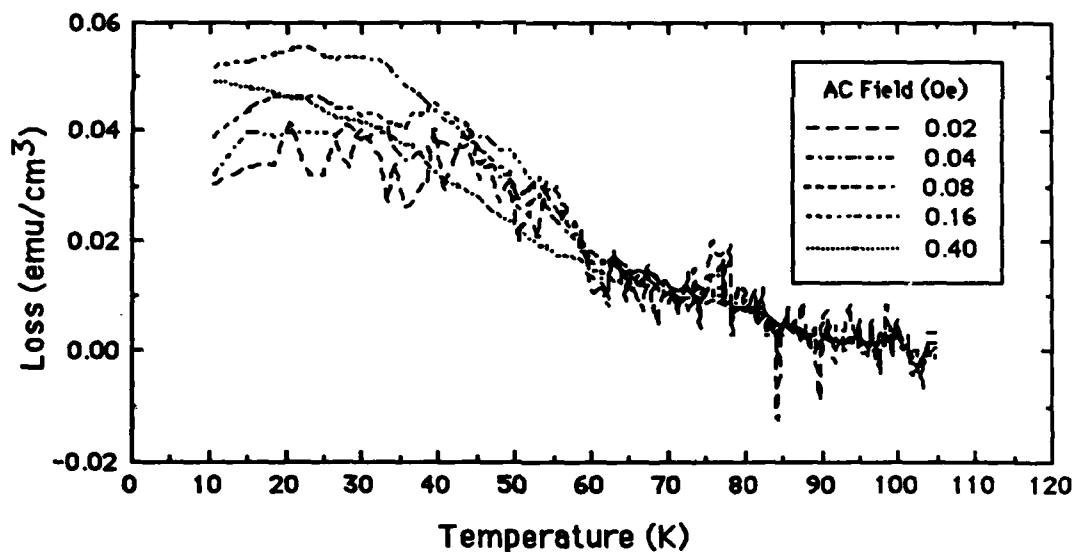


Figure 31. Magnetic Susceptibility Loss versus Temperature for the Barium Carbonate Derived Sample, Sintered at 950 °C, Not Annealed

sudden occurrence of magnetic susceptibility at about 88 K, where the AC field curves begin to split up. For the sample derived from barium carbonate, sintered at 950 °C, and annealed in oxygen, the magnetic susceptibility curve shows a much better trend than that of the unannealed sample as shown in Figure 32. The loss curves for this sample show a clearly defined peak (Figure 33).

For the samples derived from barium peroxide which were sintered at 900 °C, the magnetic susceptibility curves are similar for the annealed and the unannealed samples; however, the AC field curves are closer together for the unannealed (Figure 34) than for the annealed (Figure 35). The loss curves for the unannealed sample (Figure 36) has a sharper peak than that of the annealed sample (Figure 37), which is especially evident for the strongest field curve.

For the samples derived from barium peroxide which were sintered at 950 °C, the magnetic susceptibility curves are similar for the annealed and the unannealed samples; however, the AC field curves are closer together for the annealed (Figure 38) than for the unannealed (Figure 39). The loss curves for the annealed sample (Figure 40) has a sharper peak than that of the unannealed sample (Figure 41), which is especially evident for the strongest field curve.

The magnetic susceptibility curves for the samples derived from barium carbonate which were sintered at 900 °C showed the same trend as those for the samples derived from

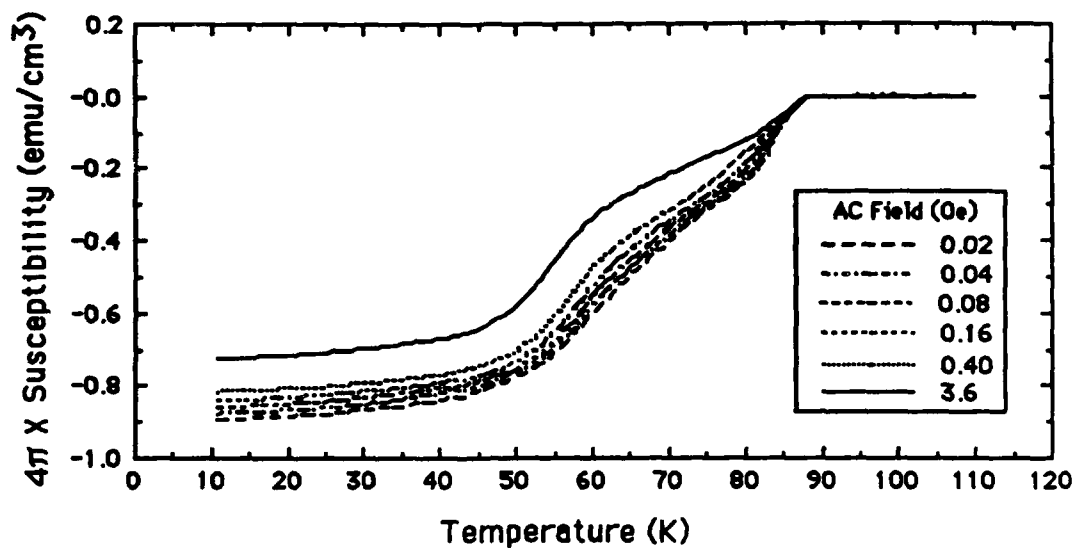


Figure 32. Magnetic Susceptibility versus Temperature for the Barium Carbonate Derived Sample, Sintered at 950 °C, Annealed in Oxygen

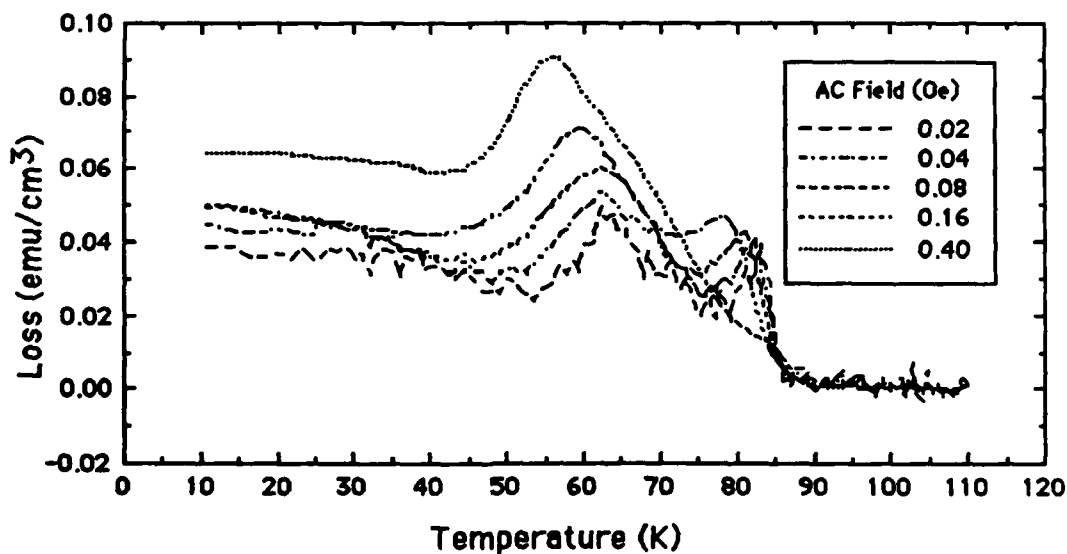


Figure 33. Magnetic Susceptibility Loss versus Temperature for the Barium Carbonate Derived Sample, Sintered at 950 °C, Annealed in Oxygen

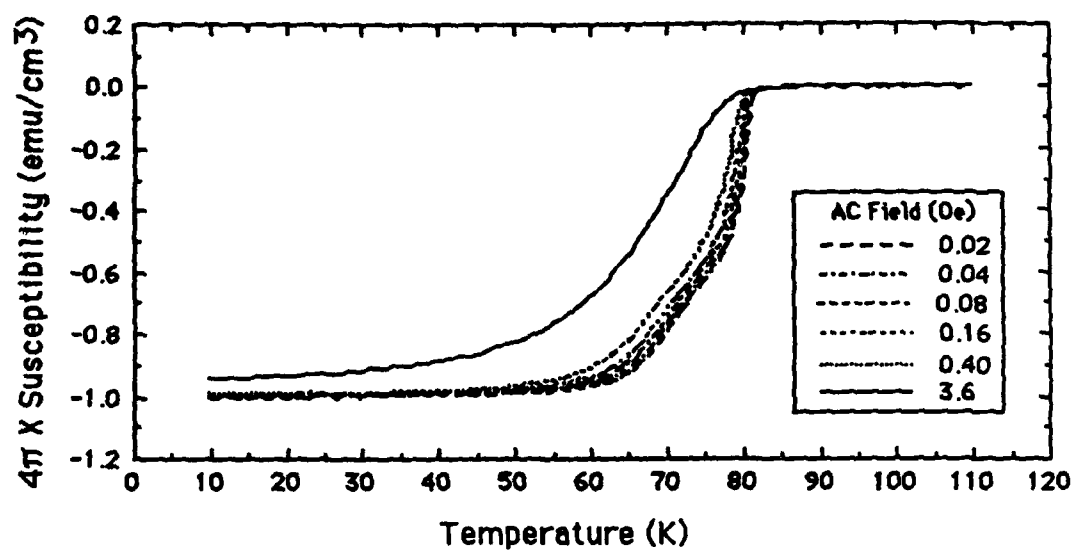


Figure 34. Magnetic Susceptibility versus Temperature for the Barium Peroxide Derived Sample, Sintered at 900 °C, Not Annealed

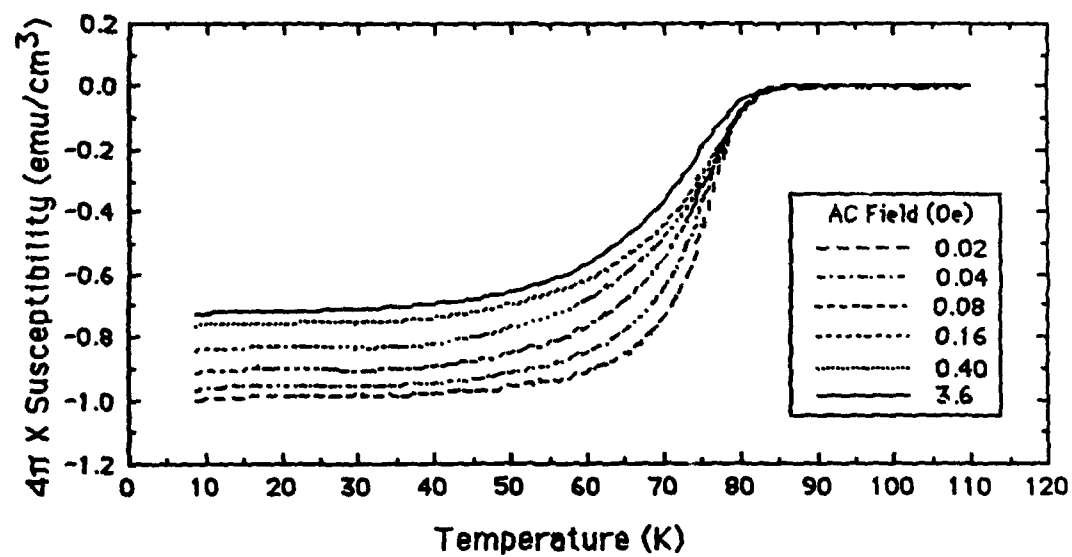


Figure 35. Magnetic Susceptibility versus Temperature for the Barium Peroxide Derived Sample, Sintered at 900 °C, Annealed in Oxygen

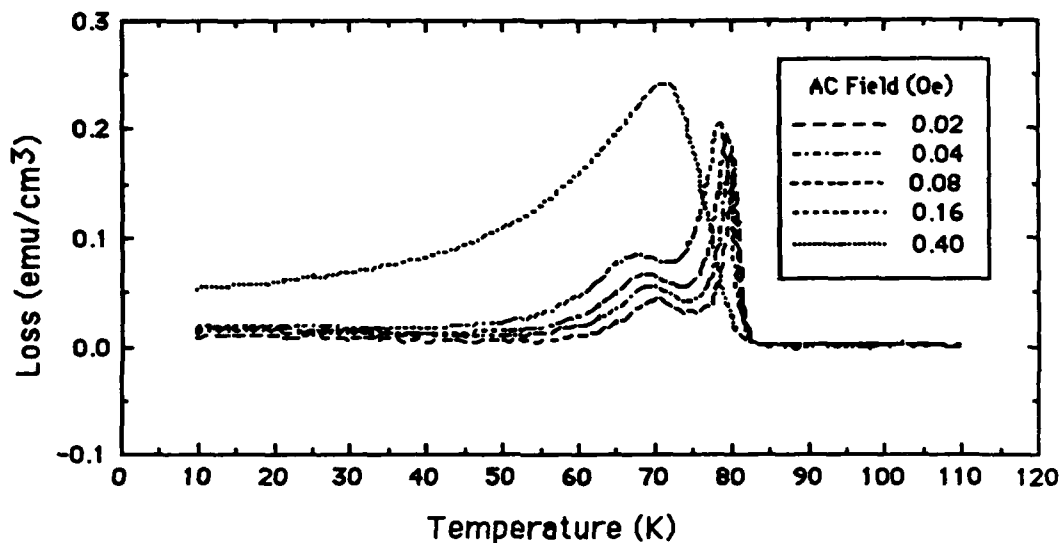


Figure 36. Magnetic Susceptibility Loss versus Temperature for the Barium Peroxide Derived Sample, Sintered at 900 °C, Not Annealed

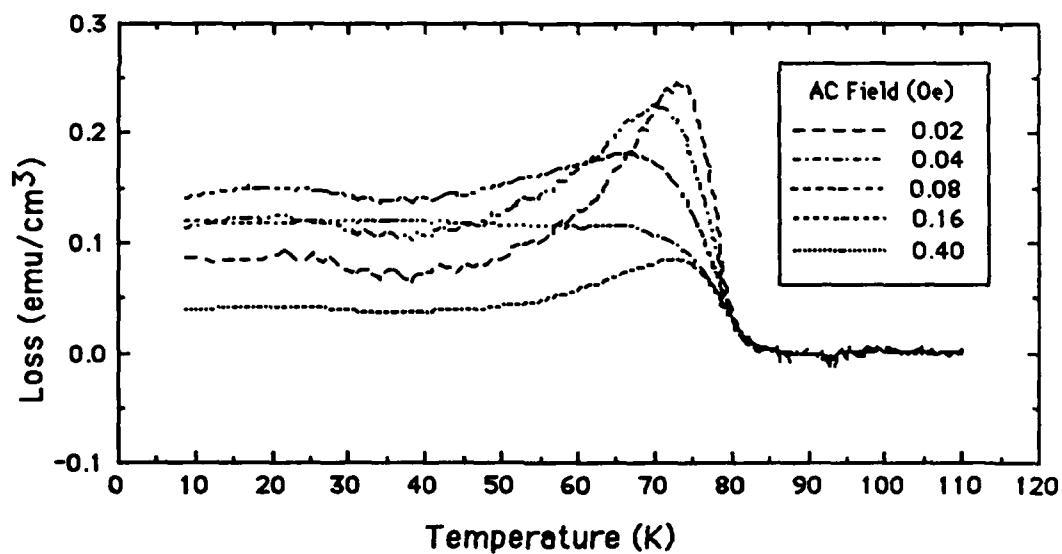


Figure 37. Magnetic Susceptibility Loss versus Temperature for the Barium Peroxide Derived Sample, Sintered at 900 °C, Annealed in Oxygen

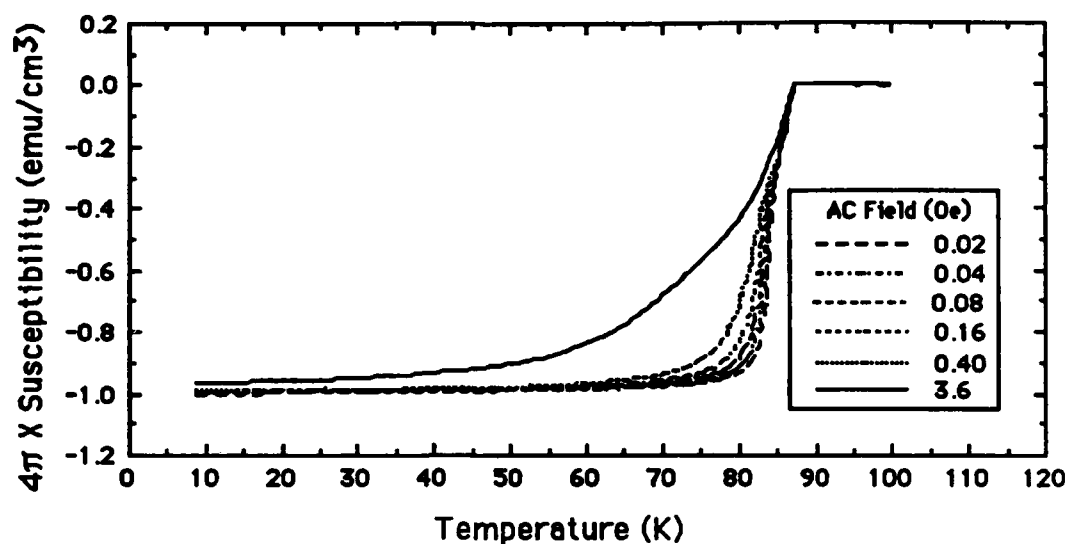


Figure 38. Magnetic Susceptibility versus Temperature for the Barium Peroxide Derived Sample, Sintered at 950 °C, Annealed in Oxygen

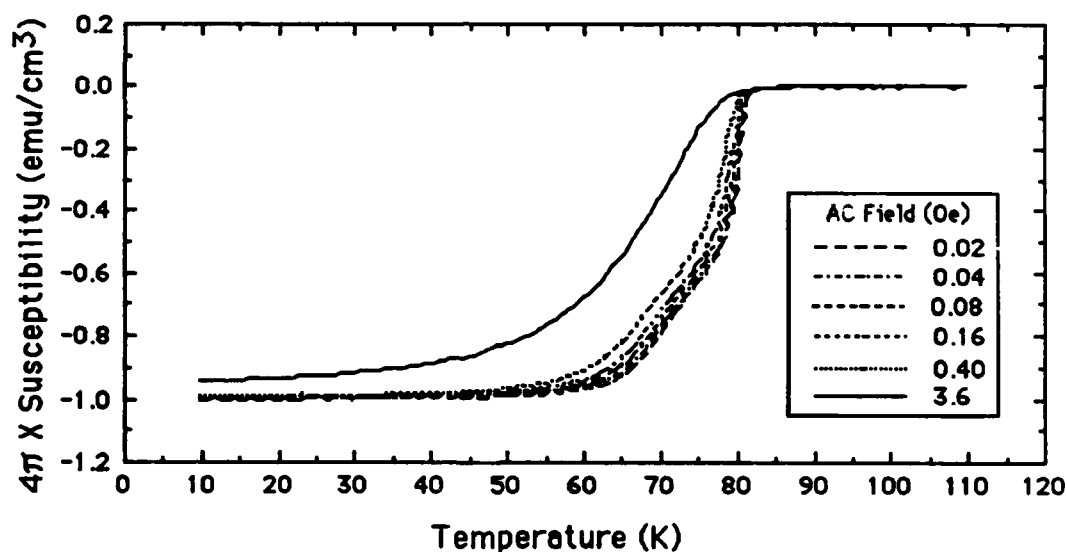


Figure 39. Magnetic Susceptibility versus Temperature for the Barium Peroxide Derived Sample, Sintered at 950 °C, Not Annealed

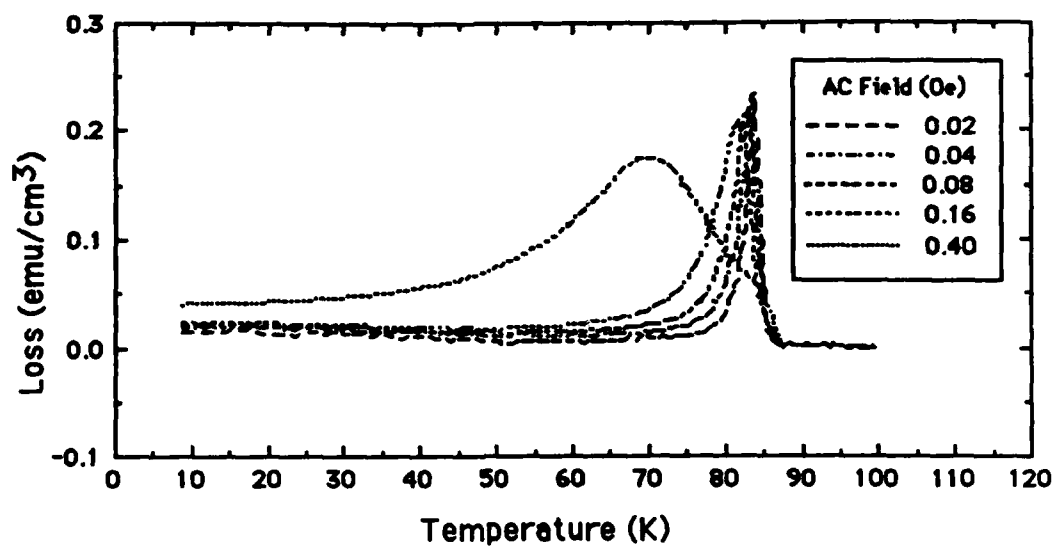


Figure 40. Magnetic Susceptibility Loss versus Temperature for the Barium Peroxide Derived Sample, Sintered at 950 °C, Annealed in Oxygen

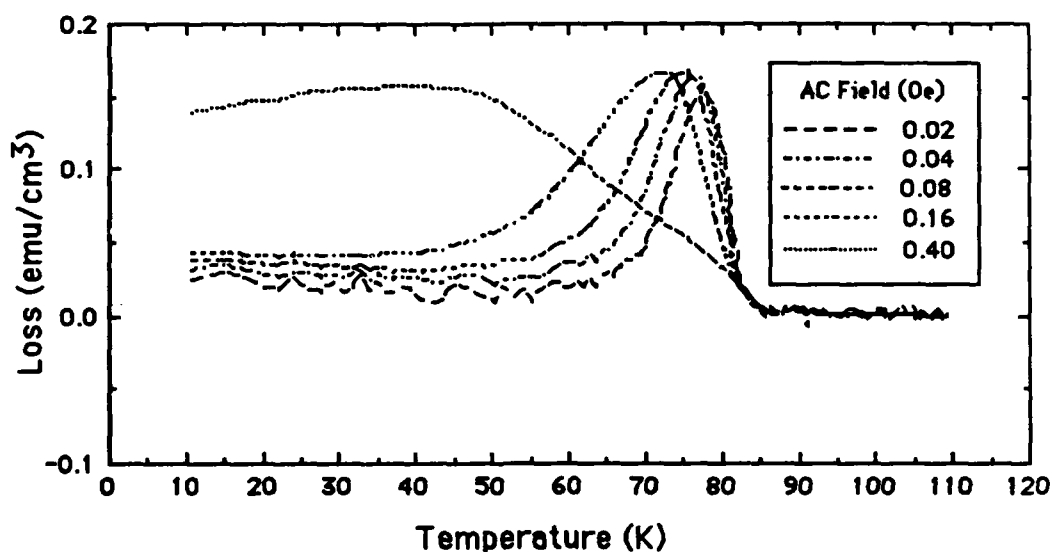


Figure 41. Magnetic Susceptibility Loss versus Temperature for the Barium Peroxide Derived Sample, Sintered at 950 °C, Not Annealed

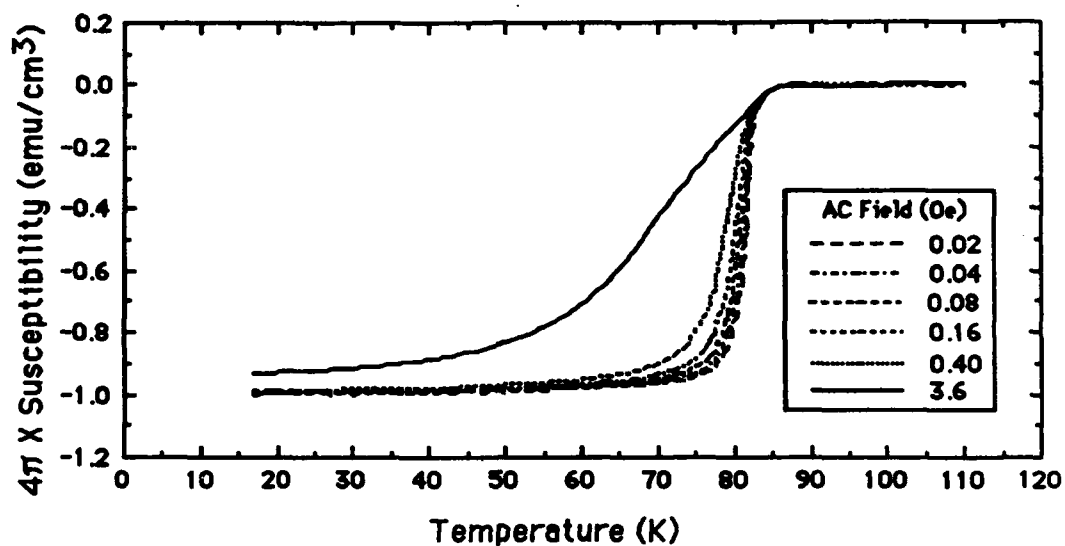


Figure 42. Magnetic Susceptibility versus Temperature for the Barium Carbonate Derived Sample, Sintered at 900 °C, Annealed in Oxygen

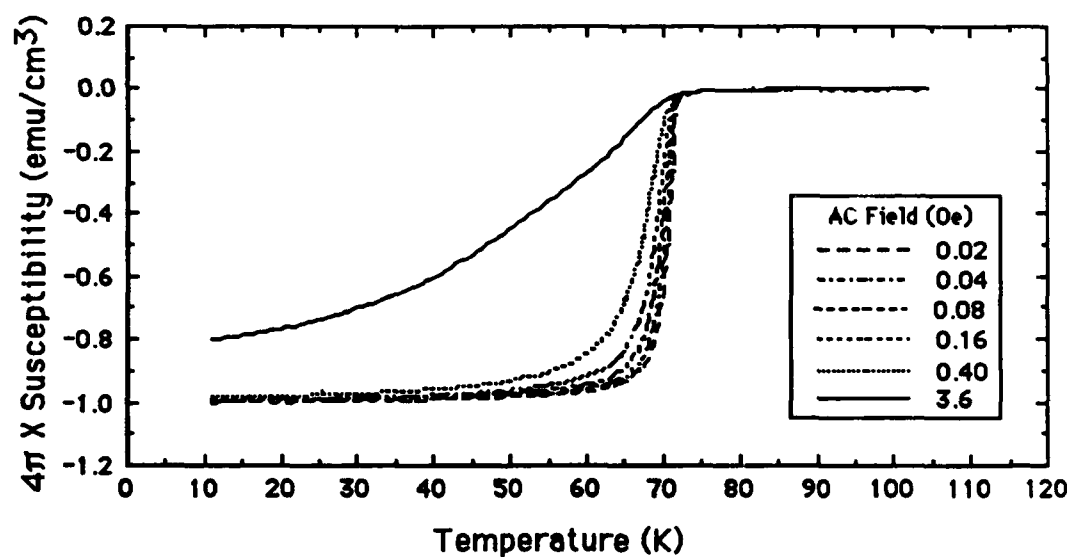


Figure 43. Magnetic Susceptibility versus Temperature for the Barium Carbonate Derived Sample, Sintered at 900 °C, Not Annealed



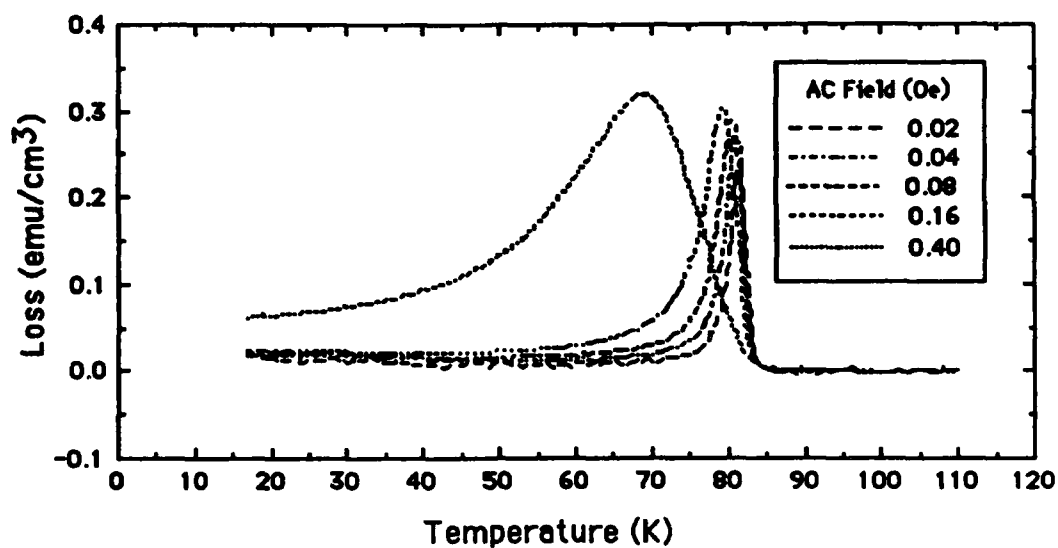


Figure 44. Magnetic Susceptibility Loss versus Temperature for the Barium Carbonate Derived Sample, Sintered at 900 °C, Annealed in Oxygen

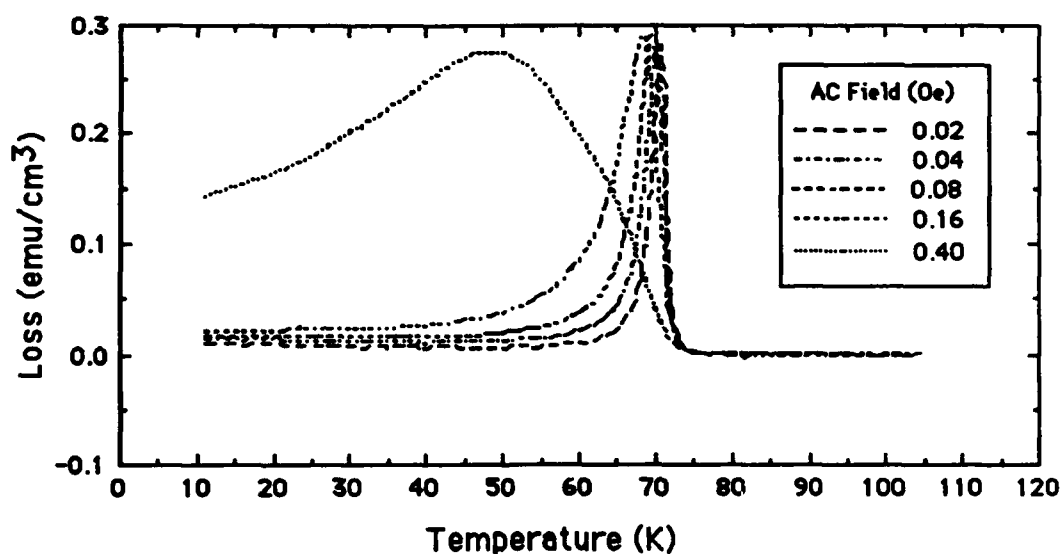


Figure 45. Magnetic Susceptibility Loss versus Temperature for the Barium Carbonate Derived Sample, Sintered at 900 °C, Not Annealed

( barium peroxide which were sintered at 950 °C (Figures 42-45) .

Resistivity Measurements. All of the samples measured showed a beginning of the transition to the superconductive state at about 88 K. Though not all of these samples reached zero resistivity, they all demonstrated a sudden drop in resistivity at about 88 K. The samples with the highest critical temperatures and the sharpest transitions into the superconductive state were those sintered at 900 °C. For these samples the oxygen annealing step had negligible effects on the critical temperatures or the transitions.

The samples derived from barium peroxide which were sintered at 850 °C increased in resistivity during cooling (Figures 46 and 47); however, they dropped suddenly in resistivity at about 88 K. The resistivity began to rise when the samples reached 70 K, and then began dropping again when the temperature reached 55 K, finally reaching zero resistivity at 30 K.

The samples derived from barium peroxide which were sintered at 900 °C had the lowest resistivity above the critical temperature of all the samples measured. These samples showed a decrease in resistivity as they were cooled (Figures 48 and 49). Also, these samples went sharply from normal resistivity to zero resistivity within a 10 K temperature drop.

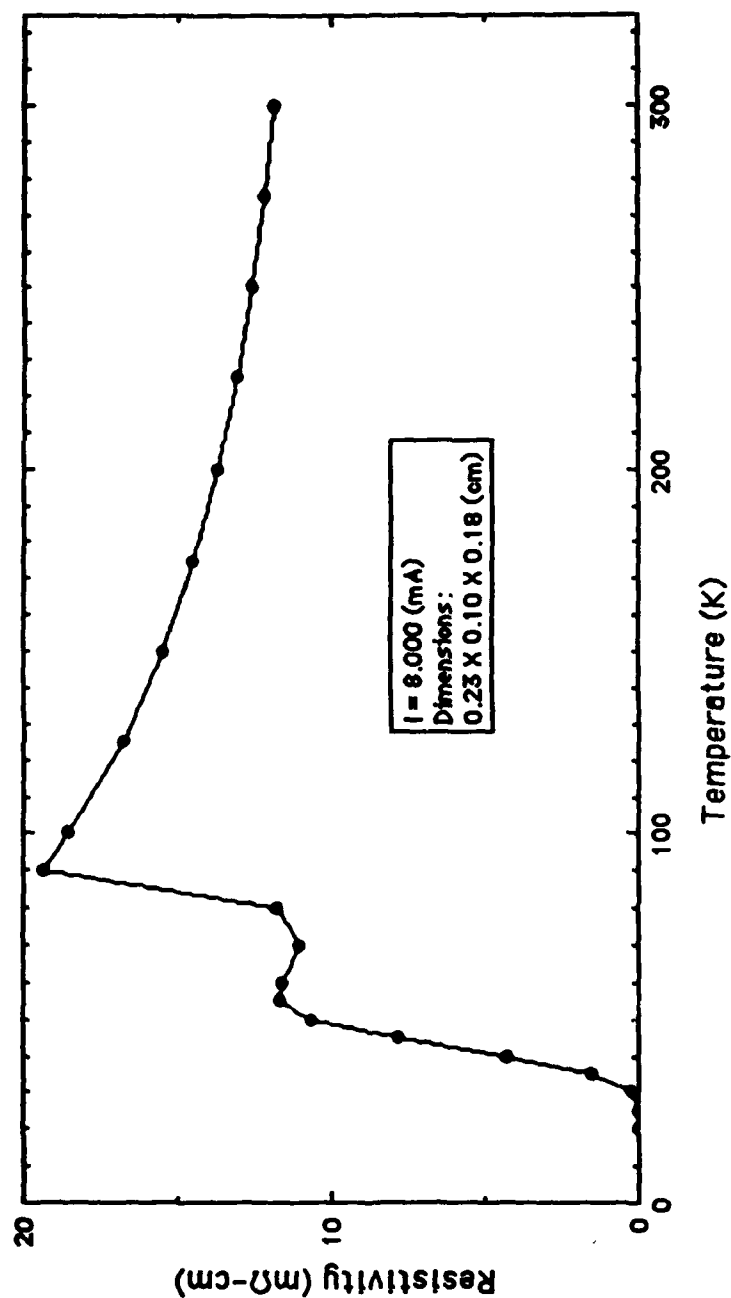


Figure 46. Resistivity versus Temperature for the Barium Peroxide Derived Sample, Sintered at 850 °C, Annealed in Oxygen

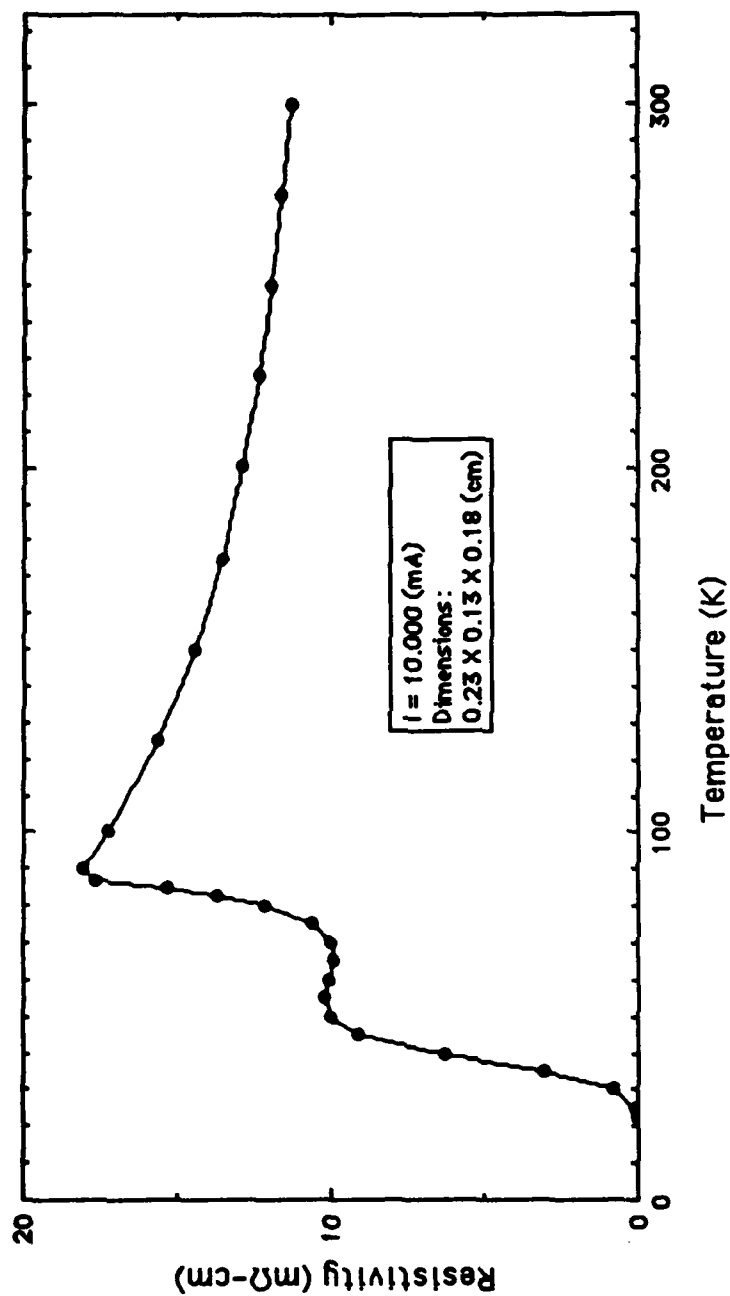


Figure 47. Resistivity versus Temperature for the Barium Peroxide Derived Sample, Sintered at 850 °C, Not Annealed

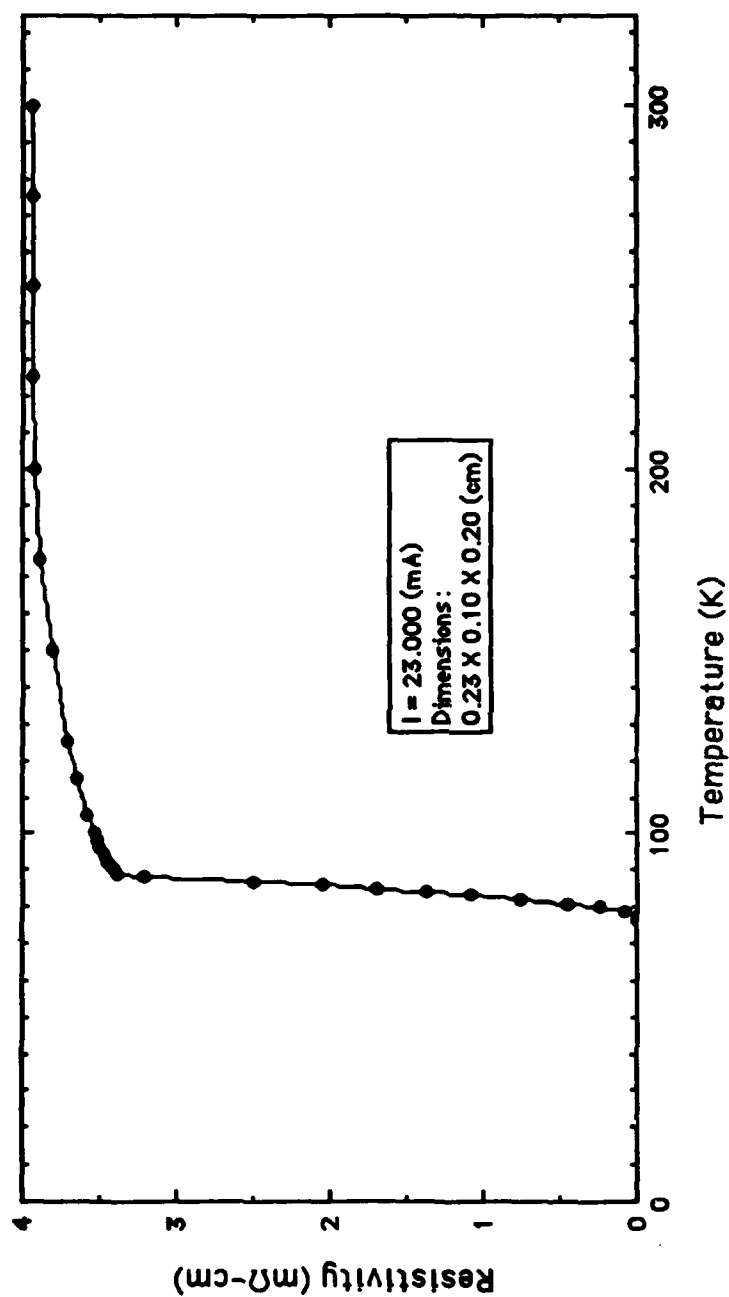


Figure 48. Resistivity versus Temperature for the Barium Peroxide Derived Sample, Sintered at 900 °C, Annealed in Oxygen

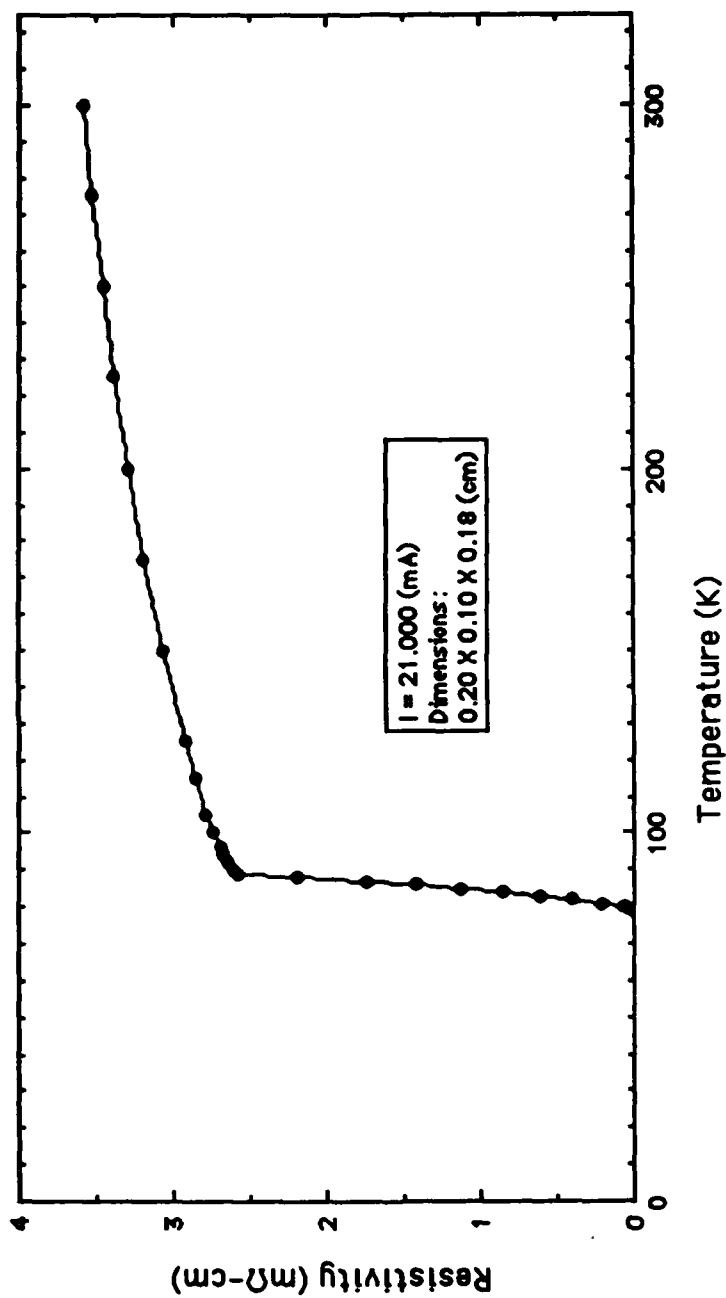


Figure 49. Resistivity versus Temperature for the Barium Peroxide Derived Sample, Sintered at 900 °C, Not Annealed

( The samples derived from barium peroxide which were sintered at 950 °C were characterized by resistivity that dropped suddenly at 88 K, but they retained a small resistivity until the temperature reached 30 K. The resistivity of these samples in the normal state was much higher than that of the barium peroxide derived samples which were sintered at 900 °C (Figures 50 and 51).

Of all the samples measured, the ones derived from barium carbonate which were sintered at 900 °C had the most linear decrease in resistivity as the temperature was reduced (Figures 52 and 53). These samples also had the sharpest transition from the normal state to the superconducting state. This transition was completed within a 9 K temperature drop.

The samples derived from barium carbonate which were sintered at 950 °C show the greatest differences between the oxygen annealed and the unannealed samples. The resistivity of the unannealed sample rose as the temperature decreased until it reached 88 K, where it dropped suddenly; though, it never reached zero (Figure 54). The oxygen annealed sample showed a decrease in resistivity as the temperature was decreased with a sudden drop at 88 K. The sample retained a small amount of resistivity until the temperature reached 30 K where zero resistivity was achieved (Figure 55).

Critical Current Density Measurements. The results of the critical current density versus temperature experiment

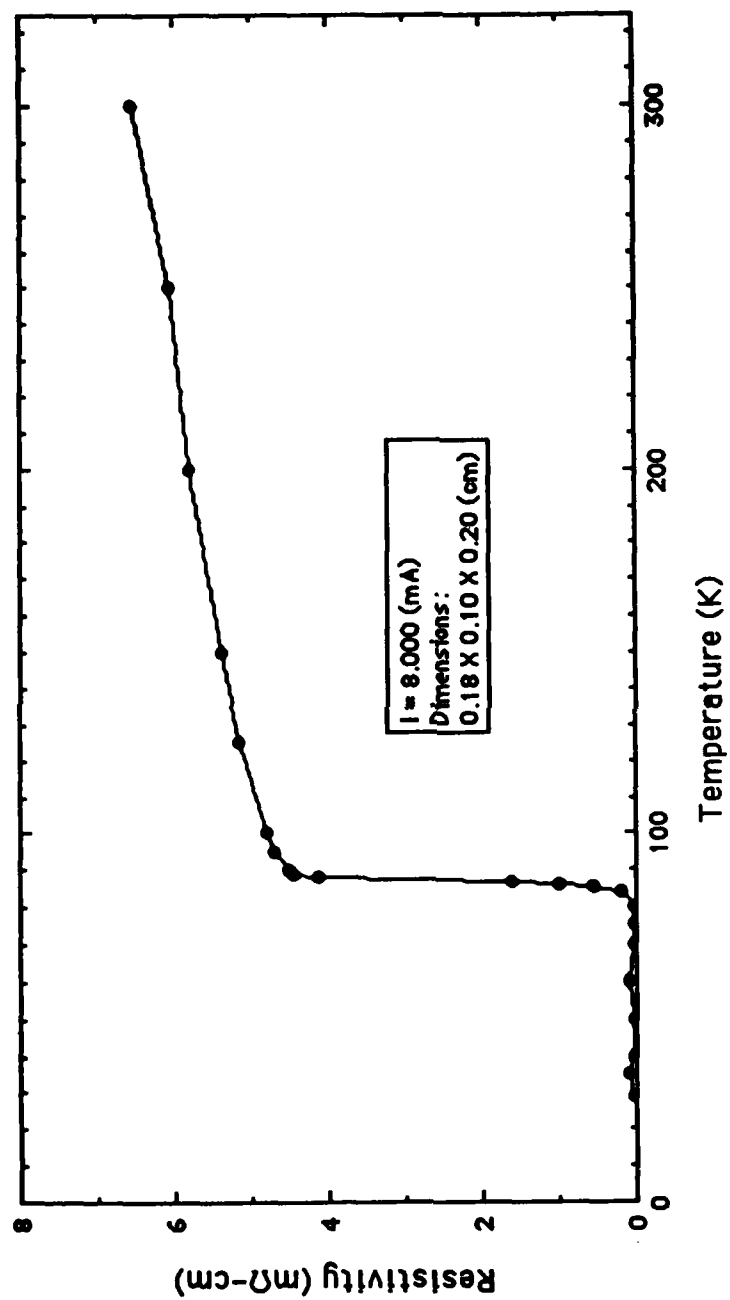


Figure 50. Resistivity versus Temperature for the Barium Peroxide Derived Sample, Sintered at 950 °C, Annealed in Oxygen



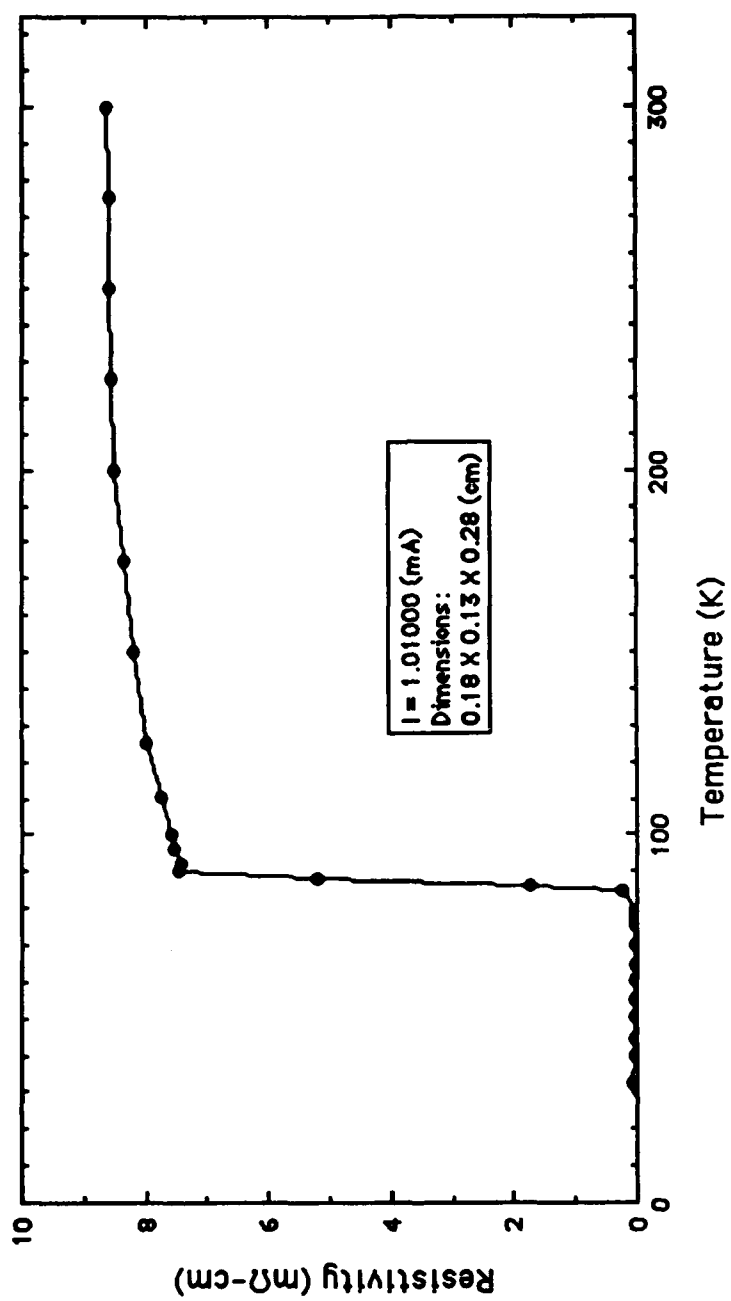


Figure 51. Resistivity versus Temperature for the Barium Peroxide Derived Sample, Sintered at 950 °C, Not Annealed

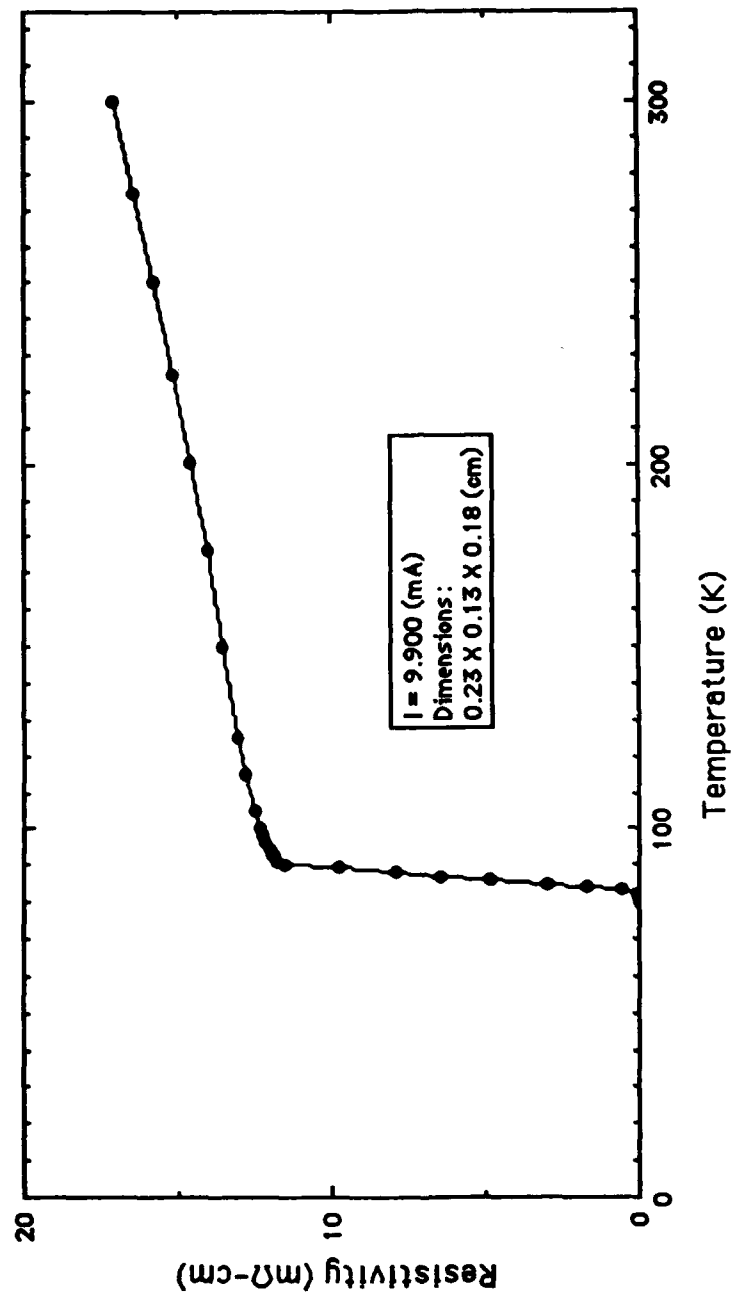


Figure 52. Resistivity versus Temperature for the Barium Carbonate Derived Sample, Sintered at 900 °C, Annealed in Oxygen

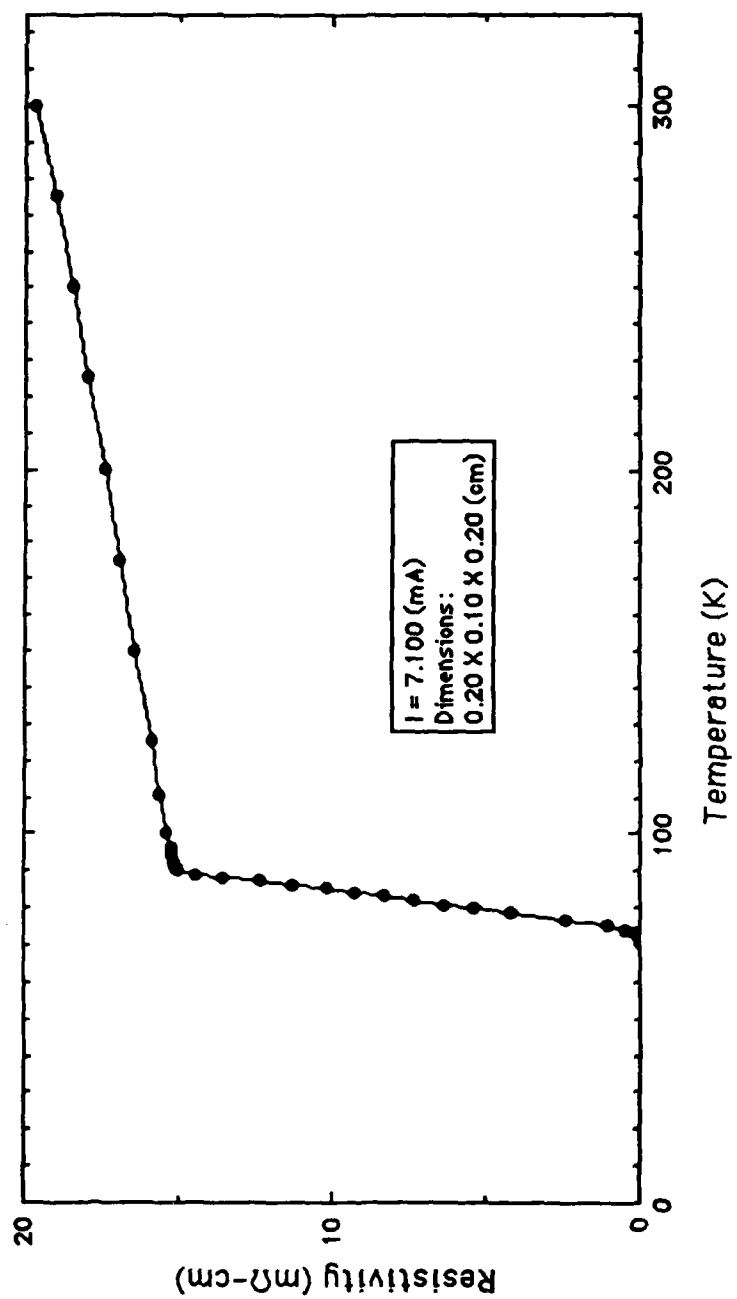


Figure 53. Resistivity versus Temperature for the Barium Carbonate Derived Sample, Sintered at 900 °C, Not Annealed

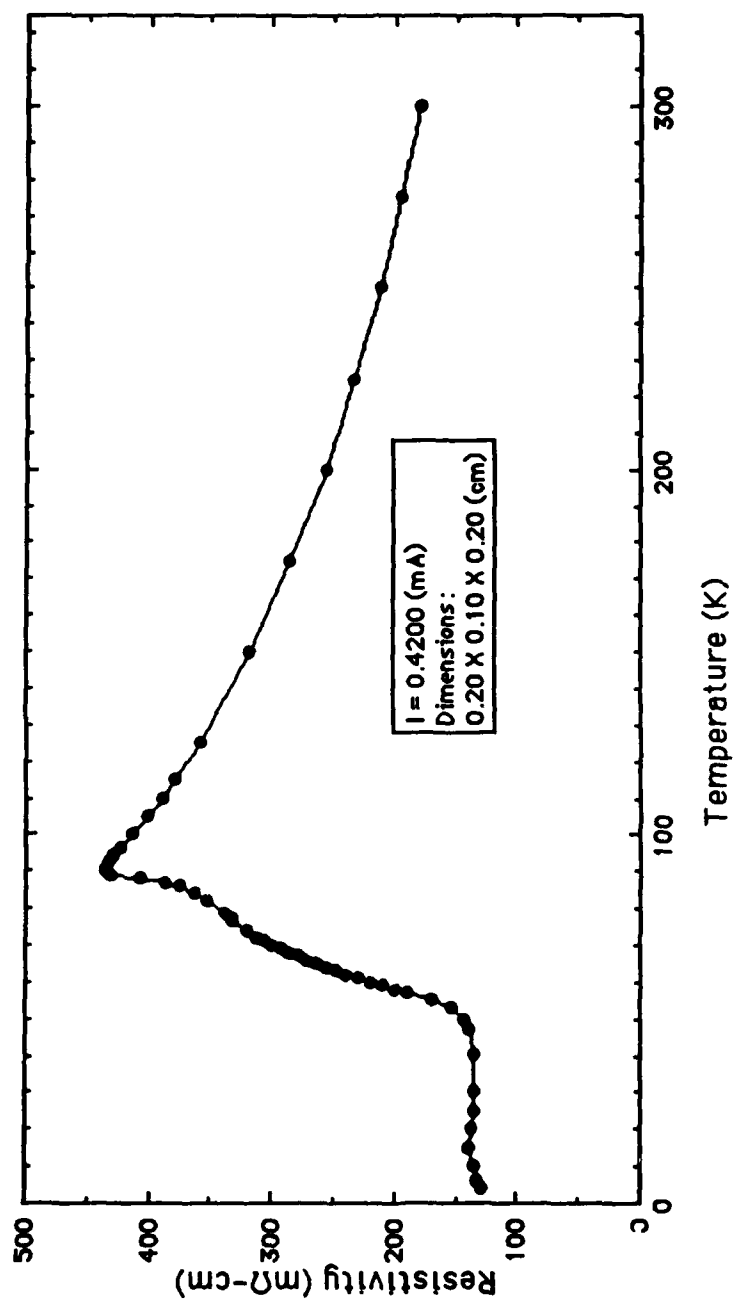


Figure 54. Resistivity versus Temperature for the Barium Carbonate Derived Sample, Sintered at 950 °C, Annealed in Oxygen

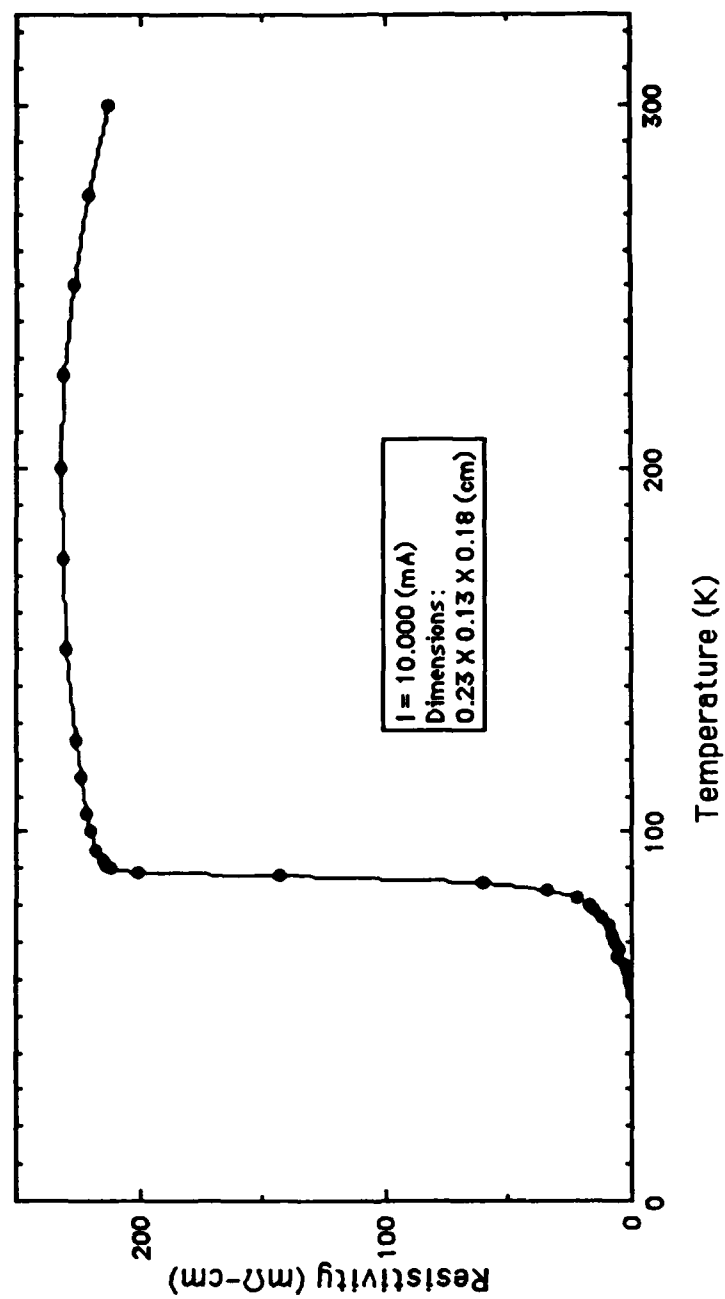


Figure 55. Resistivity versus Temperature for the Barium Carbonate Derived Sample, Sintered at 950 °C, Annealed in Oxygen

show that the critical current density for the samples derived from barium peroxide is significantly greater than that of the samples derived from barium carbonate, which indicates that these samples are more homogeneous (Figure 56). Additionally, the critical current density was lower for the samples annealed in oxygen than for those not annealed in oxygen.

### Analysis

Having looked at the results of each group of measurements taken, an analysis of these results may lead to a better understanding of the data obtained and of the materials themselves.

First, considering the samples derived from barium peroxide which were sintered at 850 °C, the increase in resistivity as the sample is cooled down shows a semiconductive nature present in the sample (3:19). When the temperature reaches about 88 K, portions of the sample begin superconducting and the series resistance of the sample drops suddenly. These regions are surrounded by non-superconducting phases. Thus, as the temperature is reduced further, the superconductive portions of the sample remain at zero resistance, while the surrounding non-superconducting phases, in series with the superconductive regions, increase in resistance due to their semiconductive behavior. The net effect is that the resistance of the sample increases until

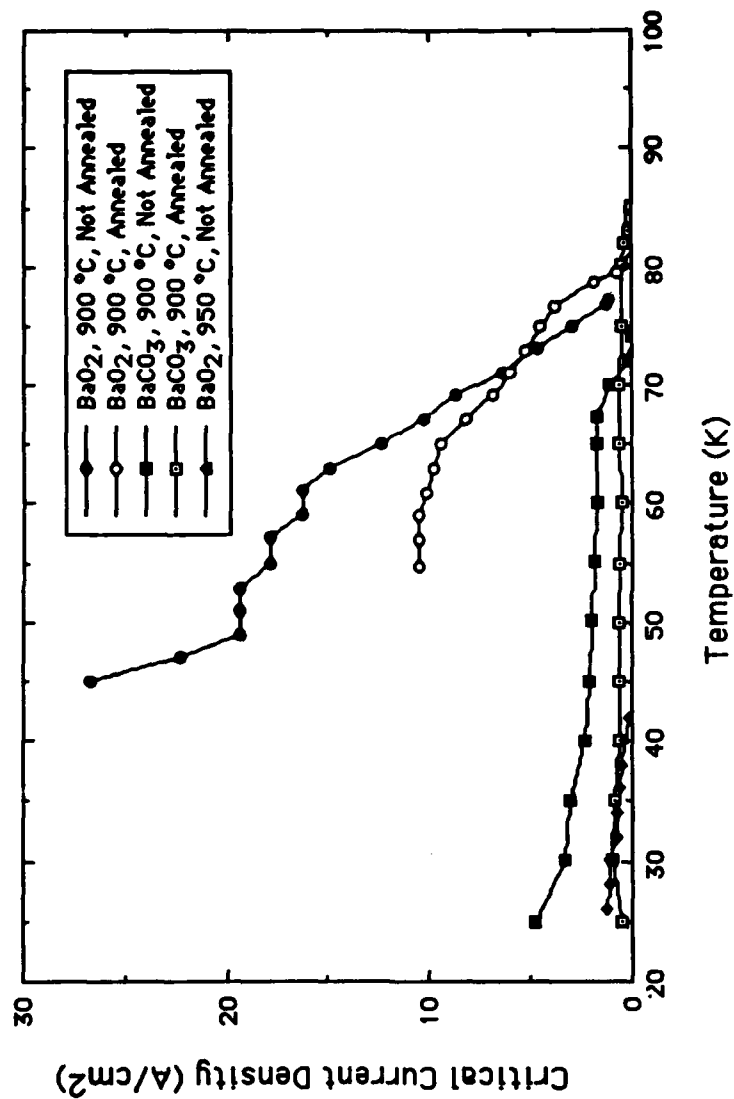


Figure 56. Critical Current Density versus Temperature for All Samples Measured

the surrounding non-superconducting phases become superconducting as shown in Figures 46 and 47. The magnetic susceptibility of the samples verifies that the grains link up at approximately the same temperature as the secondary drop ensues. The AC field curves begin separating at about 55 K for the annealed (Figure 22) and about 35 K for the unannealed (Figure 23). The semiconductive nature of the material is caused by impurities in the material shown in the x-ray diffraction patterns (Figures 16 and 17) as peaks which are not characteristic of the yttrium-barium-copper oxide superconductor.

Next, considering the samples derived from barium carbonate which were sintered at 850 °C, the lack of bulk superconductivity is due to the large amount of unreacted barium carbonate present in the material (Figures 10 and 11). The presence of the barium carbonate prevents the superconducting grains from linking together and providing a complete superconductive path through the samples.

The same effect present in the barium carbonate derived samples sintered at 850 °C is seen in the barium carbonate derived sample which was sintered at 950 °C and not annealed in oxygen. Bulk superconductivity is not reached (Figures 30 and 54) and the x-ray diffraction pattern indicates a large amount of barium carbonate remaining in the material (Figure 13). The barium carbonate derived sample which was sintered at 950 °C and annealed in oxygen, however, eventually went



superconducting after an initial drop in resistivity at about 88 K and a small persistent resistivity which remained until the temperature reached about 55 K (Figure 55). The magnetic susceptibility data shows a gradual increase in susceptibility (Figure 32). The x-ray diffraction patterns are very similar for the annealed and unannealed samples, except that the annealed samples did not retain many of the impurities contained in the unannealed samples (Figures 12 and 13). Thus, the oxygen annealing step influenced the characterization of these samples.

The samples derived from barium peroxide which were sintered at 950 °C were characterized by a sharp drop in resistivity at about 88 K, followed by a small resistivity which remained until the temperature reached about 30 K (Figures 50 and 51). Neither the x-ray diffraction patterns nor the magnetic susceptibility measurements offer any explanation of why a small resistivity persists below the initial drop in resistivity. However, the critical current density curve for the unannealed sample (Figure 56) shows that this small resistivity disappears when the current density is reduced. When the current density is near zero, the critical temperature is above 40 K. Thus it is evident that the small residual resistivity is due to the grain boundaries acting as weak links. When a current large enough to exceed the critical current density of these weak links is

passed through the sample, the weak links return to the normal state and a small resistivity is observed.

The samples derived from barium peroxide which were sintered at 900 °C were characterized by a sharp drop to zero resistivity beginning at about 88 K and ending at about 78 K (Figures 48 and 49). The annealed and unannealed samples are almost identical in most respects; however, the magnetic susceptibility shows that the AC field curves are closer together for the unannealed sample (Figures 34 and 35). This compactness generally indicates that the sample is less susceptible to losing its superconductivity in the presence of a magnetic field. Thus, since the critical current density is determined by how well a material maintains its superconductivity in the presence of a magnetic field, this compactness should indicate that the unannealed sample has a better critical current density. This conclusion is verified by the critical current versus temperature curves shown in Figure 56.

The magnetic susceptibility curves for the samples derived from barium carbonate which were sintered at 900 °C are more compact for the annealed samples (Figures 42 and 43), unlike the previous samples derived from barium peroxide. The critical current density of the unannealed sample was greater than that of the annealed at most temperatures considered (Figure 56). This seems contradictory; however, the x-ray diffraction patterns for

( the annealed sample shows a greater number of peaks which do not correspond to the yttrium-barium-copper oxide (Figures 14 and 15). These impurities are responsible for reducing the critical current density of the sample.

### Conclusions

The results of each phase of this experiment generally correlated well. The resistivity data was generally well supported by the magnetic susceptibility data, the x-ray diffraction patterns, and the critical current density measurements.

## V. Conclusions and Recommendations

### Introduction

The primary objective of this study was to gain a better understanding of how purer, more homogeneous superconductors may be fabricated so that new materials with better properties may be developed. The approach was to determine how several different parameters were changed in the yttrium-barium-copper oxide superconductor when the fabrication techniques were altered by using different barium precursors, sintering at different temperatures, and annealing in an above ambient oxygen environment. Chapter I addressed this objective and listed the different parameters that were to be considered as density, x-ray diffraction, critical temperature, critical current density, and magnetic susceptibility. Chapter II was a review of the current literature on the subject of superconductivity. Chapter III discussed the methodology used in the exercise. The scheme for generating the 12 different pellets was laid out, and the design of the devices used for taking measurements was detailed. Chapter IV showed the results of each type of measurement on each individual sample, and the correlation between the different types of measurements for each sample. The next objective is to arrive at general trends based on the results and analysis of the measurements taken.

## Conclusions

The conclusions drawn based on the results and analysis are based on the effects of barium peroxide versus barium carbonate as a precursor, the effects of varying the sintering temperature, and the effects of oxygen annealing.

Using barium peroxide as the barium precursor has several advantages over using barium carbonate. The primary advantage is that the critical current densities for the samples derived from barium peroxide were significantly better as shown in Figure 56, indicating a more homogeneous sample. The x-ray diffraction patterns indicate that these are purer samples. Also, better densities were achieved using barium peroxide (Figure 9). Also, these samples consistently showed lower resistivity in the normal state. This result, as well as the improved density and increased homogeneity, verify results achieved in a study by NASA Lewis Research Center and Cleveland State University (1:1). Finally, these samples were easier to work with from a fabrication point of view. The hand-grindings were consistently easier, cutting the samples was not as difficult, and no melting occurred even at temperatures where the barium carbonate derived samples experienced some melting.

The effects of changing the sintering temperature were dramatic. In all cases the critical temperature was higher for samples sintered at 900 °C. Also, the resistivity in the

normal state was consistently lower for the samples sintered at 900 °C. These samples also had the quickest transitions from the normal to the superconductive state. These effects can be seen in Figures 57-60. Figure 56 shows that the critical current densities for these samples are much higher than for the other samples, indicating a more homogeneous sample. The x-ray defraction patterns indicate that these are purer samples.

The effects of annealing the samples in oxygen was, generally, to degrade the samples. This is the most obvious effect seen in looking at the critical current densities of the samples (Figure 56). The unannealed samples are consistently capable of carrying more current than the annealed samples. The annealing process did, however, enhance the performance of the sample derived from barium carbonate and sintered at 950 °C. Figure 61 shows a much better resistivity curve for the annealed sample as opposed to the unannealed. In fact, the sample did not even superconduct when measured as-sintered. The annealing step made a superconductor out of this sample. The effects of the oxygen annealing on the resistivity curves of the other samples are inconclusive.

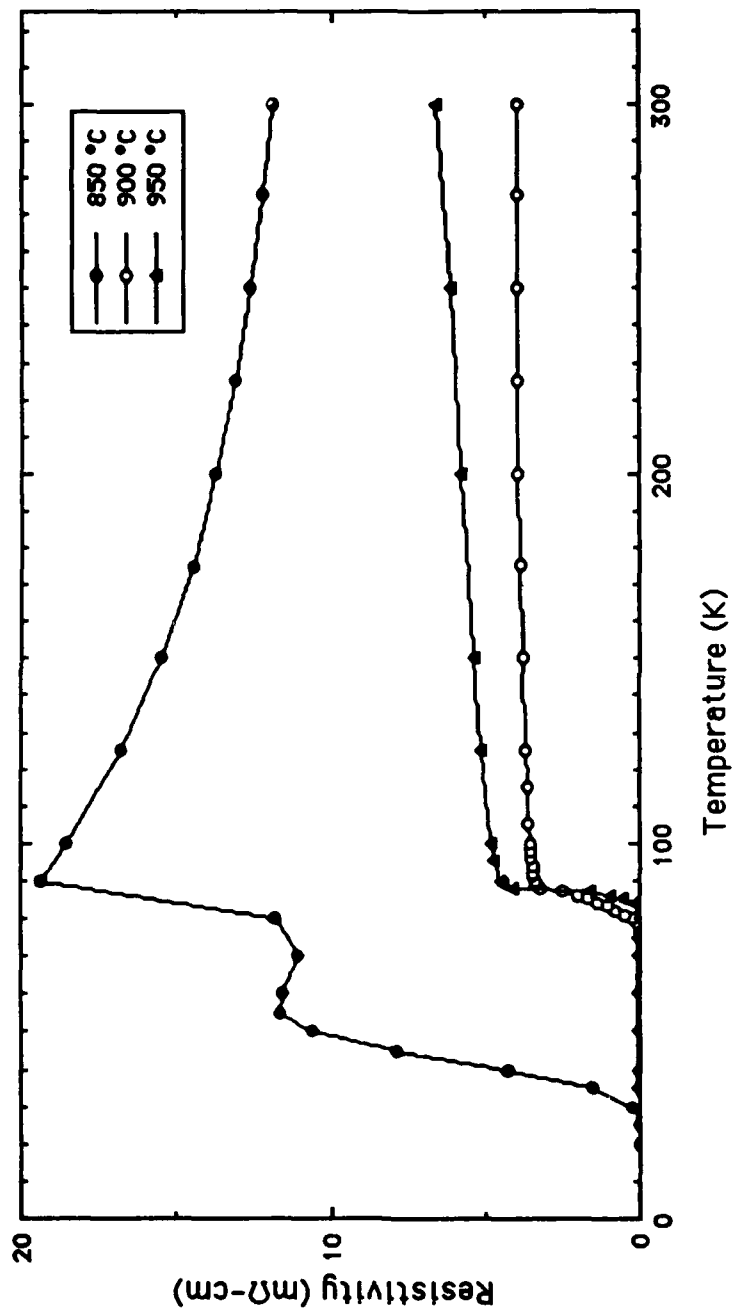


Figure 57. Resistivity versus Temperature for All Oxygen Annealed, Barium Peroxide Derived Samples

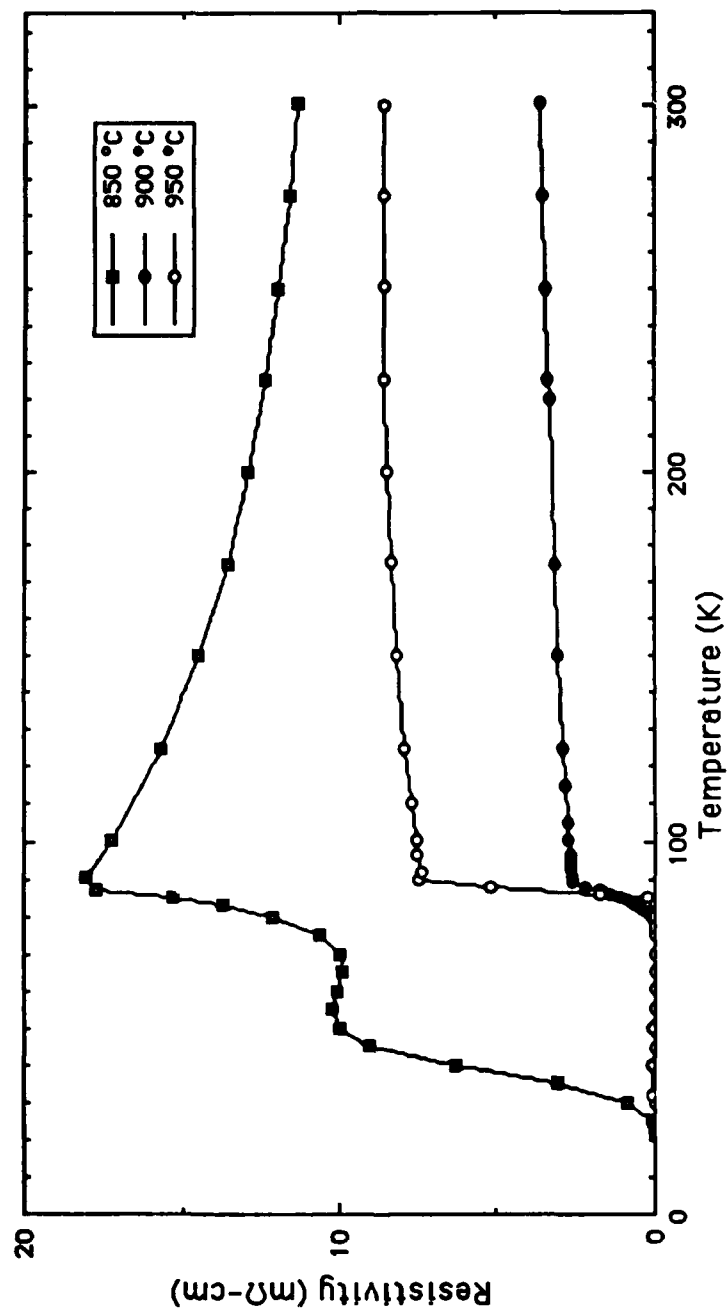


Figure 58. Resistivity versus Temperature for All Unannealed Barium Peroxide Derived Samples



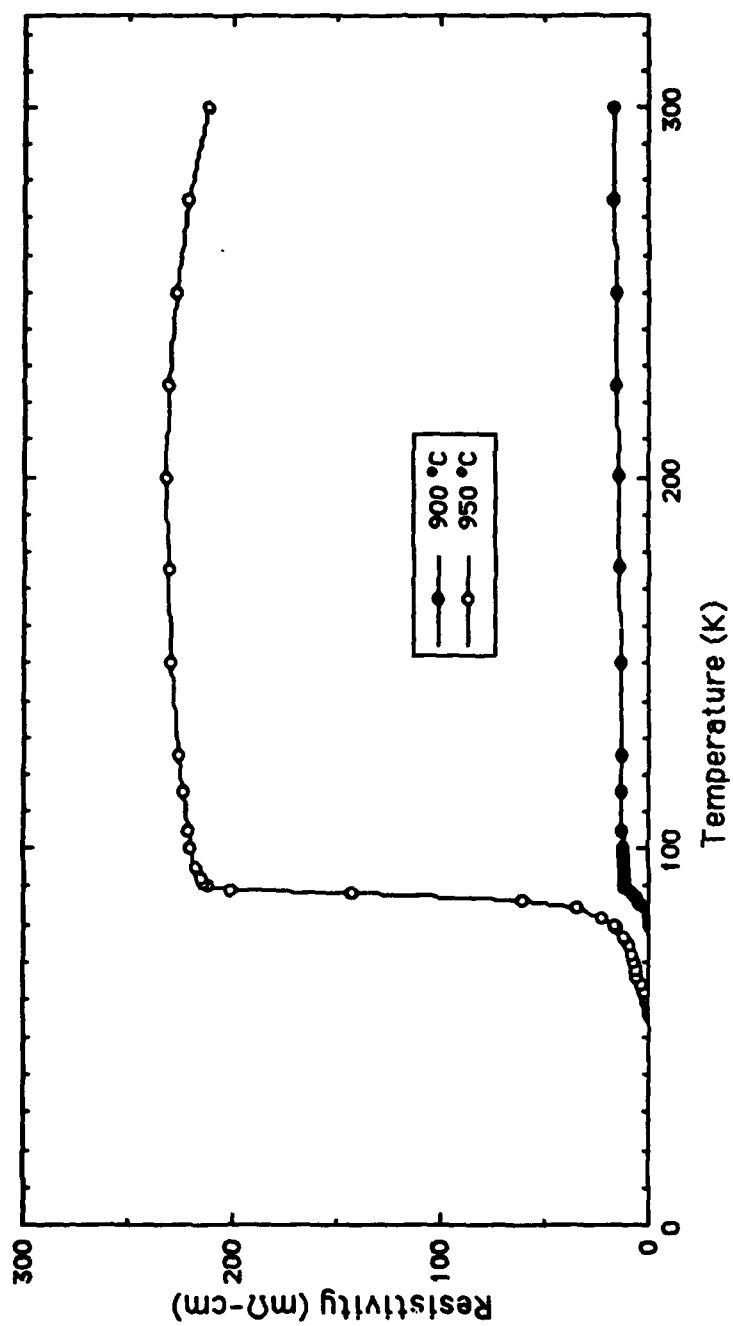


Figure 59. Resistivity versus Temperature for All Oxygen Annealed, Barium Carbonate Derived Samples

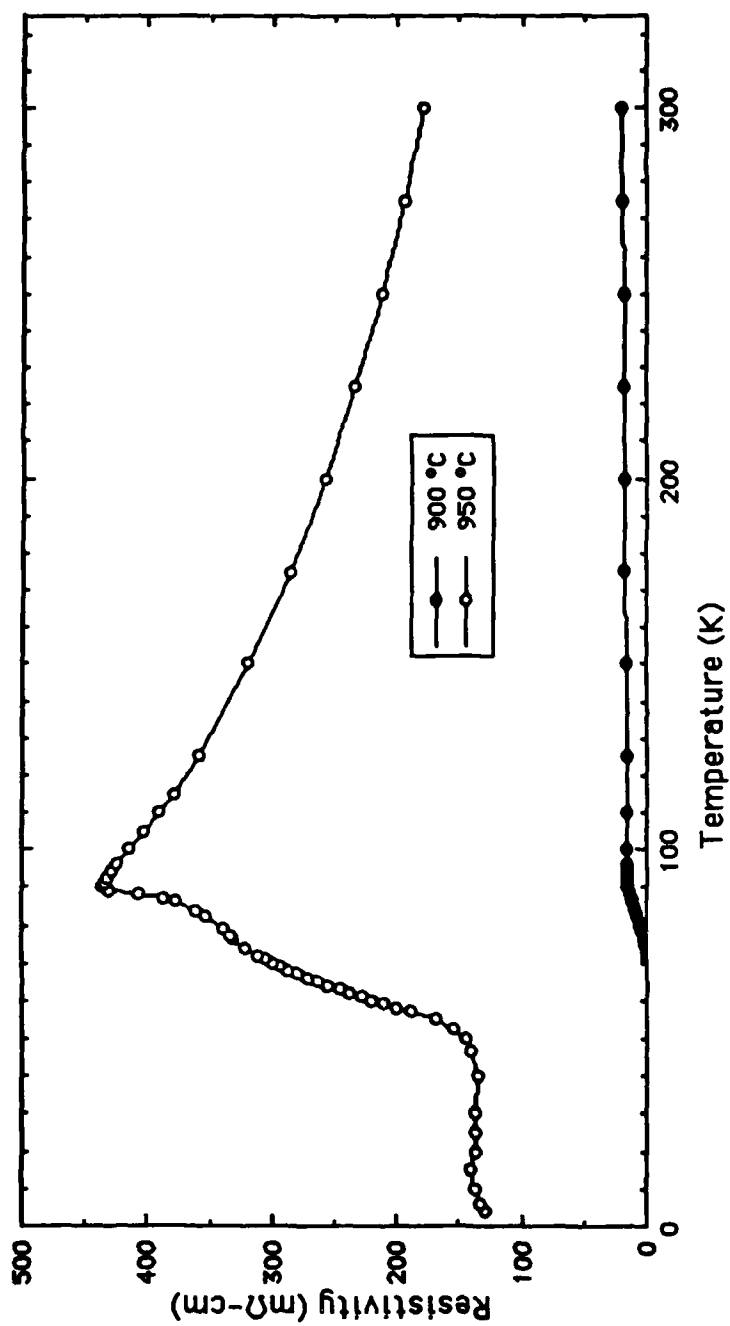


Figure 60. Resistivity versus Temperature for All Unannealed Barium Carbonate Derived Samples

### Recommendations

The opportunity for further investigation in the field of high temperature superconductivity seems inexhaustible. A study concentrating on samples derived from five different sintering temperature, such as 850, 875, 900, 925, and 950 °C, would add considerably to the knowledge gained through this current research effort. The data taken during this experiment shows that 900 °C is the best sintering temperature between the three temperatures considered, but it is not necessarily the optimum sintering temperature. More than three temperatures need to be considered in order to better pinpoint the best sintering temperature.

A more detailed study of the critical current density and the methods for measuring it would be a valuable study. A better scheme than that used in this current research effort would be to take resistivity versus temperature measurements for several current densities. This would yield a more exact critical temperature for each given current density.

Another beneficial study would be to analyze various methods for making contacts for these materials. This issue is important especially when taking critical current density measurements, where the high currents can cause heating to occur at the contacts. A study comparing gold and silver as contacts would be useful.

Other opportunities for further research include studying the new bismuth- or thallium-derived compounds, studying the effects of different cooling schemes on the performance of a superconductor, and designing an automated system for making resistivity versus temperature measurements.

## Appendix A. Calculations of Amounts of Starting Materials

This appendix contains the calculations necessary to determine the amounts of each starting material needed. It was decided that the experimental design would include two barium precursors, three sintering temperatures, and one oxygen annealing temperature. This constitutes a total of 12 pellets. The need to have two identical pellets of each type, to ensure that any abnormalities were not isolated to one pellet, leads to a total of 24 pellets. Thus there are 12 pellets for each barium precursor.

In order to produce all of the needed samples for the various measurements to be taken, the pellets were required to be not less than 0.5 inches in diameter and 0.25 inches thick. Thus, the volume of each pellet is  $1.609 \text{ cm}^3$ .

Assuming a density of  $6.3 \text{ g/cm}^3$ , the weight of each pellet is 10.14 g. So 12 samples weigh 121.7 g. Thus, the weight of the two batches was decided to be 200 g each, thus ensuring that plenty of each mixture was available.

The next step was to determine the relative weights of each of the starting materials.

$$\text{Y}_2\text{O}_3 = 2(88.91) + 3(16.00) = 225.8 \text{ (g/mole)}$$

$$\text{CuO} = 63.55 + 16.00 = 79.55 \text{ (g/mole)}$$

The next step is to look at the reaction that will occur. For the barium carbonate derived sample the reaction is



For the barium peroxide derived sample the reaction is



Since these two reactions show a one to one relationship, the relative weights of the precursors may be determined as follows:

$$\text{BaCO}_3 = 137.3 + 3(16.00) + 12.01 = 197.34 \text{ (g/mole)}$$

$$\text{BaO}_2 = 137.3 + 2(16.00) = 169.33 \text{ (g/mole)}$$

The reaction which produces the desired compound is



Thus, for the barium carbonate derived mixture the relative weight is given as follows:

$$225.8 + 4(197.3) + 6(79.55) = 1492 \text{ (g/mole)}$$

Likewise, for the barium peroxide derived mixture the relative weight is given as follows:

$$225.8 + 4(169.3) + 6(79.55) = 1380 \text{ (g/mole)}$$

From these calculations we see that, for the barium carbonate derived mixture, by weight  $\text{Y}_2\text{O}_3$  makes up 15.13% of the mixture,  $\text{BaCO}_3$  makes up 52.90%, and  $\text{CuO}$  makes up 31.99%. Similarly, for the barium peroxide derived mixture,  $\text{Y}_2\text{O}_3$  makes up 16.36% of the mixture,  $\text{BaO}_2$  makes up 49.07%, and  $\text{CuO}$  makes up 34.59%.

Thus, for a 200 g batch of the barium carbonate derived mixture, the amounts of the starting materials needed are 30.26 g of  $\text{Y}_2\text{O}_3$ , 105.8 g of  $\text{BaCO}_3$ , and 63.98 g of  $\text{CuO}$ . Also, for a 200 g batch of the barium peroxide derived mixture, the

( amounts of the starting materials needed are 32.72 g of  $\text{Y}_2\text{O}_3$ ,  
98.14 g of  $\text{BaO}_2$ , and 69.18 g of  $\text{CuO}$ .

## Appendix B. Density Measurements

This appendix includes the data required to calculate the density for all of the samples. Table 1 includes the density measurements for the samples annealed in an oxygen environment. Table 2 includes the density measurements for the samples which were not annealed.



TABLE 1

## DENSITY MEASUREMENTS FOR SAMPLES ANNEALED IN OXYGEN

| Barium<br>Precursor | Sintering<br>Temperature<br>(°C) | Sample<br>Number | w <sub>d</sub><br>(g) | w <sub>s</sub><br>(g) | w <sub>w</sub><br>(g) | Density<br>(g/cm <sup>3</sup> ) |
|---------------------|----------------------------------|------------------|-----------------------|-----------------------|-----------------------|---------------------------------|
| BaCO <sub>3</sub>   | 850                              | 1                | 3.2971                | 3.5420                | 0.7169                | 5.514                           |
|                     |                                  | 2                | 2.9748                | 3.2657                | 0.7169                | 5.512                           |
|                     | 900                              | 1                | 3.7828                | 3.9695                | 0.7169                | 5.631                           |
|                     |                                  | 2                | 3.1971                | 3.4686                | 0.7169                | 5.666                           |
|                     | 950                              | 1                | 3.4938                | 3.7040                | 0.7169                | 5.442                           |
|                     |                                  | 2                | 3.8017                | 3.9696                | 0.7169                | 5.466                           |
| BaO <sub>2</sub>    | 850                              | 1                | 3.2042                | 3.4836                | 0.7169                | 5.781                           |
|                     |                                  | 2                | 3.1708                | 3.4553                | 0.7169                | 5.788                           |
|                     | 900                              | 1                | 3.3826                | 3.6370                | 0.7169                | 5.773                           |
|                     |                                  | 2                | 3.1396                | 3.4260                | 0.7169                | 5.756                           |
|                     | 950                              | 1                | 3.8138                | 3.9965                | 0.7169                | 5.635                           |
|                     |                                  | 2                | 3.3383                | 3.5853                | 0.7169                | 5.607                           |

TABLE 2

## DENSITY MEASUREMENTS FOR SAMPLES NOT ANNEALED

| Barium<br>Precursor | Sintering<br>Temperature<br>(°C) | Sample<br>Number | w <sub>d</sub><br>(g) | w <sub>s</sub><br>(g) | w <sub>w</sub><br>(g) | Density<br>(g/cm <sup>3</sup> ) |
|---------------------|----------------------------------|------------------|-----------------------|-----------------------|-----------------------|---------------------------------|
| BaCO <sub>3</sub>   | 850                              | 1                | 3.4926                | 3.7126                | 0.7159                | 5.559                           |
|                     |                                  | 2                | 3.4870                | 3.7016                | 0.7159                | 5.490                           |
|                     | 900                              | 1                | 2.7571                | 3.0883                | 0.7159                | 5.657                           |
|                     |                                  | 2                | 3.1119                | 3.3885                | 0.7159                | 5.591                           |
|                     | 950                              | 1                | 3.4730                | 3.6834                | 0.7159                | 5.423                           |
|                     |                                  | 2                | 3.7298                | 3.9031                | 0.7159                | 5.426                           |
| BaO <sub>2</sub>    | 850                              | 1                | 3.5234                | 3.7681                | 0.7159                | 5.902                           |
|                     |                                  | 2                | 3.1183                | 3.4115                | 0.7159                | 5.823                           |
|                     | 900                              | 1                | 3.2907                | 3.5584                | 0.7159                | 5.795                           |
|                     |                                  | 2                | 3.6922                | 3.9020                | 0.7159                | 5.758                           |
|                     | 950                              | 1                | 3.6973                | 3.8900                | 0.7159                | 5.578                           |
|                     |                                  | 2                | 3.7687                | 3.9468                | 0.7159                | 5.531                           |

## Bibliography

1. Hepp, A. F., J. R. Gaier, W. H. Philipp, J. D. Warner, R. G. Garlick, J. J. Pouch, and P. D. Hambourger. "Advantages of Barium Peroxide in the Powder Synthesis of Perovskite Superconductors," Unpublished report, undated.
2. "Interview with Dr. M. Brian Maple: Professor of Physics, University of California San Diego, "Supercurrents, 2: 13-20 (February 1988).
3. Khurana, Anil. "Even Lanthanum Copper Oxide is Superconducting," Physics Today, 40: 17-22 (September 1987).
4. Khurana, Anil. "The  $T_c$  to Beat is 125 K," Physics Today, 41: 21-25 (April 1988).
5. Lemonick, Michael D. "Superconductors: The Startling Breakthrough that Could Change Our World," Time, 129: 64-75 (May 11, 1987).
6. Lewis, Clifford F. "Conductive Ceramics," Materials Engineering, 104: 27-30 (June 1987).
7. Loyd, Robert J. "Bechtel's Program in Superconducting Magnetic Energy Storage," Supercurrents, 2: 1-6 (February 1988).
8. Maartense, Iman, SYSTRAN Corporation. Electrical and Magnetic Properties of High Temperature Superconductors. Contract F33615-84-C-5116. Report to AFWAL/MLPO, Materials Laboratory, Wright-Patterson AFB, OH. February 1988.
9. Miller, K. Alex and Georg Bednorz. "The Discovery of a Class of High-Temperature Superconductors," Science, 237: 1133-1139 (September 4, 1987).

10. "New Superconducting Materials," Supercurrents, 3: 2-5 (March 1988).
11. Pool Robert. "New Superconductors Answer Some Questions," Science, 240: 146-147 (April 8, 1988).
12. Pool, Robert. "Superconductors' Material Problems," Science, 240: 25-27 (April 1, 1988).
13. Robinson, Arthur L. "IBM Superconductor Leaps Current Hurdle," Science, 236: 1189 (June 5, 1987).
14. Robinson, Arthur L. "A New Route to Oxide Superconductors," Science, 236: 1526 (June 19, 1987).
15. Voss, David F. "Superconductivity: the FAX Factor," Science, 240: 280-281 (April 15, 1988).
16. Waldrop, M. Mitchell. "Thallium Superconductor Reaches 125 K," Science, 239: 1243 (March 11, 1988).
17. Wong-Ng, W., R. S. Roth, L. J. Swartzendruber, L. H. Bennett, C. K. Chiang, F. Beech, and C. R. Hubbard. "X-ray Powder Characterization of  $\text{Ba}_2\text{YCu}_3\text{O}_{7-x}$ ," Advanced Ceramics Materials, 2: 571 (1987).

Vita

First Lieutenant Paul A. Rhea [REDACTED]

[REDACTED] [REDACTED]  
[REDACTED] in 1979 [REDACTED] went on to attend Tennessee Technological University from which he received the degree of Bachelor of Science in Electrical Engineering. He graduated Magna Cum Laude in 1983. He received a commission in the USAF through Officers' Training School in 1985. He was assigned to the Air Logistics Center at Oklahoma City, Oklahoma, where he served as the NATO E-3 Software Release Manager. He was then assigned to the School of Engineering, Air Force Institute of Technology.

[REDACTED]  
[REDACTED]

REPORT DOCUMENTATION PAGE

Form Approved  
OMB No. 0704-0188

|  |                    |   |   |   |  |
|--|--------------------|---|---|---|--|
| 1. REPORT SECURITY CLASSIFICATION<br><b>UNCLASSIFIED</b>   |                    |   | 1b. RESTRICTIVE MARKINGS  |   |  |
| 2a. SECURITY CLASSIFICATION AUTHORITY  |                    |   | 3. DISTRIBUTION/AVAILABILITY OF REPORT<br><b>Approved for public release;<br/>distribution unlimited.</b> |   |  |
| 2b. DECLASSIFICATION/DOWNGRADING SCHEDULE  |                    |   |   |   |  |
| 4. PERFORMING ORGANIZATION REPORT NUMBER(S)<br><b>AFIT/GE/ENG/88D-42</b>   |                    |   | 5. MONITORING ORGANIZATION REPORT NUMBER(S)   |   |  |
| 6a. NAME OF PERFORMING ORGANIZATION<br><b>School of Engineering</b>  |                    | 6b. OFFICE SYMBOL<br>(If applicable)<br><b>AFIT/ENG</b> | 7a. NAME OF MONITORING ORGANIZATION   |   |  |
| 6c. ADDRESS (City, State, and ZIP Code)<br><b>Air Force Institute of Technology<br/>Wright-Patterson AFB OH 45433-6583</b>   |                    |   | 7b. ADDRESS (City, State, and ZIP Code)   |   |  |
| 8a. NAME OF FUNDING/SPONSORING ORGANIZATION<br><b>AFWAL Materials Lab</b>  |                    | 8b. OFFICE SYMBOL<br>(If applicable)<br><b>MLPO</b>     | 9. PROCUREMENT INSTRUMENT IDENTIFICATION NUMBER   |   |  |
| 8c. ADDRESS (City, State, and ZIP Code)<br><b>AFWAL/MLPO<br/>Wright-Patterson AFB OH 45433-6533</b>  |                    |   | 10. SOURCE OF FUNDING NUMBERS   |   |  |
|  |                    |   | PROGRAM ELEMENT NO.<br><b>6.1</b>   | PROJECT NO.<br><b>2306</b>                                    | TASK NO.<br><b>2306Q1</b>                  |
|  |                    |   |   |   | WORK UNIT ACCESSION NO.<br><b>2306Q106</b> |
| 11. TITLE (Include Security Classification)<br><b>See Box 19</b>   |                    |   |   |   |  |
| 12. PERSONAL AUTHOR(S)<br><b>Paul A. Rhea, B.S., 1 Lt, USAF</b>  |                    |   |   |   |  |
| 13a. TYPE OF REPORT<br><b>MS Thesis</b>  |                    | 13b. TIME COVERED<br>FROM _____ TO _____                |   | 14. DATE OF REPORT (Year, Month, Day)<br><b>1988 December</b> |  |
| 15. PAGE COUNT<br><b>110</b>   |                    |   |   |   |  |
| 16. SUPPLEMENTARY NOTATION   |                    |   |   |   |  |
| 17. COSATI CODES   |                    |   | 18. SUBJECT TERMS (Continue on reverse if necessary and identify by block number)                         |   |  |
| FIELD<br><b>20</b>   | GROUP<br><b>03</b> | SUB-GROUP   | Superconductivity, Yttrium-Barium-Copper Oxide,<br>High Temperature Superconductivity, <i>THESE (JET)</i> |   |  |
| 19. ABSTRACT (Continue on reverse if necessary and identify by block number)<br>Title: <b>EFFECTS OF DIFFERENT FABRICATION TECHNIQUES ON THE YTTRIUM-BARIUM-COPPER OXIDE HIGH TEMPERATURE SUPERCONDUCTOR</b><br><br>Thesis Advisor: <b>Y. K. Yeo, PhD<br/>Associate Professor of Physics</b> |                    |   |   |   |  |
| 20. DISTRIBUTION/AVAILABILITY OF ABSTRACT<br><input checked="" type="checkbox"/> UNCLASSIFIED/UNLIMITED <input type="checkbox"/> SAME AS RPT. <input type="checkbox"/> DTIC USERS  |                    |   | 21. ABSTRACT SECURITY CLASSIFICATION<br><b>UNCLASSIFIED</b>   |   |  |
| 22a. NAME OF RESPONSIBLE INDIVIDUAL<br><b>Y. K. Yeo, PhD</b>   |                    |   | 22b. TELEPHONE (Include Area Code)<br><b>(513) 255-2012</b>   |   | 22c. OFFICE SYMBOL<br><b>AFIT/ENP</b>      |

UNCLASSIFIED

↓ This study examines how several different parameters were changed in the yttrium-barium-copper oxide superconductor when the fabrication techniques were altered by using different barium precursors, including barium peroxide and barium carbonate; sintering at different temperatures, including 850, 900, 950 °C; and annealing in an above ambient oxygen environment. Twelve different pellets were fabricated, and measurements were taken on them which included density, x-ray diffraction, critical temperature, critical current density, and magnetic susceptibility. The results showed that the barium peroxide derived samples had higher densities, better critical current densities, and lower resistivities in the normal state. The samples sintered at 900 °C for both barium precursors, had higher critical temperatures, higher critical current densities, sharper transitions from the normal to the superconducting state, and lower resistivities in the normal state. The samples which were annealed in an oxygen environment varied little from those samples measured as-sintered.

→ 4, 5, 6, 7

UNCLASSIFIED